

ChemMedChem

Supporting Information

Adsorption to the Surface of Hemozoin Crystals: Structure-Based Design and Synthesis of Amino-Phenoxazine β -Hematin Inhibitors

Tania Olivier, Leigh Loots, Michéle Kok, Marianne de Villiers, Janette Reader, Lynn-Marié Birkholtz, Gareth E. Arnott, and Katherine A. de Villiers*

Table of Contents

1. Supporting data for <i>in silico</i> investigations.....	2
Crystal morphology.....	2
Clinically-relevant antimalarial drugs	4
Cyclic scaffolds.....	18
2. Crystallographic data	28
3. Synthetic details.....	30
Synthesis of 3-substituted phenoxazines.....	30
Synthesis of 2-substituted phenoxazines.....	32
Experimental details	35
General.....	35
Towards the 2-substituted phenoxazines	36
Towards the 3-substituted phenoxazines	38
Spectra for new compounds reported in the manuscript	40
1-(2-((5-(diethylamino)pentan-2-yl)amino)-10 <i>H</i> -phenoxazin-10-yl)ethan-1-one (N-Ac-P2a)	40
<i>N</i> ¹ , <i>N</i> ¹ -diethyl- <i>N</i> ⁴ -(10 <i>H</i> -phenoxazin-2-yl)pentane-1,4-diamine (P2a).....	42
1-(2-(cyclohexylamino)-10 <i>H</i> -phenoxazin-10-yl)ethan-1-one (N-Ac-P2b).....	43
<i>N</i> -cyclohexyl-10 <i>H</i> -phenoxazin-2-amine (P2b).....	45
1-(2-(phenylamino)-10 <i>H</i> -phenoxazin-10-yl)ethan-1-one (N-Ac-P2c).....	49
<i>N</i> -phenyl-10 <i>H</i> -phenoxazin-2-amine (P2c)	51
<i>tert</i> -butyl 3-bromo-10 <i>H</i> -phenoxazine-10-carboxylate (Boc-protected 2)	53
<i>tert</i> -butyl 3-([5-(diethylamino)pentan-2-yl]amino)-10 <i>H</i> -phenoxazine-10-carboxylate (N-Boc-P3a)	54
<i>tert</i> -butyl 3-(cyclohexylamino)-10 <i>H</i> -phenoxazine-10-carboxylate (N-Boc-P3b).....	56
<i>N</i> ¹ , <i>N</i> ¹ -diethyl- <i>N</i> ⁴ -(10 <i>H</i> -phenoxazin-3-yl)pentane-1,4-diamine (P3a).....	58
(<i>E</i>)-4-[(3 <i>H</i> -phenoxazin-3-ylidene)amino]- <i>N,N</i> -diethylpentan-1-amine HCl salt (P3a') ...	59
<i>N</i> -cyclohexyl-10 <i>H</i> -phenoxazin-3-amine (P3b).....	60
4. References	61

1. Supporting data for *in silico* investigations

Crystal morphology

Table S1 Parameters used for the growth morphology calculations

Property	Details
Force field	cvff (parameterized for β -haematin)
Charges	QEq
Quality	2×10^{-5} kcal.mol ⁻¹
Summation method – electrostatics	Ewald
Summation method – van der Waals	Group based

Table S2 Calculated attachment energies for the four morphologically-relevant faces of a β -hematin crystal

Crystal face	This study		Previous study ^[1]	
	E_{att} (kcal.mol ⁻¹)	Morphological importance relative to (100)	E_{att} (kcal.mol ⁻¹)	Morphological importance relative to (100)
(001)	-124.4	0.17	-101.5	0.30
(011)	-100.8	0.21	-82.4	0.37
(010)	-38.1	0.56	-27.7	1.10
(100)	-21.4	1.00	-30.6	1.00

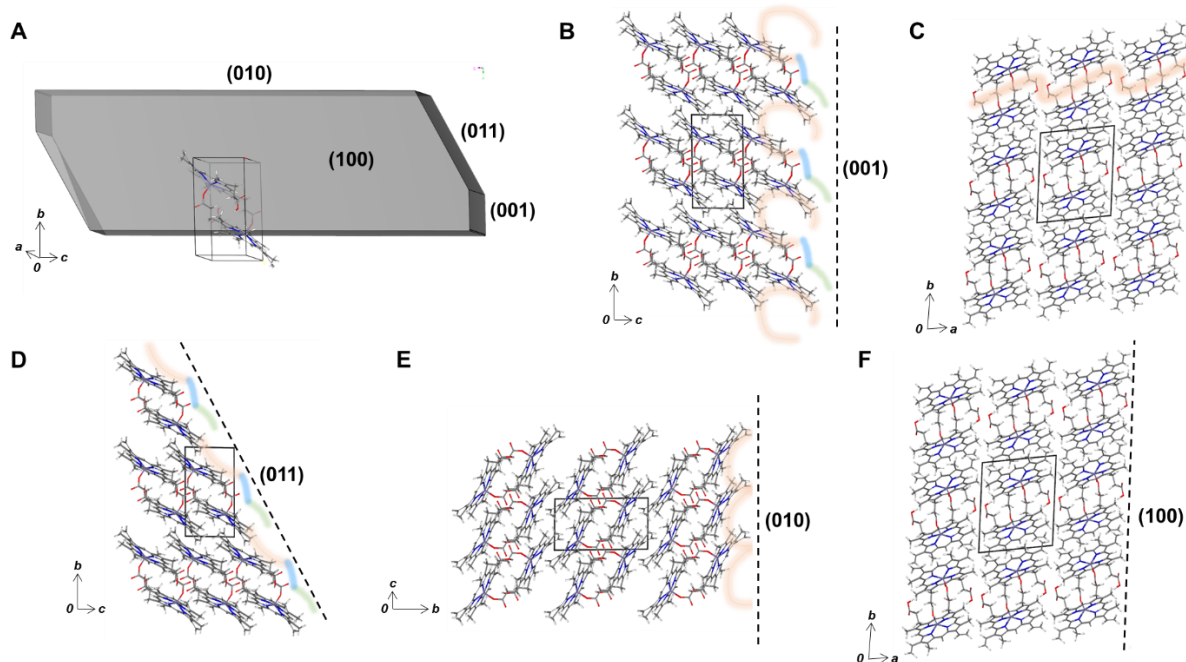


Figure S1 The structure of synthetic hemozoin (β -hematin). **A** The theoretical morphology of the crystal was determined using the Morphology tool in BIOVIA MS.^[2] The four faces with greatest morphological importance were identified using relative attachment energies, and are indicated on the structure, together with the unit cell. The slow growing (100) face dominates the external morphology, while the fastest-growing (001) and (011) faces are considered likely targets for adsorption of inhibitors. **B** The corrugated topology of the (001) face is evident when viewed down the a -axis. Fe(III)PPIX molecules line the deep furrows indicated in orange and promote π -stacking interactions; hydrogen-bonding sites are indicated in blue, while additional π -stacking may take place in regions indicated in green. **C** A view down the c -axis onto the (001) face showing the zig-zag shaped furrow (orange). **D** Viewed down the a -axis, the corrugations on the (011) face are less marked compared to the (001) face, although π -stacking (orange and green) and hydrogen bonding (blue) sites are still present. **E** Viewed down the a -axis, shallow π -stacking sites (orange) are evident on the (010) face. **F** The (100) face is molecularly flat. The unit cell is outlined in black in (b) – (f).

Clinically-relevant antimalarial drugs

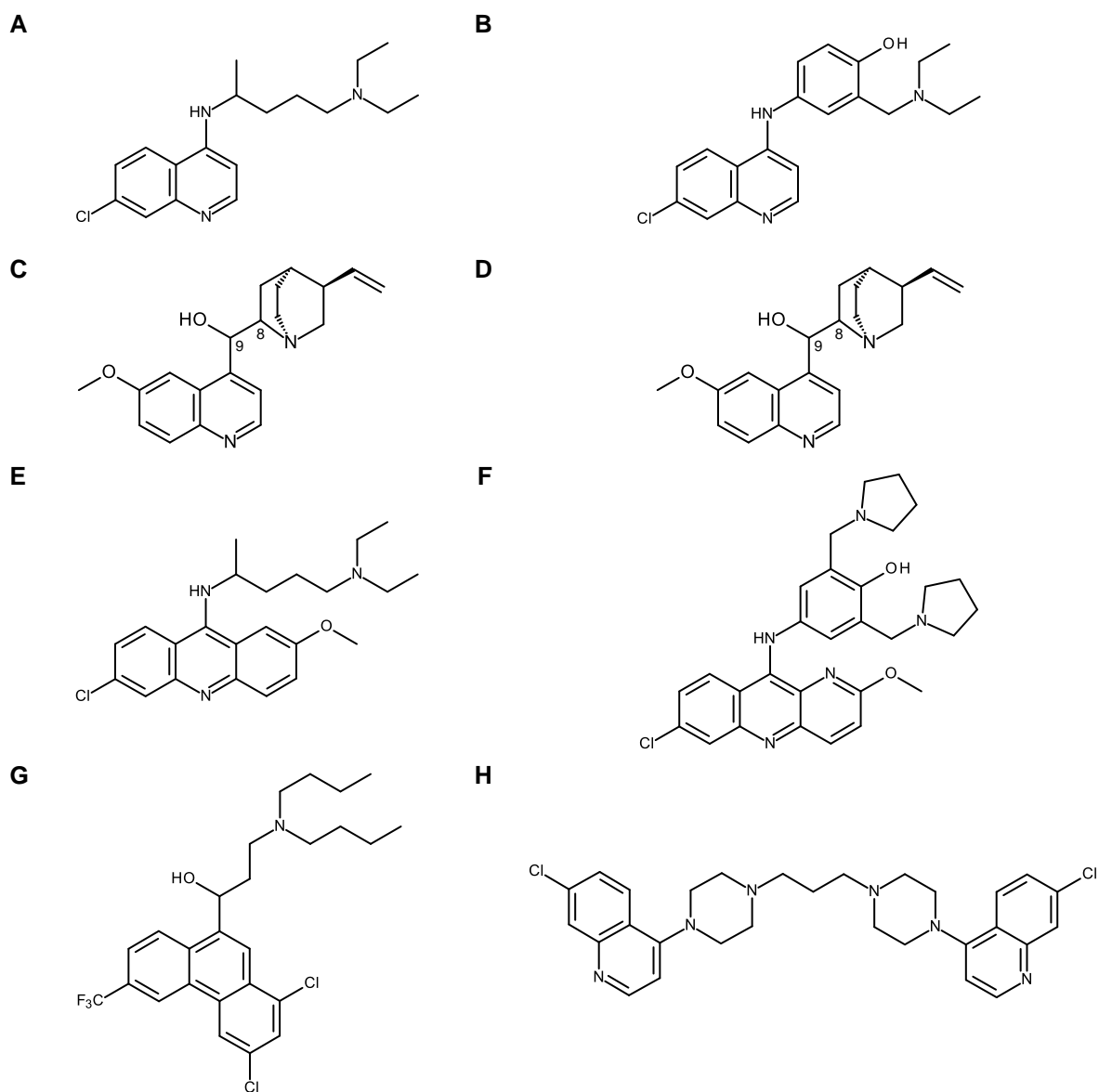


Figure S2 Molecular structures of antimalarial drugs investigated. **A** chloroquine, CQ; **B** amodiaquine, AQ; **C** quinine (8*S*, 9*R*), QN; **D** quinidine (8*R*, 9*S*), QD; **E** quinacrine (mepacrine), QC; **F** pyronaridine, PYR; **G** halofantrine, Hf; and **H** piperavaquine, PPQ.

Table S3 Predicted pK_a values^[3] and relative abundances of different protic forms of the antimalarial drugs at pH 4.8

Inhibitor	$pK_{a,1}$	$pK_{a,2}$	$pK_{a,3}$	$pK_{a,4}$	% 1+	% 2+	% 3+	% 4+
CQ	7.29	10.29	-	-	1	99	-	-
AQ	6.46	10.23	-	-	2	98	-	-
QN	4.02	9.05	-	-	86	14	-	-
QD	4.05	9.05	-	-	86	14	-	-
QC	8.37	10.33	-	-	-	100	-	-
PYR	5.95	7.97	9.23	10.16	-	7	93	-
Hf	10.05	14.47	-	-	100	-	-	-
PPQ	6.08	6.81	7.40	8.75	-	-	5*	95

* Two different 3+ species, where either one or both quinoline scaffolds are protonated, were considered totalling 5% abundance.

Table S4 Calculated adsorption energies ($E_{ads}/kcal.mol^{-1}$) for the adsorption of antimalarial drugs* onto the (001), (011), (010) and (100) faces of β -hematin

Drug	Scaffold	Number of rings	E_{ads} (001)	σ	E_{ads} (011)	σ	E_{ads} (010)	σ	E_{ads} (100)	σ	Avg E_{ads}	σ
CQ2+	Quinoline	2	-61.8	0.2	-53.3	0.0	-52.4	0.0	-42.0	0.1	-52.4	0.1
AQ2+	Quinoline	2	-68.9	0.4	-57.6	0.1	-57.4	0.0	-48.0	0.0	-58.0	0.1
QN1+	Quinoline	2	-60.5	0.0	-52.7	0.9	-53.8	0.9	-40.7	0.3	-51.9	0.3
QN2+	Quinoline	2	-65.9	0.6	-54.9	0.6	-57.3	0.0	-41.6	0.0	-54.9	0.2
QD1+	Quinoline	2	-61.2	0.6	-52.7	0.7	-50.2	0.0	-38.1	0.2	-50.5	0.2
QD2+	Quinoline	2	-60.0	0.5	-52.6	0.3	-50.3	0.9	-38.7	0.5	-50.4	0.3
QC2+	Acridine	3	-82.2	0.3	-65.8	0.9	-61.3	0.5	-50.0	0.0	-64.8	0.2
PYR2+	benzo[b][1,5]-naphthyridine	3	-87.2	0.5	-68.8	0.6	-70.2	0.0	-57.1	0.5	-70.8	0.2
PYR3+	benzo[b][1,5]-naphthyridine	3	-85.4	0.9	-71.7	0.5	-71.2	0.7	-57.6	0.2	-71.5	0.2
Hf1+	Phenanthrene	3	-70.3	0.5	-73.4	0.3	-56.4	0.3	-51.2	0.4	-62.8	0.3
PPQ3+ ^a	<i>bis</i> -Quinoline	4 (2 × 2)	-83.0	0.1	-81.1	0.0	-78.3	0.2	-57.5	0.6	-75.0	0.3
PPQ3+ ^b	<i>bis</i> -Quinoline	4 (2 × 2)	-90.0	0.6	-85.7	0.8	-80.6	0.6	-73.5	0.4	-82.5	0.2
PPQ4+	<i>bis</i> -Quinoline	4 (2 × 2)	-79.5	0.1	-70.6	0.8	-75.3	0.1	-50.1	0.6	-68.9	0.3

* Protonation states that are relevant at the pH of the digestive vacuole (4.8) are shown.

^a Two quinoline and one side chain N-atoms protonated; ^b One quinoline and two side chain N-atoms protonated

Table S5 Hierarchical ordering of antimalarial drugs* based on adsorption energies# on (001), (011), (010) and (100) faces compared to average (Avg.) adsorption energy

Rank	(001)		(011)		(010)		(100)		Avg.	
1	Piperaquine	3+ (1 Qn)	Piperaquine	3+ (1 Qn)	Piperaquine	3+ (2Qn)	Piperaquine	3+ (1 Qn)	Piperaquine	3+ (1 Qn)
2	Pyronaridine	2+	Piperaquine	3+ (2 Qn)	Piperaquine	3+ (1Qn)	Pyronaridine	3+	Piperaquine	3+ (2 Qn)
3	Pyronaridine	3+	Halofantrine	1+	Piperaquine	4+	Piperaquine	3+ (2 Qn)	Pyronaridine	3+
4	Piperaquine	3+ (2 Qn)	Pyronaridine	3+	Pyronaridine	3+	Pyronaridine	2+	Pyronaridine	2+
5	Quinacrine	2+	Piperaquine	4+	Pyronaridine	2+	Halofantrine	1+	Piperaquine	4+
6	Piperaquine	4+	Pyronaridine	2+	Amodiaquine	2+	Piperaquine	4+	Quinacrine	2+
7	Halofantrine	1+	Quinacrine	2+	Quinacrine	2+	Quinacrine	2+	Halofantrine	1+
8	Amodiaquine	2+	Amodiaquine	2+	Halofantrine	1+	Amodiaquine	2+	Amodiaquine	2+
9	Quinine	2+	Quinine	2+	Quinine	2+	Chloroquine	2+	Quinine	2+
10	Chloroquine	2+	Chloroquine	2+	Quinine	1+	Quinine	2+	Chloroquine	2+
11	Quinidine	1+	Quinine	1+	Chloroquine	2+	Quinine	1+	Quinine	1+
12	Quinine	1+	Quinidine	1+	Quinidine	2+	Quinidine	2+	Quinidine	1+
13	Quinidine	2+	Quinidine	2+	Quinidine	1+	Quinidine	1+	Quinidine	2+

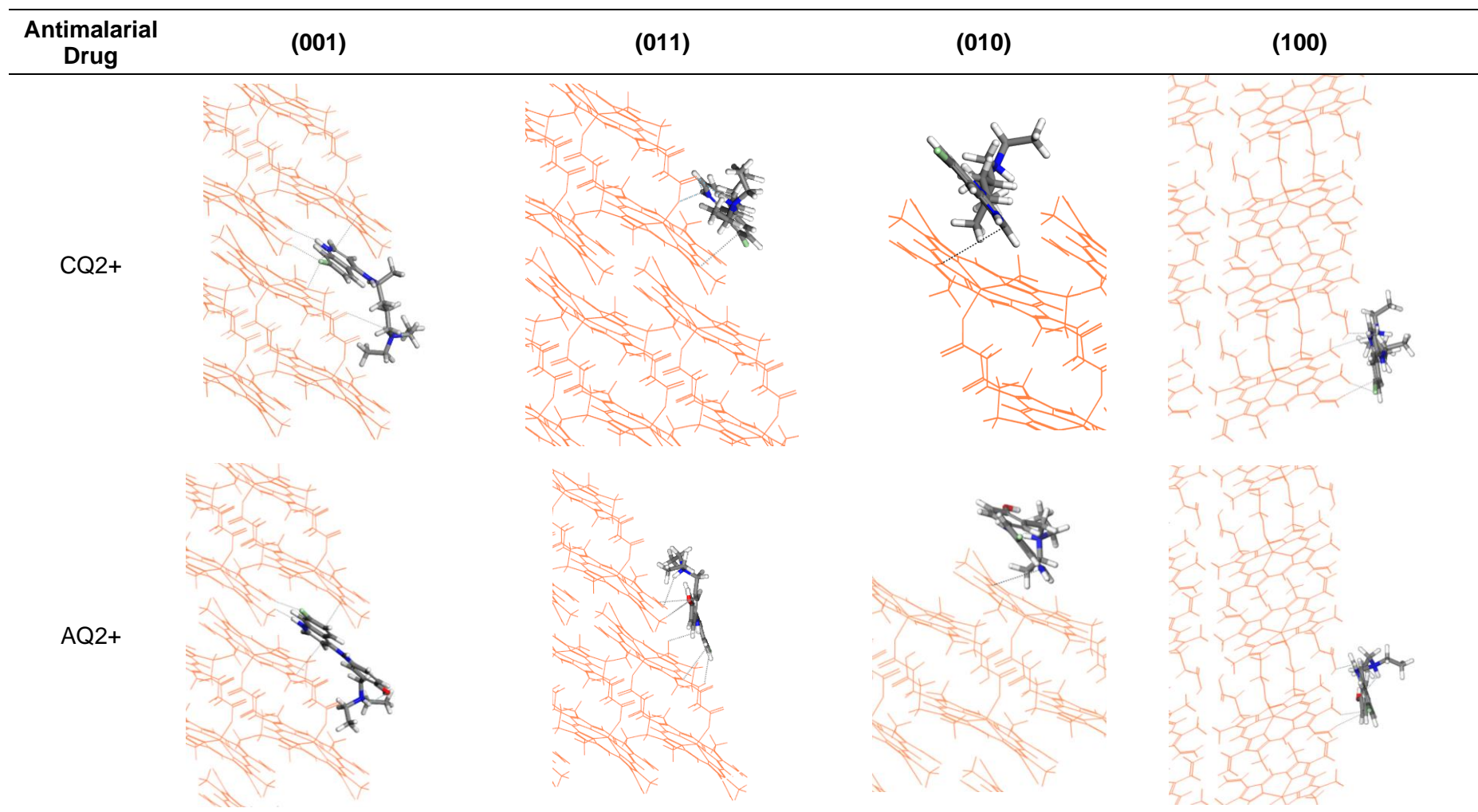
* Antimalarial drug contains: white – quinoline scaffold; green – benzo[b][1,5]naphthyridine scaffold; blue – acridine scaffold and orange – phenanthrene scaffold. When more than one protic form is considered, the most abundant species at pH 4.8 is shown in bold.

The adsorption energies are reported in Table 2 of the main text.

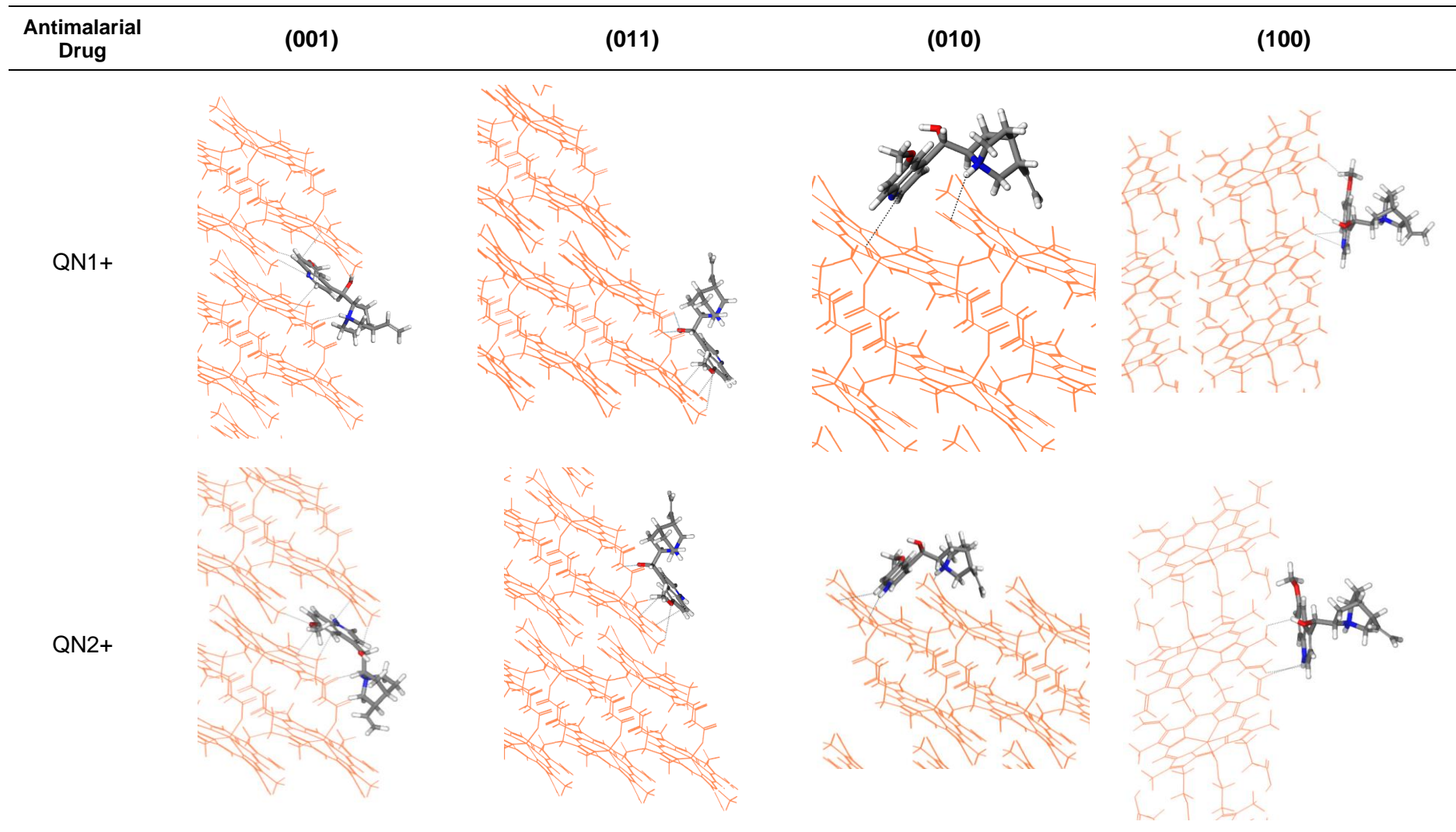
Table S6 Close contacts previously identified during *manual docking* of CQ1+ on the (001) crystal face^[1]

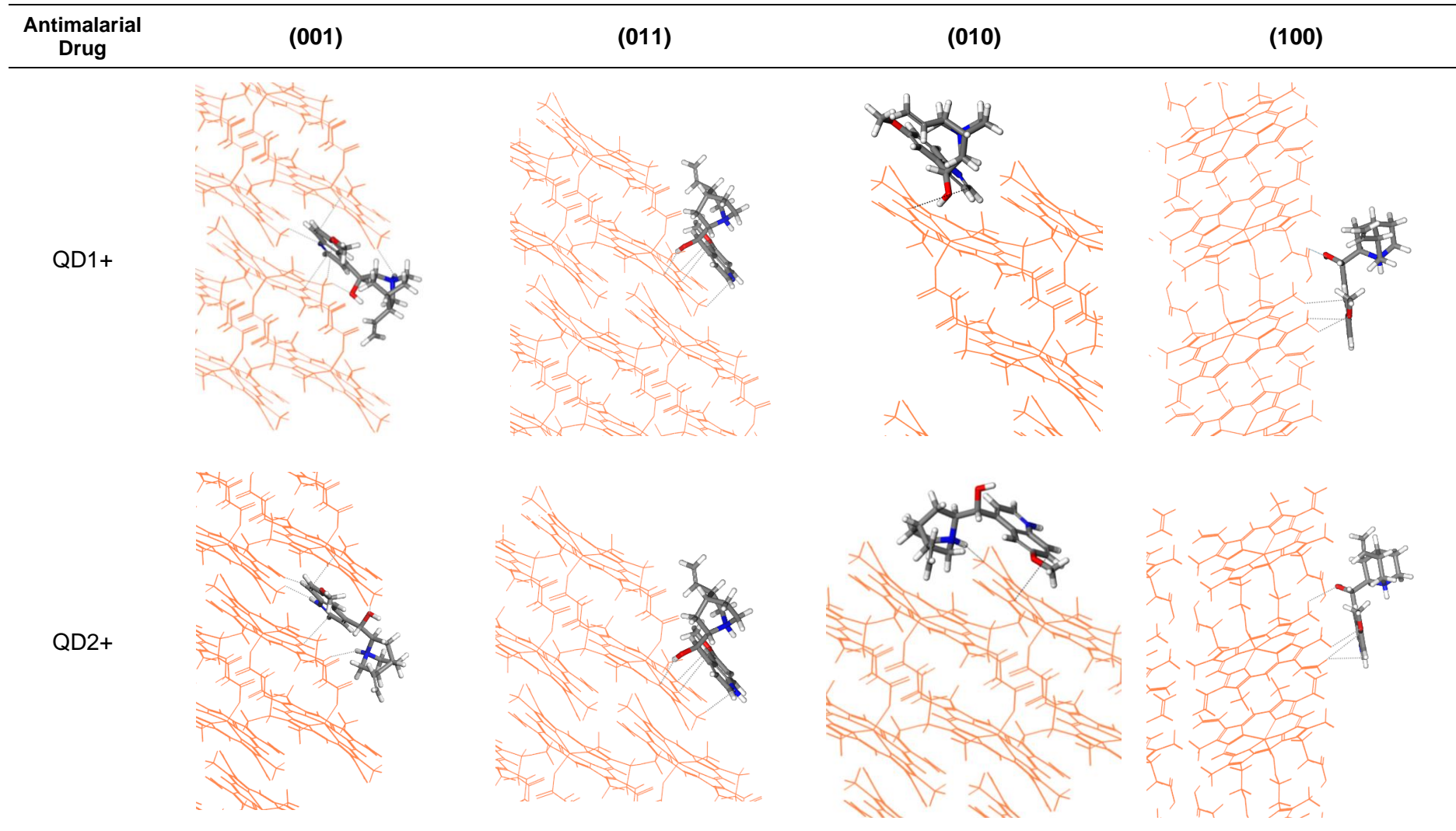
Inhibitor	Fe(III)PPIX	Distance / Å
(CQ) N _{quinoline}	(vinyl)CH	2.4
(CQ) C ₇ -Cl	(methyl)CH ₃	3.0
(CQ) R ₃ NH ⁺	(propionic acid)COO ⁻	2.7 (salt bridge)
(CQ) C ₄ -NRH	(π cloud)C=C	2.7

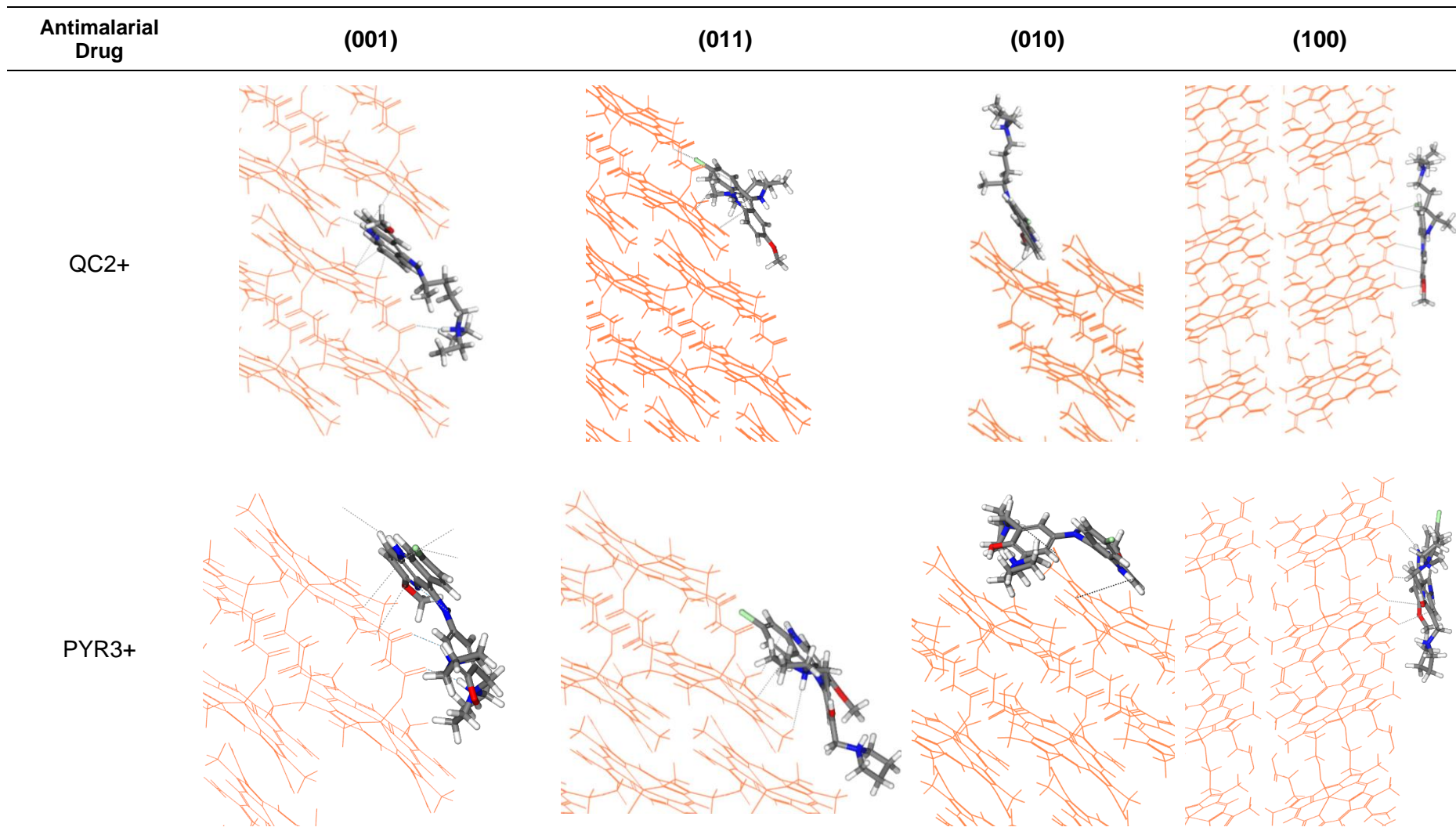
Table S7 *In silico* adsorption of antimalarial drugs on (001), (011), (010) and (100) faces.



For clarity, the β -haematin crystal is shown in orange, and the orientation of each face corresponds to that shown in **Figure S1**. Close contacts are indicated as dashed black lines. For further details of the latter, please consult **Tables S7a-d** for the (001), (011), (010) and (100) faces, respectively.







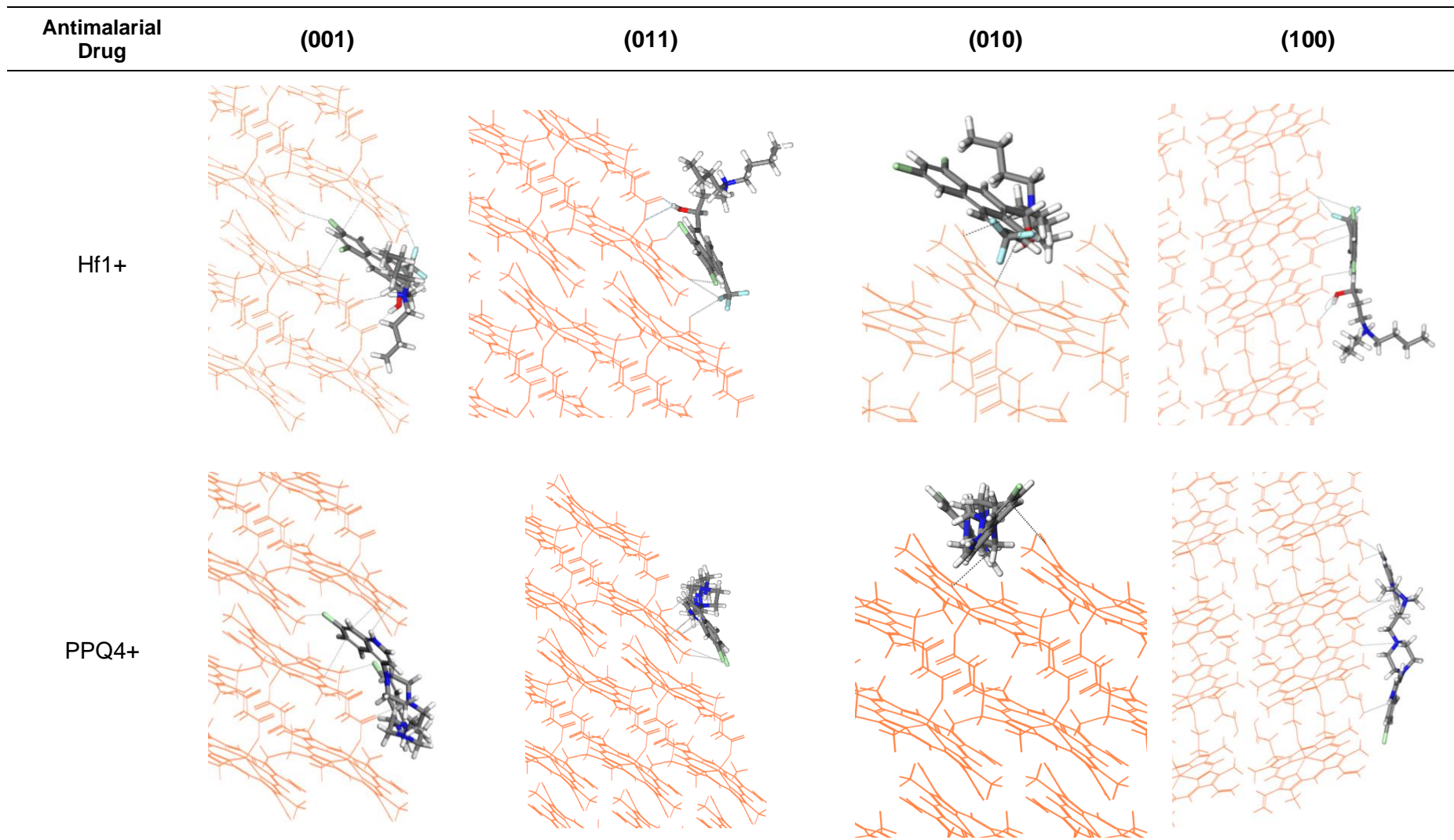


Table S8a Close contacts (< 4Å) determined for the adsorption of antimalarial drugs onto the (001) face of β -haematin.

Drug	Interaction	Type	Distance	Description [#]	Angle
CQ2+	π - π	1	3.4	(Cyclic scaffold)C---C(Porphyrin)	
	π - π	1	3.7	(Cyclic scaffold)N---C(Porphyrin)	
	Heteroatom	2	2.9	(Cyclic scaffold)NH---H(vinyl)	
	Heteroatom	3	2.8	(Cyclic scaffold)7Cl---H(methyl)	
	H-Bond	4	4.0	(Side chain)NH---O=C(Propionic acid)	104.6
AQ2+	π - π	1	3.4	(Cyclic scaffold)C---C(Porphyrin)	
	π - π	1	3.5	(Cyclic scaffold)C---C(Porphyrin)	
	Heteroatom	2	1.8	(Cyclic scaffold)NH---H(Methyl)	
	Heteroatom	3	2.7	(Cyclic scaffold)7Cl---H(Vinyl)	
	H-bond*	6	2.3	(Side Chain)NH---O(Side chain-phenol)	115.1
QN1+	π - π	1	3.3	(Cyclic scaffold)C---N(Porphyrin)	
	π - π	1	3.5	(Cyclic scaffold)C---C(Porphyrin)	
	Heteroatom	2	3.3	(Cyclic scaffold)N---H(Methyl)	
	Heteroatom	3	3.1	(6-Methoxy)O---H(Vinyl)	
	Heteroatom	5	1.9	(Side chain)OH---H (Methyl)	
QN2+	π - π	1	3.4	(Cyclic scaffold)C---C(Porphyrin)	
	π - π	1	3.7	(Cyclic scaffold)C---C(Porphyrin)	
	Heteroatom	3	2.6	(6-Methoxy)O---H(Methyl)	
	H-bond	4	2.3	(Side chain)NH---O=C(Propionic acid)	141.6
	Heteroatom	5	2.3	(Side chain)OH---H (Methyl)	
QD1+	π - π	1	3.4	(Cyclic scaffold)C---N(Porphyrin)	
	π - π	1	3.7	(Cyclic scaffold)C---C(Porphyrin)	
	Heteroatom	2	2.7	(Cyclic scaffold)N---H(Methyl)	
	Heteroatom	5	2.5	(Side chain)NH---H(Methyl)	
QD2+	π - π	1	3.5	(Cyclic scaffold)C---C(Porphyrin)	
	π - π	1	3.3	(Cyclic scaffold)C---N(Porphyrin)	
	Heteroatom	2	2.4	(Cyclic scaffold)NH---H(Methyl)	
	Heteroatom	3	3.1	(6-Methoxy)O---H(Vinyl)	
	Heteroatom	5	2.7	(Side chain)OH---H (Methyl)	
QC2+	π - π	1	3.4	(Cyclic scaffold)C---N(Porphyrin)	
	π - π	1	3.7	(Cyclic scaffold)C---C(Porphyrin)	
	Heteroatom	2	1.8	(Cyclic scaffold)NH---H(Methyl)	
	Heteroatom	3	2.5	(Cyclic scaffold)6Cl---H(Methyl)	
	H-Bond	4	2.1	(Side chain)NH---O=C(Propionic acid)	170.5
PYR3+	π - π	1	3.6	(Cyclic scaffold)C---C(Porphyrin)	
	π - π	1	3.5	(Cyclic scaffold)C---C(Porphyrin)	
	Heteroatom	2	3.7	(Cyclic scaffold)5NH---H(Vinyl)	
	Heteroatom	3	3.1	(Cyclic scaffold)7Cl---H(Vinyl)	
	Heteroatom	3	3.7	(2-Methoxy)O---H(methyl)	
	H-Bond	4	2.1	(Side chain)NH---O=C(Propionate)	154.6
	H-Bond	4	2.0	(Side chain)NH---O=C(Propionic acid)	142.7
	H-Bond*	6	2.4	(Cyclic scaffold)1N---HN(Side chain)	107.2
Hf1+	π - π	1	3.6	(Cyclic scaffold)C---C(Porphyrin)	
	π - π	1	3.7	(Cyclic scaffold)C---C(Porphyrin)	
	Heteroatom	3	2.5	(Cyclic scaffold)1Cl---H(Vinyl)	
	Heteroatom	3	3.5	(Cyclic scaffold)F---C(Vinyl)	
	H-Bond	4	3.4	(side chain)NH---O=C(Propionic acid)	126.4
	H-Bond	5	1.7	(Side chain)OH---O=C(Propionic acid)	169.5
PPQ4+	π - π	1	3.8	(Cyclic scaffold)C---C(Porphyrin)	
	π - π	1	3.9	(Cyclic scaffold)C---C(Porphyrin)	
	Heteroatom	2	2.1	(Cyclic scaffold)NH---C(Vinyl)	149.4
	Heteroatom	3	2.8	(Cyclic scaffold)7Cl---H(Methyl)	
	Heteroatom	3	2.5	(Cyclic scaffold)7Cl---H(Methyl)	
	H-Bond	4	1.9	(Side chain)NH---O=C(Propionic acid)	168.0

*Intramolecular interaction

For simplicity, charges on relevant atoms have been omitted from descriptions

Table S8b Close contacts (< 4Å) determined for the adsorption of antimalarial drugs onto the (011) face of β -haematin.

Drug	Interaction	Type	Distance	Description [#]	Angle
CQ2+	π - π	1	3.7	(Cyclic scaffold)C---C(Porphyrin)	
	H-Bond	4a ^a	2.0	(Cyclic scaffold)NH---O=C(Propionate)	160.1
	H-Bond	4a	2.5	(Cyclic scaffold)NH---O(Propionate)	141.3
	H-Bond	4	2.2	(Side Chain)NH---O=C(Propionate)	174.8
AQ2+	π - π	1	3.9	(Cyclic scaffold)C---C(Porphyrin)	
	π - π	7	3.7	(Side chain benzene)C---C(Vinyl)	
	Heteroatom	2	3.0	(Cyclic scaffold)NH---H(Methyl)	
	Heteroatom	5	2.6	(Side chain-phenol)O---H(Methyl)	
QN1+	Heteroatom	5	3.3	(Side Chain)NH---H(Vinyl group)	
	π - π	1	3.7	(Cyclic scaffold)C---C(Porphyrin)	
	Heteroatom	2	3.7	(Cyclic scaffold)N---C(Vinyl)	
	Heteroatom	5	3.5	(6-Methoxy)O---H(Methyl)	
	H-Bond	5	2.5	(Side chain)OH---O(Propionic acid)	125.8
QN2+	H-Bond	5	2.3	(Side chain)OH---O=C(Propionic acid)	124.3
	π - π	1	3.5	(Cyclic scaffold)C---C(Vinyl)	
	π - π	1	3.7	(Cyclic scaffold)C---C(Porphyrin)	
	Heteroatom	2	3.3	(Cyclic scaffold)N---H(Methyl)	
	Heteroatom	5	3.5	(6-Methoxy)O---H(Methyl)	
QD1+	H-Bond	4	2.3	(Side chain)OH---O(Propionic acid)	123.8
	π - π	1	3.7	(Cyclic scaffold)C---C(Porphyrin)	
	Heteroatom	2	3.0	(Cyclic scaffold)N---H(Methyl)	
	Heteroatom	5	2.7	(Side chain)OH---H(Methyl)	
QD2+	π - π	1	3.7	(Cyclic scaffold)C---C(Porphyrin)	
	Heteroatom	2	3.0	(Cyclic scaffold)N---H(Methyl)	
	Heteroatom	5	2.7	(Side chain)OH---H(Methyl)	
QC2+	π - π	1	3.5	(Cyclic scaffold)C---C(Vinyl)	
	π - π	1	3.6	(Cyclic scaffold)C---C(Porphyrin)	
	H-Bond	4	3.5	(Side Chain)NH---O=C(Propionate)	120.0
PYR3+	H-Bond	4	3.5	(Side Chain)NH---O=C(Propionate)	
	π - π	1	3.4	(Cyclic scaffold)C---C(Porphyrin)	
	H-Bond*	6	2.4	(Side chain)NH---N(Cyclic scaffold)	109.2
	Heteroatom	2	3.7	(Cyclic scaffold)NH---H(Methyl)	
Hf1+	Heteroatom	5	3.2	(Side chain)NH---H(Methyl)	
	Heteroatom	3	3.2	(Cyclic scaffold)1Cl---H (Methyl)	
	Heteroatom	3	3.3	(Cyclic scaffold)3Cl---H(Vinyl)	
	Heteroatom	3	3.2	(Cyclic scaffold)F---H(Methyl)	
	H-Bond	4	1.7	(Alcohol)OH---O=C(Propionic acid)	172.4
PPQ4+	H-Bond	4	2.8	(Side chain)OH---O(Propionic acid)	132.2
	π - π	1	3.7	(Cyclic scaffold)N---C(Porphyrin)	
	π - π	1	3.3	(Cyclic scaffold)C---C(Vinyl)	
	Heteroatom	2	2.3	(Cyclic scaffold)NH---HC(Vinyl)	
	Heteroatom	2	2.8	(Cyclic scaffold)NH---C(Vinyl)	
	Heteroatom	3	3.7	(Cyclic scaffold)7Cl---H(Methyl)	
	Heteroatom	3	3.9	(Cyclic scaffold)7Cl---H(Methyl)	
	Heteroatom	5	2.4	(Side Chain)NH---H(Methyl)	

*Intramolecular interaction

[#] For simplicity, charges on relevant atoms have been omitted from descriptions

^a A variation of type 4 H-bond, where the interaction involves the scaffold NH rather than side chain NH/OH.

Table S8c Close contacts (< 4Å) determined for the adsorption of antimalarial drugs onto the (010) face of β -haematin.

Drug	Interaction	Type	Distance Å	Description	Angle
CQ2+	π - π	1	4.0	(cyclic scaffold)C---C(porphyrin)	
AQ2+	π - π	1	3.8	(cyclic scaffold)C-C(porphyrin)	
QN1+	π - π	1	3.9	(cyclic scaffold)C---C(Porphyrin)	
	Heteroatom	5	2.9	(Side chain)NH---H(Vinyl)	
QN2+	π - π	1	3.5	(Cyclic scaffold)C---C(Porphyrin)	158.8
	H-bond	4a	2.3	(Cyclic scaffold)NH---N(Porphyrin)	
QD1+	Heteroatom	5	3.4	(Side chain)NH---H(Vinyl)	
	π - π	1	3.9	(Cyclic scaffold)C---C(Porphyrin ring)	
QD2+	π - π	1	3.6	(Cyclic scaffold)C---C(Porphyrin ring)	
	Heteroatom	5	2.6	(Side chain)NH---H(Methyl)	
QC2+	π - π	1	3.6	(Cyclic scaffold)C-C(Porphyrin ring)	
PYR3+	π - π	1	4.0	(Cyclic scaffold)C-C(Porphyrin ring)	
	Heteroatom	5	2.6	(Side chain)NH---C(Methyl)	
Hf1+	π - π	1	3.9	(Cyclic scaffold)C-C(Porphyrin ring)	
	Heteroatom	5	3.0	(Side chain)NH---C(Vinyl)	
PPQ4+	π - π	1a ^a	3.9	(Cyclic scaffold)C---C(Vinyl)	
	π - π	1	3.1	(Cyclic scaffold)N-C(Porphyrin ring)	

*Intramolecular interaction

^a A variation of type 1 π - π stacking, where the interaction involves the drug scaffold and porphyrin vinyl group (rather than core).

Table S8d Close contacts (< 4Å) determined for the adsorption of antimalarial drugs onto the (100) face of β -haematin

Drug	Interaction	Type	Distance	Description [#]	Angle
CQ2+	π - π	1a	3.2	(Cyclic scaffold)C---H(Vinyl)	138.4
	H-bond	4a	2.3	(Cyclic scaffold)NH---O(Propionic acid)	
	Heteroatom	3	2.6	(Cyclic scaffold)7Cl---H(Methyl)	
	Heteroatom	5	3.9	(Side Chain)NH---H(Methyl)	
AQ2+	π - π	1	3.6	(Cyclic scaffold)C---C(Vinyl)	129.7
	H-Bond	4a	2.9	(Cyclic scaffold)NH---O(Propionic acid)	
	Heteroatom	3	2.7	(Cyclic scaffold)7Cl---H(Methyl)	
	H-bond*	6	2.7	(Side chain-phenol)O---HN(Side chain)	
QN1+	H-bond	4a	1.8	(Alcohol)OH---O(Propionic acid)	160.2
	Heteroatom	2	2.8	(Cyclic scaffold)N---H(methyl)	
	Heteroatom	5	2.7	(6-methoxy)O---H(Methyl)	
	Other	8	2.8	(Cyclic scaffold)C---H(methyl)	
QN2+	π - π	1	2.9	(Cyclic scaffold)C---C(Vinyl)	
	Heteroatom	2	2.9	(Cyclic scaffold)NH---H(Vinyl)	
QD1+	Heteroatom	2	3.0	(Cyclic scaffold)N---H(Methyl)	143.5
	Heteroatom	3	2.5	(6-Methoxy)O---H(Methyl)	
	H-Bond	4a	2.9	(Side chain)OH---O=C(Propionic acid)	
	Other	8	2.9	(Cyclic scaffold)C---H(Methyl)	
QD2+	π - π	1	3.2	(Cyclic scaffold)C---H(Vinyl)	
	Heteroatom	2	3.0	(Cyclic scaffold)NH---H(Vinyl)	
	Heteroatom	3	2.8	(6-Methoxy)O---H(Methyl)	
	Heteroatom	5	2.7	(Side chain)OH---H(Methyl)	
QC2+	π - π	1	3.3	(Cyclic scaffold)C---H(Vinyl)	
	π - π	1a	2.9	(Cyclic scaffold)N---H(Vinyl)	
	Heteroatom	3	2.8	(Cyclic scaffold)6Cl---H(Methyl)	
	Heteroatom	3	2.6	(2-Methoxy)O---H(Methyl)	
PYR3+	H-Bond*	4a	2.5	(Cyclic scaffold)N---HN(Side chain)	104.1
	Heteroatom	2	2.1	(Cyclic scaffold)NH---H(Methyl)	
	Heteroatom	5	3.1	(Side chain-phenol)O---H(Methyl)	
	Other	8	3.3	(Cyclic scaffold)C---O(Propionic acid)	
	Other	8	3.3	(Side chain)C---H(Methyl)	
Hf1+	π - π	1	2.5	(Cyclic scaffold)C---H(Vinyl)	147.8
	Heteroatom	3	2.8	(Cyclic scaffold)1Cl---H(Methyl)	
	Heteroatom	3	3.3	(Cyclic scaffold)3Cl---H(Methyl)	
	Heteroatom	3	2.4	(Cyclic scaffold)F---H(Methyl)	
	Heteroatom	3	2.5	(Cyclic scaffold)F---H(Vinyl)	
	H-Bond	4	2.0	(Side chain)OH---O=C(Propionic acid)	
PPQ4+	π - π	1	3.4	(Cyclic scaffold)C---H(Vinyl)	143.3
	H-Bond	4a	2.5	(Cyclic scaffold)NH---O=C(Propionic acid)	
	H-Bond	4a	2.5	(Cyclic scaffold)NH---O(Propionic acid)	
	H-Bond	4a	2.7	(Cyclic scaffold)NH---O(Propionic acid)	
	Heteroatom	3	3.9	(Cyclic scaffold)7Cl---H(Methyl)	
	Heteroatom	5	3.8	(Side Chain)N---H(Methyl)	
	Heteroatom	5	3.7	(Side Chain)N---H(Vinyl)	

*Intramolecular interaction

For simplicity, charges on relevant atoms have been omitted from descriptions

Table S9 pH-weighted adsorption energy values (kcal.mol⁻¹)* used to determine correlations between NP-40 β -haematin inhibitory activity and *in silico* adsorption.

Drug	β H (NP-40) IC ₅₀ / μ M	log(IC ₅₀)	E_{ads} 001	log (E_{ads} 001) [#]	E_{ads} 011	log (E_{ads} 011) [#]	E_{ads} 010	log (E_{ads} 010) [#]	E_{ads} 100	log (E_{ads} 100) [#]	Avg E_{ads}	log (Avg E_{ads}) [#]
CQ	15 \pm 1.0	1.2 \pm 0.034	-61.8	1.791	-53.3	1.727	-52.4	1.719	-42.0	1.623	-52.4	1.719
AQ	5.8 \pm 0.30	0.76 \pm 0.022	-68.9	1.838	-57.6	1.760	-57.4	1.759	-48.0	1.681	-58.0	1.763
QN	47 \pm 8.0	1.7 \pm 0.080	-61.2 [*]	1.787	-53.0 [*]	1.725	-54.3 [*]	1.735	-40.8 [*]	1.611	-52.3 [*]	1.719
QD	22 \pm 2.0	1.4 \pm 0.034	-61.0 [*]	1.785	-52.7 [*]	1.721	-50.2 [*]	1.701	-38.2 [*]	1.582	-50.5 [*]	1.704
QC	12 \pm 0.50	1.1 \pm 0.021	-82.2	1.915	-65.8	1.818	-61.3	1.788	-50.0	1.699	-64.8	1.812
PYR	3.3 \pm 0.60	0.23 \pm 0.054	-85.5 [*]	1.931	-71.5 [*]	1.854	-71.2 [*]	1.751	-57.5 [*]	1.760	-71.4 [*]	1.854
Hf	7.0 \pm 0.30	0.97 \pm 0.027	-70.3	1.847	-73.4	1.866	-56.4	1.852	-51.2	1.709	-62.8	1.798
PPQ	2.7 \pm 0.10	0.62 \pm 0.047	-79.7 [*]	1.902	-71.2 [*]	1.853	-75.4 [*]	1.877	-50.7 [*]	1.705	-69.3 [*]	1.840

* The adsorption energy values reported in **Table S4** were weighted based on the fractional abundance of different protic species at pH 4.8 (Table S3) and summed together in order to obtain a single adsorption value for each drug.

Log values are determined for the absolute values of E_{ads} .

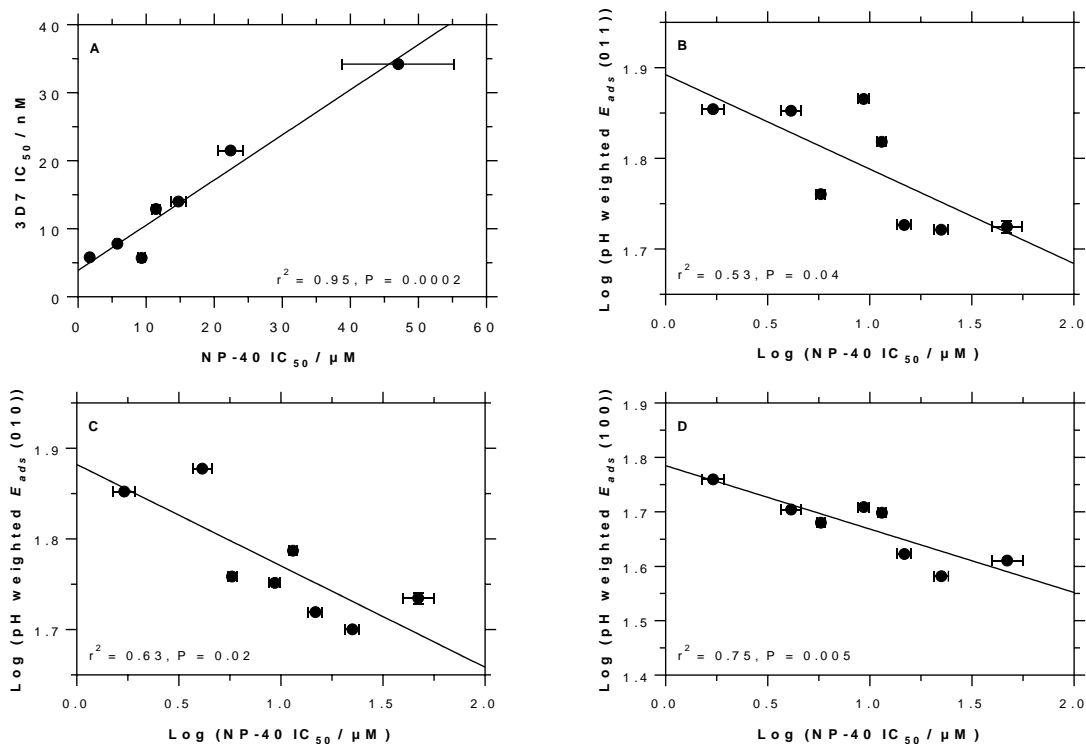


Figure S3 Relationship between *in silico* adsorption energy and β -haematin inhibitory activity. **A** Direct correlation observed between β -haematin inhibitory activity determined using the biomimetic NP-40 assay,^[4] and biological activity (3D7 strain).^[5] Linear correlations observed between the log of the NP-40 β -haematin inhibitory and **B** the log of the adsorption energy determined for the (011) crystal face ($r^2 = 0.53$, $P = 0.04$); **C** the log of the adsorption energy determined for the (010) crystal face ($r^2 = 0.63$, $P = 0.02$); **D** the log of the adsorption energy determined for the (100) crystal face ($r^2 = 0.75$, $P = 0.005$) The plotted data are reported in **Table S9** above.

Cyclic scaffolds

Table S10a Monocyclic scaffolds investigated using *in silico* Adsorption Locator protocol

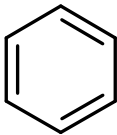
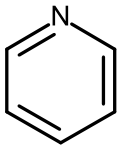
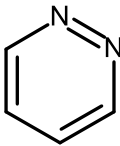
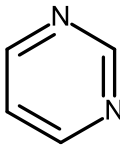
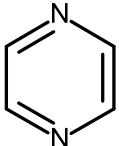
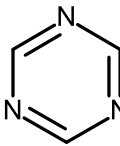
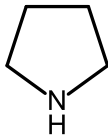
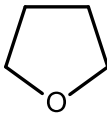
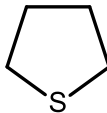
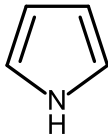
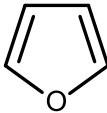
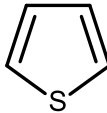
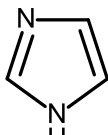
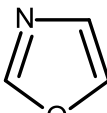
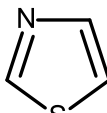
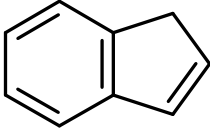
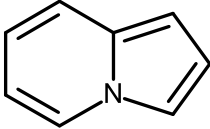
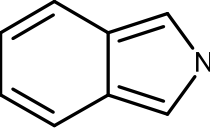
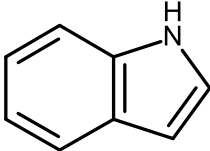
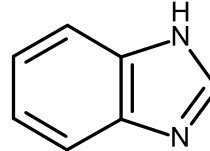
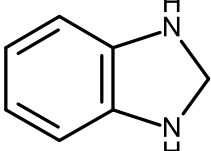
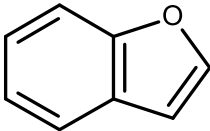
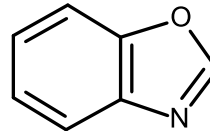
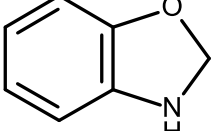
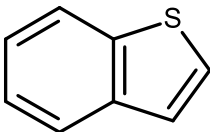
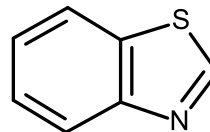
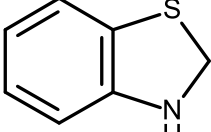
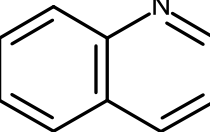
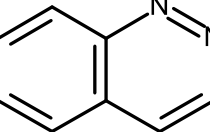
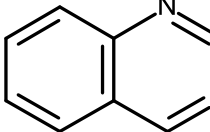
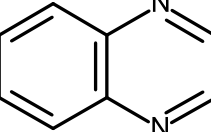
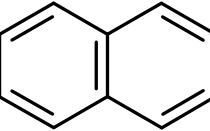
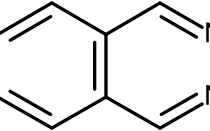
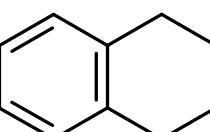
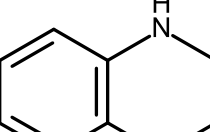
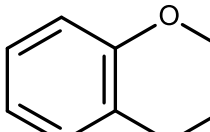
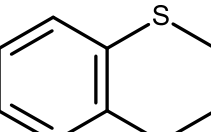
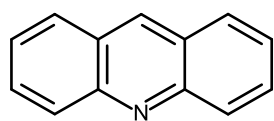
					
M1. Benzene					
					
M2. Pyridine	M3. Pyridazine	M4. Pyrimidine	M5. Pyrazine	M6. 1,3,5-triazine	
					
M7. Pyrrolidine	M8. Tetrahydrofuran	M9. Tetrahydrothiophene			
					
M10. Pyrrole	M11. Furan	M12. Thiophene			
					
M13. Imidazole	M14. Oxazole	M15. Thiazole			

Table S10b Bicyclic scaffolds investigated using *in silico* Adsorption Locator protocol

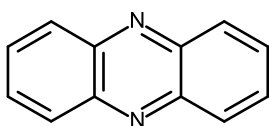
			
B1. 1H-indene	B2. indolizine	B3. 2H-isoindole	
			
	B4. Indole	B5. benzimidazole	B6. 2,3-dihydro-1H-benzimidazole
			
	B7. benzofuran	B8. 1,3-benzoxazole	B9. 2,3-dihydro-1,3-benzoxazole
			
	B10. benzothiophene	B11. 1,3-benzothiazole	B12. 2,3-dihydro-1,3-benzothiazole
			
B13. Quinoline[#]	B14. Cinnoline	B15. Quinazoline	B16. Quinoxaline
			
B17. Naphthalene	B18. Phthalazine		
			
B19. Tetralin	B20. 1,2,3,4-Tetrahydroquinoline	B21. Chromane	B22. Thiochromane

[#] This scaffold is present in a number of current antimalarial drugs: CQ, AQ, QN, QN and PPQ.

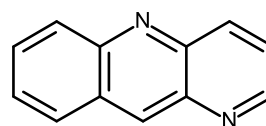
Table S10c Tricyclic scaffolds investigated using *in silico* Adsorption Locator protocol



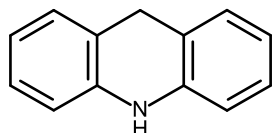
T1. **Acridine**[#]



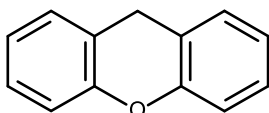
T2. Phenazine



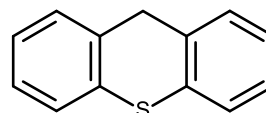
T3.
Benzo[b][1,5]naphthyridine[#]



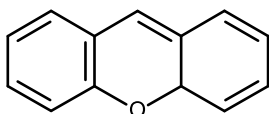
T4. 9,10-Dihydroacridine



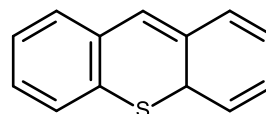
T5. 9H-Xanthene



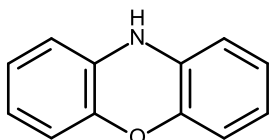
T6. 9H-Thioxanthene



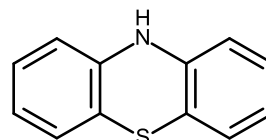
T7. 4aH-Xanthene



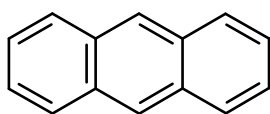
T8. 4aH-Thioxanthene



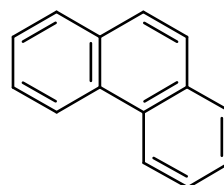
T9. Phenoxazine



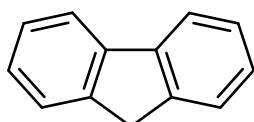
T10. **Phenothiazine**[#]



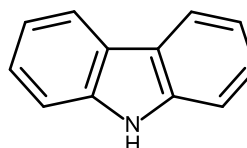
T11. Anthracene



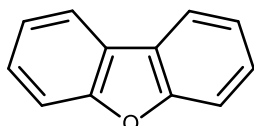
T12. **Phenanthrene**[#]



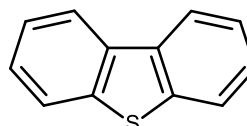
T13. **Fluorene**[#]



T14. Carbazole



T15. Dibenzofuran



T16. Dibenzothiophene

[#] This scaffold is present in current antimalarial drugs/compounds: T1 – QC; T3 – PYR; T10 – methylene blue; T12 – Hf; T13 – lumefantrine.

Table S10d Alphabetical reference list of scaffolds investigated

Scaffold	Code*
Acridine	T1
Acridine (9,10-dihydro-)	T4
Anthracene	T11
Benzene	M1
Benzimidazole	B5
benzimidazole (2,3-dihydro-1H-)	B6
Benzo[b][1,5]naphthyridine	T3
benzofuran	B7
Benzothiazole (1,3-)	B11
Benzothiazole (2,3-dihydro-1,3-)	B12
Benzothiophene	B10
Benzoxazole (1,3-)	B8
Benzoxazole (2,3-dihydro-1,3-)	B9
Carbazole	T14
Chromane	B21
Cinnoline	B14
Dibenzofuran	T15
Dibenzothiophene	T16
Fluorene	T13
Furan	M11
Imidazole	M13
Indene (1H-)	B1
Indole	B4
Indolizine	B2
Isoindole (2H-)	B3
Naphthalene	B17
Oxazole	M14
Phenanthrene	T12
Phenazine	T2
Phenothiazine	T10
Phenoxazine	T9
Phthalazine	B18
Pyrazine	M5
Pyridazine	M3
Pyridine	M2
Pyrimidine	M4
Pyrrole	M10
Pyrrolidine	M7
Quinazoline	B15
Quinoline	B13
Quinoxaline	B16
Tetrahydrofuran	M8
Tetrahydroquinoline (1,2,3,4-)	B20

Tetrahydrothiophene	M9
Tetralin	B19
Thiazole	M15
Thiochromane	B22
Thiophene	M12
Thioxanthene (4aH-)	T8
Thioxanthene (9H-)	T6
Triazine (1,3,5-)	M6
Xanthene (4aH-)	T7
Xanthene (9H-)	T5

* The code relates to the monocyclic (M), bicyclic (B) and tricyclic (T) structures in Tables S3a, S3b and S3c, respectively.

Table S11 Predicted pK_a values^[3] and relative abundances of different protic forms of the scaffolds at pH 4.8

Scaffold	Scaffold Code	Predicted pK_a	Protonation state	%
Benzene	M1	na	0	100
Pyridine	M2	5.12	0	32
Pyridine	M2	-	1+	68
Pyridazine	M3	2.52	0	99
Pyrimidine	M4	1.58	0	100
Pyrazine	M5	0.88/ -1.52	0	100
1,3,5-triazine	M6	-1.18	0	100
pyrrolidine	M7	11.4	1+	100
tetrahydrofuran	M8	na	0	100
tetrahydrothiophene	M9	na	0	100
Pyrrole	M10	na	0	100
Furan	M11	na	0	100
thiophene	M12	na	0	100
imidazole	M13	6.97	1+	99
Oxazole	M14	0.63	0	100
Thiazole	M15	2.89	0	99
1H-indene	B1	na	0	100
Indolizine	B2	na	0	100
2H-isoindole	B3	na	0	100
Indole	B4	na	0	100
benzimidazole	B5	5.79	0	9 [#]
2,3-dihydro-1H-benzimidazole	B6	1.22; 3.47	0	96
2,3-dihydro-1H-benzimidazole	B6	-	1+	4
Benzofuran	B7	na	0	100
1,3-benzoxazole	B8	0.18	0	100
2,3-dihydro-1,3-benzoxazole	B9	1.47	0	100
benzothiophene	B10	na	0	100
1,3-benzthiazole	B11	2.28	0	100
2,3-dihydro-1,3-benzothiazole	B12	2.37	0	100
Quinoline	B13	4.5	0	66
Quinoline	B13	-	1+	34
Cinnoline	B14	3.07	0	98
Cinnoline	B14	-	1+	2
Quinazoline	B15	2.19	0	100
Quinoxaline	B16	-1.95; 1.86	0	100
Napthalene	B17	na	0	100
Phthalazine	B18	2.89	0	98
Phthalazine	B18	-	1+	2
Tetralin	B19	na	0	100
1,2,3,4-tetrahydroquinoline	B20	4.93	0	42
1,2,3,4-tetrahydroquinoline	B20	-	1+	58
Chromane	B21	na	0	100
thiochromane	B22	na	0	100

Table continues on next page

Acridine	T1	6.15	0	4
Acridine	T1	-	1+	96
Phenazine	T2	2.7	0	99
benzo[b][1,5]naphthyridine	T3	-1.19; 3.48	0	95
benzo[b][1,5]naphthyridine	T3	-	1+ (=NH, ring 2)	4
9,10-dihydroacridine	T4	-0.03	0	100
9H-xanthene	T5	na	0	100
9H-thioxanthene	T6	na	0	100
4aH-xanthene	T7	na	0	100
4aH-thoixanthene	T8	na	0	100
Phenoxazine	T9	-0.66	0	100
Phenothiozine	T10	-0.95	0	100
Anthracene	T11	na	0	100
Phenanthrene	T12	na	0	100
Fluorene	T13	na	0	100
Carbazole	T14		0	100
Dibenzofuran	T15	na	0	100
Dibenzothiophene	T16	na	0	100

Materials Studio repeatedly gave an error for calculations of the major species (91 %) benzimidazole

1+

Table S12a Monocyclic scaffolds: Calculated adsorption energies ($E_{ads}/\text{kcal.mol}^{-1}$) and size-independent ligand efficiency (SILE)^[6] values determined on the (001), (011), (010) and (100) faces of β -hematin.

Scaffold	#non-H	MW	E_{ads} (001)	SILE	Rank	E_{ads} (011)	SILE	Rank	E_{ads} (010)	SILE	Rank	E_{ads} (100)	SILE	Rank	Average	SILE	Rank
M1	6	78.1	-31.1	-18.2	47	-19.6	-11.4	55	-23.9	-14.0	48	-14.5	-8.5	58	-22.3	-13.0	54
M2	6	79.1	-31.3	-18.3	44	-21.5	-12.6	50	-24.2	-14.1	46	-17.2	-10.0	52	-23.6	-13.8	47
M2(1+)	6	80.1	-31.0	-18.1	49	-20.0	-11.7	54	-23.8	-13.9	49	-15.4	-9.0	54	-22.5	-13.2	53
M3	6	80.1	-31.2	-18.2	45	-22.3	-13.0	45	-24.4	-14.3	45	-17.9	-10.5	47	-24.0	-14.0	45
M4	6	80.1	-31.0	-18.1	50	-21.7	-12.7	49	-24	-14.0	47	-17.4	-10.2	50	-23.5	-13.7	48
M5	6	80.1	-31.4	-18.3	43	-22.5	-13.2	44	-20.8	-12.2	58	-18.2	-10.6	46	-23.2	-13.6	49
M6	6	81.1	-29.6	-17.3	56	-19.2	-11.2	56	-23.1	-13.5	53	-15.0	-8.8	56	-21.7	-12.7	57
M7(1+)	5	71.1	-13.2	-8.1	61	-14.0	-8.6	61	-22.5	-13.9	50	-11.0	-6.8	61	-15.2	-9.4	61
M8	5	72.1	-20.0	-12.4	59	-19.9	-12.3	52	-15.7	-9.7	61	-14.0	-8.6	57	-17.4	-10.7	59
M9	5	88.2	-19.4	-12.0	60	-18.0	-11.1	57	-17.4	-10.7	59	-13.1	-8.1	60	-16.9	-10.5	60
M10	5	67.1	-28.7	-17.7	55	-17.7	-10.9	60	-15.8	-9.7	60	-14.3	-8.8	55	-19.1	-11.8	58
M11	5	68.1	-28.9	-17.8	52	-20.2	-12.5	51	-21.6	-13.3	54	-16.7	-10.3	49	-21.8	-13.5	50
M12	5	84.1	-29.5	-18.2	46	-19.2	-11.8	53	-21.6	-13.3	54	-16.9	-10.4	48	-21.8	-13.5	51
M13(1+)	5	68.1	-27.7	-17.1	57	-17.8	-11.0	59	-22	-13.6	52	-15.2	-9.4	53	-20.7	-12.8	56
M14	5	69.1	-29.2	-18.0	51	-21.9	-13.5	40	-21.1	-13.0	56	-17.6	-10.9	43	-22.5	-13.9	46
M15	5	85.1	-28.9	-17.8	53	-20.8	-12.8	48	-20.9	-12.9	57	-16.4	-10.1	51	-21.7	-13.4	52

* Scaffolds in bold are present in clinically-relevant antimalarial drugs. Colour scale (conditional formatting): **red** – worst adsorbers; **green** – best adsorbers

Table S12b Bicyclic scaffolds: Calculated adsorption energies ($E_{ads}/\text{kcal.mol}^{-1}$) and size-independent ligand efficiency (SILE) values determined on the (001), (011), (010) and (100) faces of β -hematin.

Scaffold	#non-H	MW	E_{ads} (001)	SILE	Rank	E_{ads} (011)	SILE	Rank	E_{ads} (010)	SILE	Rank	E_{ads} (100)	SILE	Rank	Average	SILE	Rank
B1	9	116.2	-35.1	-18.1	48	-21.4	-11.1	58	-26.3	-13.6	51	-16.2	-8.4	59	-24.7	-12.8	55
B2	9	117.2	-42.8	-22.1	20	-27.1	-14.0	30	-32.7	-16.9	22	-22.5	-11.7	29	-31.3	-16.2	25
B3	9	117.2	-41.2	-21.3	30	-27.0	-14.0	31	-31.1	-16.1	33	-21.3	-11.0	40	-30.1	-15.6	35
B4	9	117.2	-42.1	-21.8	25	-25.5	-13.2	43	-31.6	-16.3	30	-21.5	-11.1	39	-30.2	-15.6	33
B5	9	118.1	-42.2	-21.8	24	-26.2	-13.5	39	-30.8	-15.9	34	-22.0	-11.4	36	-30.3	-15.7	32
B6	9	120.1	-39.6	-20.5	34	-25.6	-13.2	42	-29.7	-15.4	42	-20.8	-10.8	45	-28.9	-15.0	40
B6(1+)	9	121.1	-39.9	-20.7	33	-26.5	-13.7	34	-29.8	-15.4	40	-21.0	-10.9	42	-29.3	-15.2	36
B7	9	118.1	-42.6	-22.0	22	-27.5	-14.2	29	-31.4	-16.2	31	-22.9	-11.8	28	-31.1	-16.1	26
B8	9	119.1	-42.7	-22.1	21	-26.4	-13.6	36	-31.3	-16.2	32	-22.1	-11.4	35	-30.6	-15.8	31
B9	9	121.1	-39.5	-20.4	35	-25.1	-13.0	47	-30	-15.5	39	-22.3	-11.5	31	-29.2	-15.1	37
B10	9	134.2	-41.8	-21.6	27	-27.9	-14.4	27	-31.8	-16.4	29	-22.9	-11.9	27	-31.1	-16.1	27
B11	9	135.2	-42.3	-21.9	23	-27.6	-14.3	28	-30.6	-15.8	35	-22.3	-11.5	32	-30.7	-15.9	30
B12	9	137.2	-38.2	-19.7	37	-26.2	-13.5	38	-29.1	-15.1	44	-21.2	-11.0	41	-28.7	-14.8	43
B13	10	129.2	-45.4	-22.8	14	-29.5	-14.8	23	-34	-17.0	19	-24.0	-12.0	23	-33.2	-16.7	17
B13(1+)	10	130.2	-45.2	-22.7	15	-29.2	-14.6	24	-33.7	-16.9	23	-24.0	-12.0	24	-33.0	-16.5	19
B14	10	130.2	-44.9	-22.5	16	-30.4	-15.2	18	-34.1	-17.1	18	-24.3	-12.2	19	-33.4	-16.8	16
B14(1+)	10	131.2	-44.6	-22.4	17	-28.8	-14.4	26	-33.8	-16.9	21	-24.1	-12.1	22	-32.8	-16.4	20
B15	10	130.2	-44.6	-22.3	18	-30.2	-15.1	19	-33.7	-16.9	23	-24.2	-12.1	20	-33.2	-16.6	18
B16	10	130.2	-45.5	-22.8	13	-27.7	-13.9	32	-33.2	-16.6	27	-23.8	-11.9	25	-32.6	-16.3	22
B17	10	128.2	-42.2	-21.2	31	-29.1	-14.6	25	-33.7	-16.9	23	-23.2	-11.6	30	-32.1	-16.1	29
B18	10	130.2	-43.0	-21.6	29	-30.7	-15.4	15	-33.3	-16.7	26	-24.2	-12.1	21	-32.8	-16.4	21
B18(1+)	10	131.2	-43.3	-21.7	26	-30.1	-15.1	20	-33	-16.5	28	-23.7	-11.9	26	-32.5	-16.3	23
B19	10	134.2	-35.4	-17.8	54	-26.0	-13.0	46	-30.5	-15.3	43	-21.5	-10.8	44	-28.3	-14.2	44
B20	10	133.2	-38.5	-19.3	39	-27.0	-13.6	37	-31.3	-15.7	37	-22.5	-11.3	38	-29.8	-14.9	41
B20(1+)	10	134.2	-37.4	-18.8	41	-27.3	-13.7	35	-31.5	-15.8	36	-22.6	-11.3	37	-29.7	-14.9	42
B21	10	134.2	-40.1	-20.1	36	-26.8	-13.4	41	-30.7	-15.4	41	-23.0	-11.5	33	-30.1	-15.1	39
B22	10	150.2	-39.3	-19.7	38	-27.5	-13.8	33	-31	-15.5	38	-22.9	-11.5	34	-30.2	-15.1	38

Table S12c Tricyclic scaffolds: Calculated adsorption energies ($E_{ads}/\text{kcal.mol}^{-1}$) and size-independent ligand efficiency (SILE) values determined on the (001), (011), (010) and (100) faces of β -hematin.

Scaffold	#non-H	MW	E_{ads} (001)	SILE	Rank	E_{ads} (011)	SILE	Rank	E_{ads} (010)	SILE	Rank	E_{ads} (100)	SILE	Rank	Average	SILE	Rank
T1	14	179.1	-54.3	-24.6	6	-35.7	-16.2	7	-40.4	-18.3	4	-30.5	-13.8	4	-40.2	-18.2	4
T1(1+)	14	180.2	-53.5	-24.3	10	-37.3	-16.9	1	-40.2	-18.2	5	-29.4	-13.3	13	-40.1	-18.2	6
T2	14	180.2	-47.6	-21.6	28	-33.9	-15.4	16	-39.1	-17.7	10	-29.3	-13.3	14	-37.5	-17.0	15
T3	14	180.2	-53.5	-24.2	11	-35.3	-16.0	9	-40.8	-18.5	3	-30.6	-13.9	3	-40.0	-18.1	7
T3(1+)	14	181.2	-58.1	-26.3	1	-37.1	-16.8	2	-41	-18.6	2	-30.1	-13.7	9	-41.6	-18.8	1
T4	14	181.2	-48.9	-22.1	19	-34.6	-15.7	13	-38.8	-17.6	13	-28.9	-13.1	16	-37.8	-17.1	13
T5	14	182.2	-40.6	-18.4	42	-32.7	-14.8	22	-38.4	-17.4	16	-30.2	-13.7	7	-35.5	-16.1	28
T6	14	198.2	-37.4	-17.0	58	-32.9	-14.9	21	-37.6	-17.0	20	-29.8	-13.5	10	-34.4	-15.6	34
T7	14	181.2	-52.9	-24.0	12	-36.0	-16.3	6	-39.6	-17.9	7	-31.5	-14.3	1	-40.0	-18.1	8
T8	14	197.2	-46.2	-20.9	32	-35.7	-16.2	8	-38.7	-17.5	14	-30.3	-13.7	5	-37.7	-17.1	14
T9	14	183.2	-55.2	-25.0	3	-36.4	-16.5	4	-39.5	-17.9	8	-30.2	-13.7	8	-40.3	-18.3	3
T10	14	199.3	-41.7	-18.9	40	-33.8	-15.3	17	-38.1	-17.3	17	-29.5	-13.4	12	-35.8	-16.2	24
T11	14	178.2	-54.3	-24.6	7	-35.2	-15.9	11	-40.2	-18.2	5	-29.1	-13.2	15	-39.7	-18.0	10
T12	14	178.2	-55.4	-25.1	2	-35.2	-16.0	10	-41.7	-18.9	1	-29.6	-13.4	11	-40.5	-18.3	2
T13	13	166.2	-53.9	-25.0	4	-33.4	-15.5	14	-38.6	-17.9	9	-27.2	-12.6	18	-38.3	-17.7	12
T14	13	167.2	-52.7	-24.4	8	-34.4	-15.9	12	-38.1	-17.6	12	-28.0	-13.0	17	-38.3	-17.7	11
T15	13	168.2	-52.7	-24.4	9	-35.4	-16.4	5	-37.7	-17.5	15	-29.9	-13.9	2	-38.9	-18.0	9
T16	13	184.2	-53.7	-24.9	5	-35.8	-16.6	3	-38.2	-17.7	11	-29.6	-13.7	6	-39.3	-18.2	5

* Scaffolds in bold are present in clinically-relevant antimalarial drugs. Colour scale (conditional formatting): **red** – worst adsorbers; **green** – best adsorbers

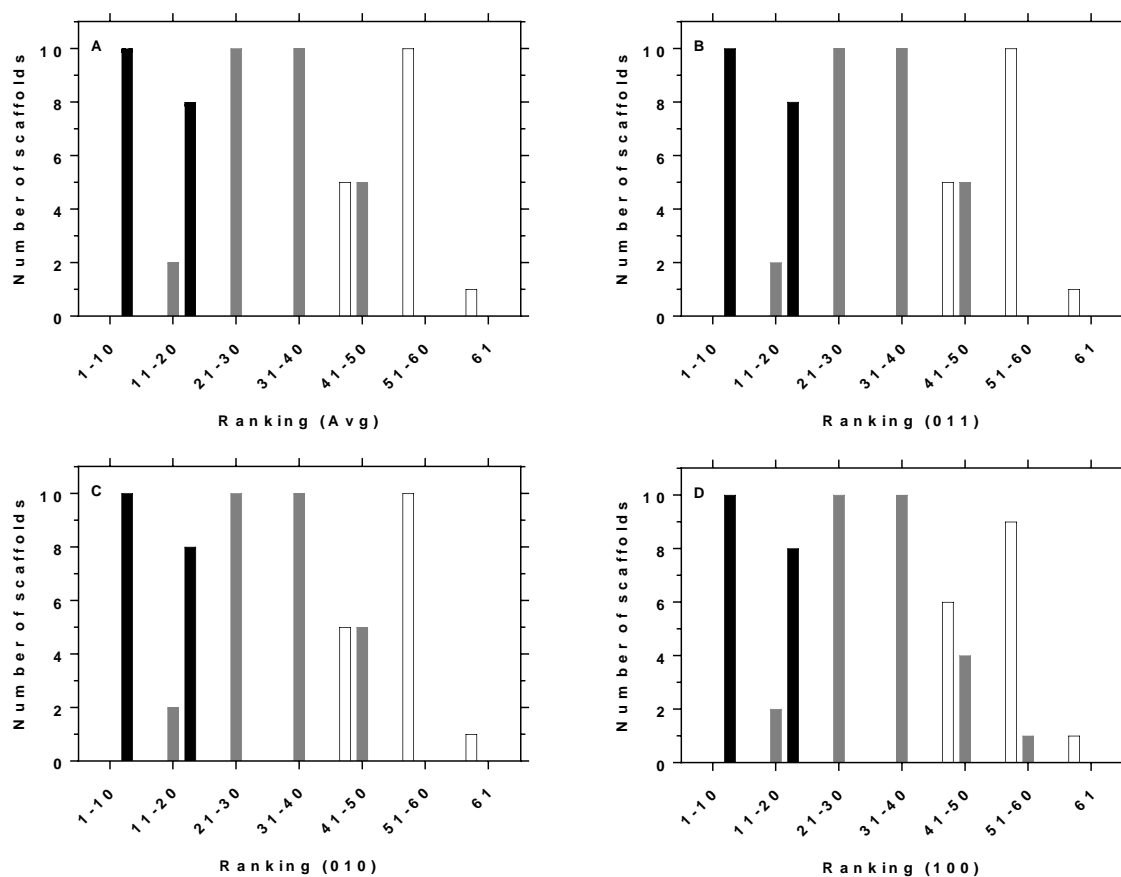


Figure S4 Adsorption of diverse scaffolds to β -hematin. Ranking of adsorption energies ($E_{ads}/\text{kcal.mol}^{-1}$) determined for 61 scaffolds (including neutral and protonated forms) on **A** average (for all four faces), **B** the (011) face, **C** the (010) face, and **D** the (100) face. The bars indicate the number of monocyclic (white), bicyclic (grey) and tricyclic (black) scaffolds in each group of 10. In total, 16 monocyclic, 27 bicyclic and 18 tricyclic scaffolds were considered.

2. Crystallographic data

Table S13 Crystallographic data for **P2b** hydrochloric salt, the covalent dimer of **P2b**, Boc-2, and **P3b** hydrochloride salt.

Species	P2b.HCl	P2b dimer.Cl.EtOH	Boc-2	P3b.HCl
Empirical Formula	C ₁₈ H ₂₁ ClN ₂ O	C ₃₈ H ₄₅ ClN ₄ O ₃	C ₁₇ H ₁₆ BrNO ₃	C ₁₈ H ₂₁ ClN ₂ O
Formula Weight	316.82	641.23	362.22	316.82
Crystal system	monoclinic	monoclinic	monoclinic	orthorhombic
Space group	<i>P2₁/c</i>	<i>P2₁/c</i>	<i>P2₁/n</i>	<i>Pbca</i>
Unit cell dimensions (Å, °)	<i>a</i> = 7.9536(6) <i>b</i> = 9.0593(7) <i>c</i> = 21.9251(16) α = 90 β = 95.4090(10) γ = 90	<i>a</i> = 9.9539(8) <i>b</i> = 30.6429(17) <i>c</i> = 11.8376(7) α = 90 β = 108.973(2) γ = 90	<i>a</i> = 6.9135(2) <i>b</i> = 13.6017(4) <i>c</i> = 16.5814(5) α = 90 β = 94.048(1) γ = 90	<i>a</i> = 16.028(5) <i>b</i> = 7.734(3) <i>c</i> = 25.561(9) α = 90 β = 90 γ = 90
Volume (Å ³)	1572.8(2)	3414.5(3)	1555.53 (8)	3168.7(19)
Z	4	4	4	8
Calculated density (g cm ⁻³)	1.338	1.247	1.547	1.328
Absorption coefficient (mm ⁻¹)	0.247	0.155	2.655	0.245
<i>F</i> ₀₀₀	672	1368	736.00	1344
Crystal size (mm ³)	0.178 × 0.114 × 0.056	0.288 × 0.218 × 0.149	0.285 × 0.110 × 0.085	0.163 × 0.072 × 0.044
θ range for data collection (°)	1.866 to 28.311	1.937 to 26.391	1.938 to 28.305	1.593 to 27.149
Miller index ranges	-10 > <i>h</i> < 10, -12 > <i>k</i> < 12, -29 > <i>l</i> < 29	-12 > <i>h</i> < 12, -38 > <i>k</i> < 38, -14 > <i>l</i> < 14	-9 > <i>h</i> < 9, -18 > <i>k</i> < 18, -22 > <i>l</i> < 22	-20 < <i>h</i> < 20, -9 < <i>k</i> < 9, -32 < <i>l</i> < 32
Reflections collect	42897	129944	49363	64811
Independent reflections	3902 [<i>R</i> _{int} = 0.0405]	6995 [<i>R</i> _{int} = 0.1554]	3874 [<i>R</i> _{int} = 0.0263]	3499 [<i>R</i> _{int} = 0.1198]
Completeness to θ_{\max} (%)	0.997	0.998	0.999	0.997
Data / restraints / parameters	3902 / 0 / 211	6995 / 1 / 440	3874 / 1 / 212	3499 / 0 / 211
Goodness-of-fit on <i>F</i> ²	1.065	1.094	1.045	1.031
Final <i>R</i> indices [<i>I</i> > 2 σ (<i>I</i>)]	<i>R</i> ₁ = 0.0339, <i>wR</i> ₂ = 0.0869	<i>R</i> ₁ = 0.0338, <i>wR</i> ₂ = 0.0877	<i>R</i> ₁ = 0.0277, <i>wR</i> ₂ = 0.0663	<i>R</i> ₁ = 0.0434, <i>wR</i> ₂ = 0.0916
<i>R</i> indices (all data)	<i>R</i> ₁ = 0.0390, <i>wR</i> ₂ = 0.0902	<i>R</i> ₁ = 0.0489, <i>wR</i> ₂ = 0.0933	<i>R</i> ₁ = 0.0311, <i>wR</i> ₂ = 0.0678	<i>R</i> ₁ = 0.0713, <i>wR</i> ₂ = 0.105

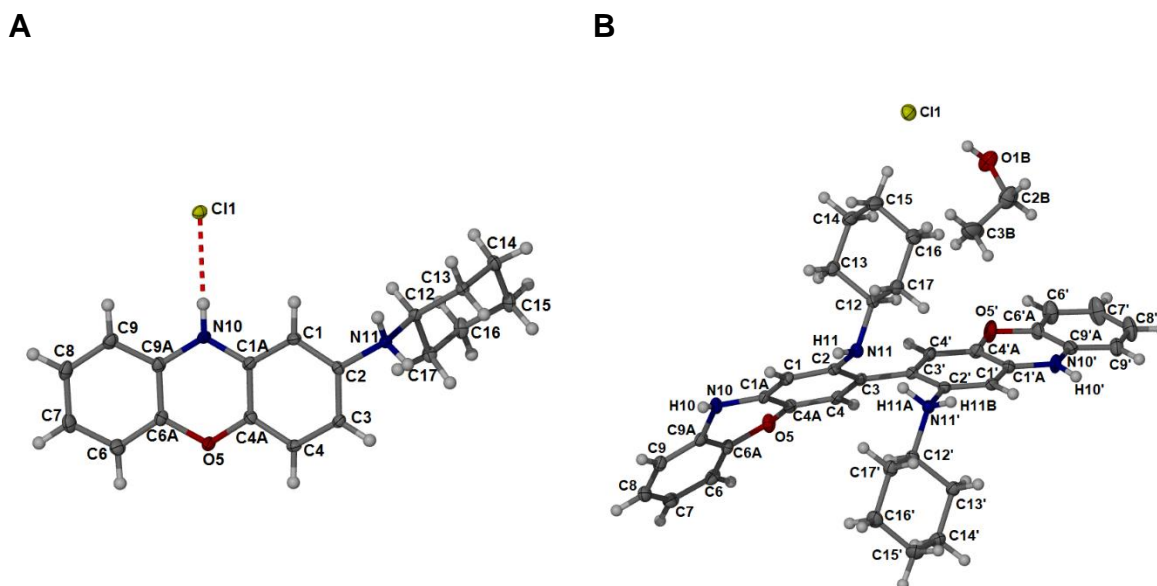


Figure S5 Single crystal X-ray diffraction structures of **P2b**. **A** The compound was isolated as a hydrochloride salt, and the structure of **P2b.HCl** confirms protonation of the side chain N-atom. CCDC deposition number: 2155681. **B** The main impurity in the synthesis of the 2-substituted amino-phenoxazine compounds was found to be a dimer formed via covalent bonding between C3 and C3'. CCDC deposition number: 2155683.

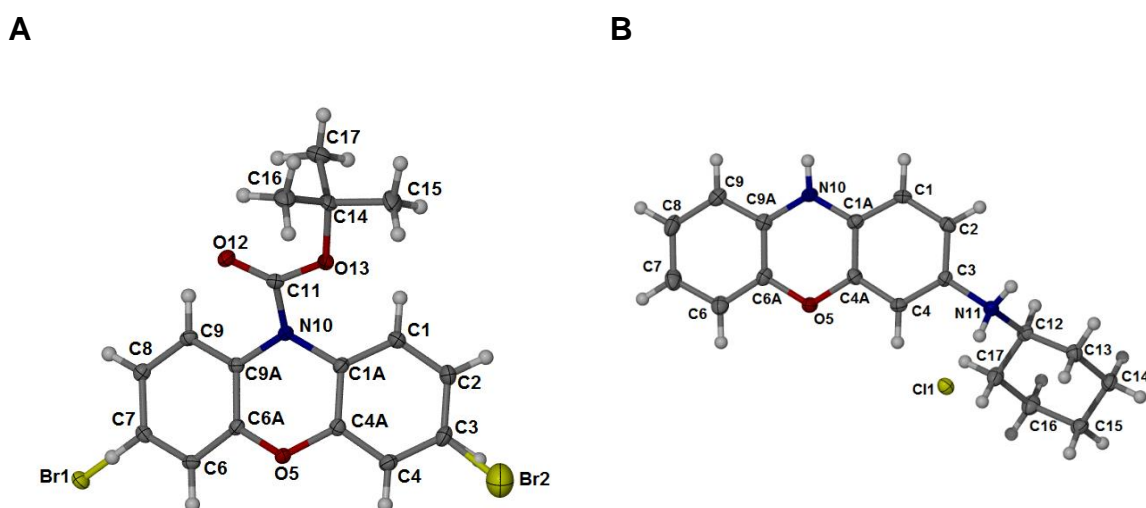
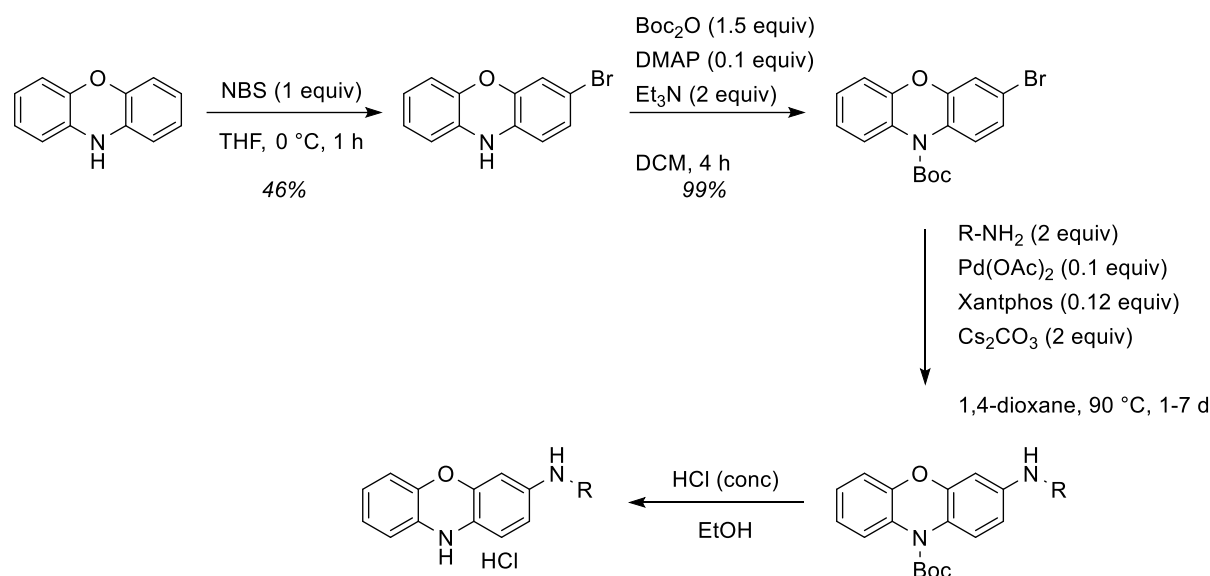


Figure S6 Single crystal X-ray diffraction structure of **A** *tert*-butyl 3-bromo-10H-phenoxazine-10-carboxylate (Boc-2). The partial occupancies for the two bromine atoms (Br1, 95% and Br2, 5%) confirm the presence of a mono-brominated species. CCDC deposition number: 2155682; **B** the hydrochloride salt of **P3b**. The structure confirms protonation of the side chain N-atom. CCDC deposition number: 2155684.

3. Synthetic details

Synthesis of 3-substituted phenoxazines

The 3-substituted phenoxazines were synthesised first owing to their shorter synthetic route from known 3-bromophenoxazine (**Scheme S3.1**).



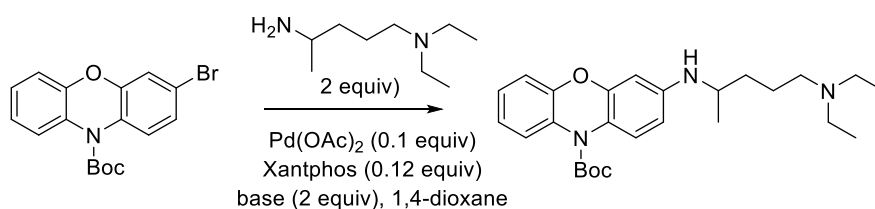
Scheme S3.1 General synthetic procedure for the synthesis of 3-substituted phenoxazines

The synthesis of 3-bromophenoxazine (**2**) has been reported previously.^[7] In our hands though it was found that an important factor was the elimination of light from the reaction, otherwise the starting material and product decomposed, and the yields were dramatically reduced. We also found that DCM or DMF were unsuitable as solvents and did not give any of the desired product. The *tert*-butyloxycarbonyl (Boc) protecting group was then introduced under conventional conditions in essentially quantitative yields. It should be noted that we did investigate a *p*-toluene sulfonate (tosylate) protecting group but found that this was incompatible with the subsequent amination reaction, returning material that was very difficult to purify. A crystal structure of Boc-protected 3-bromophenoxazine **2** was obtained, details of which can be found in **Table S13** and **Figure S6** in section 2 above.

The amination procedure began by applying a representative procedure reported by Kawatsura and co-workers,^[8] which employed Pd(OAc)₂ as the catalyst, Xantphos as the ligand and NaO^tBu as the base in 1,4-dioxane as a solvent at 100 °C. These

conditions however returned no obvious major product, but rather a slew of more than eleven compounds as well as consuming all the starting material (**Table S3.1**, entry 1). We eliminated the possibility that the Boc-group was falling off at the high temperatures with a control experiment, so our attention turned to the base. Fortunately changing the base to caesium carbonate (Cs_2CO_3) gave a small amount of product with none of the degradation we had previously observed being seen on TLC. This strongly suggested that the NaO^tBu was having a deleterious effect on our substrate. Nevertheless, the Cs_2CO_3 did slow the reaction down dramatically, and after some fine-tuning (**Table S3.1**, entries 3-6) we managed to get reasonable yields albeit after a 7 day reaction.

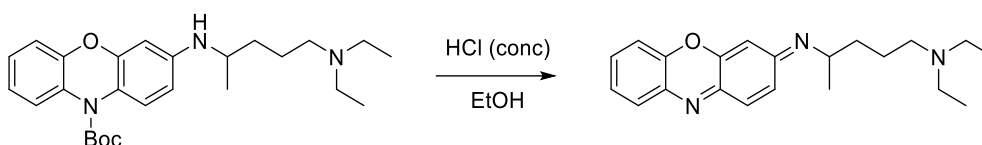
Table S3.1 Optimisation of amination reaction with 3-bromophenoxazine **2**



Entry	Base	Time (h)	Temp (°C)	Product (%) (SM %)
1	NaO^tBu	18	100	- (0) ^a
2	Cs_2CO_3	18	100	12 (62)
3	Cs_2CO_3	24	100	20 (60)
4	Cs_2CO_3	48	80	44 (21)
5	Cs_2CO_3	60	80	45 (22)
6	Cs_2CO_3	168	90	60-66 (1) ^b

^a more than 11 products detected on TLC; ^b range based on 4 reactions.

The deprotection of the Boc-group was then investigated, where it became clear that the product was unstable and rapidly decomposed. Although Boc-deprotections have been reported in pure water at high temperatures,^[9] this did not work effectively in our hands. However, the addition of conc. HCl quickly furnished a product in moderate yields. After analysis though, it became clear that the product isolated was the oxidised form **P3a'** (**Scheme S3.2** and main text for more details).

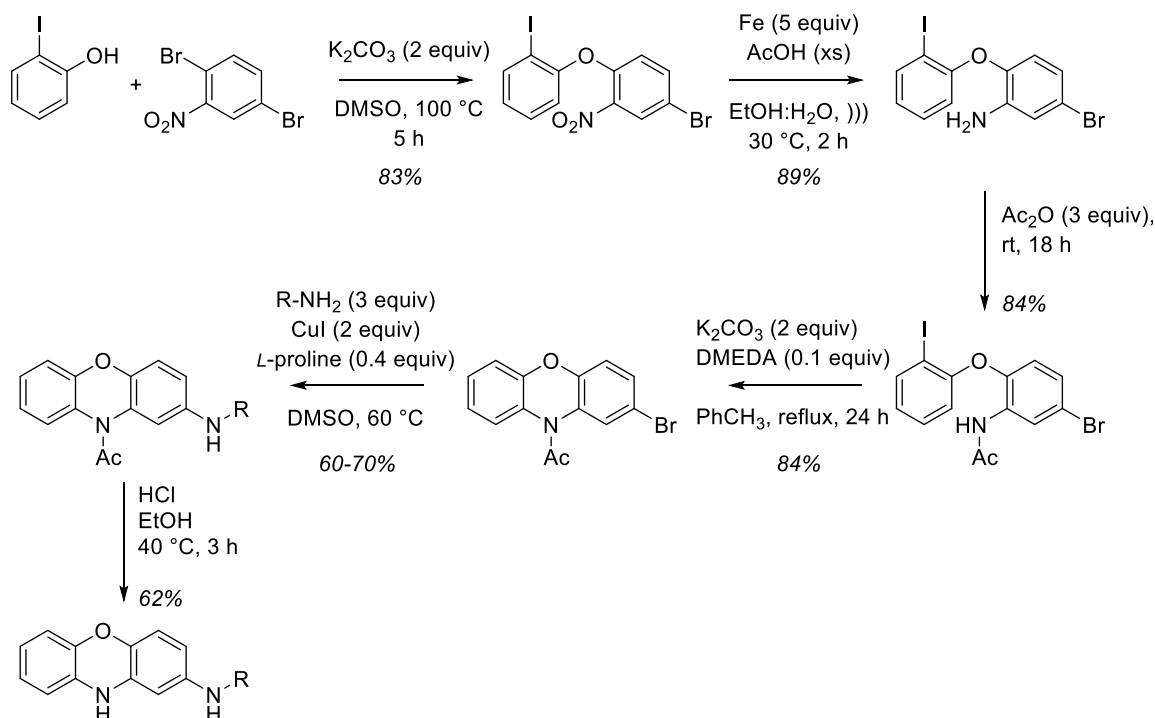


Scheme S3.2 Formation of the oxidised phenoxazine **P3a'** on deprotection of the Boc-group.

In the case of the cyclohexyl derivative (**P3b**), the Ullmann coupling gave a low yield (23%), which was not further optimised, whilst the deprotection under acidic conditions gave the 3-cyclohexylamino-phenoxazine **P3b** and not the oxidised form observed with the chloroquine sidechain. A crystal structure of the hydrochloride salt of **P3b** was obtained (see **Table S13** and **Figure S6** above). Nevertheless, purity above 95% could never be conclusively determined (see main text for details).

Synthesis of 2-substituted phenoxazines

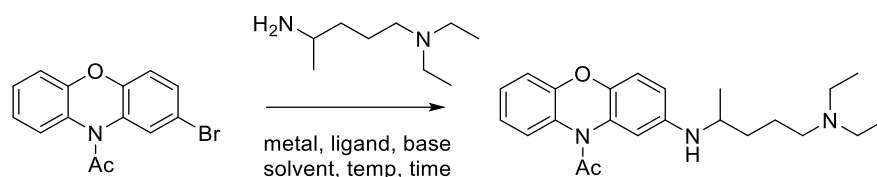
A synthesis reported by Thomé and Bolm provided the basic framework for obtaining the required 2-bromo phenoxazine intermediate **1** (**Scheme S3.3**).^[10]



Scheme S3.3 General synthetic procedure for the synthesis of 2-substituted phenoxazines.

The first modification of the reported procedure was to use the cheaper dibromo derivative for the S_NAr reaction. Thomé and Bolm employed a fluoro derivative,^[10] but in our hands the additional expense did not warrant the very minor reduction in yield that we obtained. Thomé and Bolm also reported a classical $SnCl_2$ reduction of the nitro group, but in our hands the yields ended up varying between 35-87%. By changing the procedure to one reported by Keller,^[11] using iron powder under ultrasonic conditions, we found a reproducible method with consistently high yields. The following two steps were followed as per the published procedures. Whilst the original paper did not delve into the necessity of the acetyl group, we examined this and found that the ring-closing reaction essentially failed without the acetyl group. Nevertheless, the acetyl group was needed for the subsequent step, so this was not a problem.

As with the 3-substituted phenoxazines, the aryl amination reactions to form the 2-substituted phenoxazines required some optimisation before a suitable method could be found. The details of the experiments that were tried can be found in **Table S3.2**. Entries 1-11 all resulted in >10 products being seen on TLC, with no discernible major product. Varying the metal catalyst (CuI vs $Pd(OAc)_2$), equivalents of amine, temperature, base, solvent, ligand and time all gave the same reaction profile. In desperation, a model (4-bromo-anisole) was investigated and this too resulted in multiple product spots. Deldaele and Evano have reported a base-free, room temperature, copper(I) catalysed reaction, which we then tried.^[12] Although we had low expectations for success as Deldaele and Evano used aryl iodides, we were extremely grateful to observe a clean reaction profile with some product (29%). Extending the reaction time to seven days at 60 °C gave the best yield (typically between 60-70%). It was clear that the base was the major problem in these reactions, although it is not understood exactly why this was so. The failure of the model reaction (with 4-bromo anisole) suggests that the amine itself may be unstable to prolonged treatment with strong bases, but we could not eliminate the acetyl group as a factor either.

Table S3.2 Optimisation of amination reaction with 2-bromophenoxazine 1

Entry	Amine Eq.	Catalyst (Eq.)	Ligand (Eq.)	Base (Eq.)	Solvent	Temp. °C	Time (h)	Yield (%)
1 ^a	1.5	CuI (0.1)	-	NaO ^t Bu (2.5)	THF	60	18	-
2 ^a	5	CuI (0.1)	-	NaO ^t Bu (2)	Toluene	80	18	-
3 ^a	5	CuI (0.1)	-	NaO ^t Bu (2)	Dioxane	80	18	-
4 ^b	3	CuI (0.1)	L-proline (0.2)	NaO ^t Bu (2)	DMSO	RT (18)	24	-
5 ^a	2	Pd(OAc) ₂ (0.2)	L-proline (0.2)	NaO ^t Bu (2)	DMSO	RT (18)	24	-
6 ^a	2	Pd(OAc) ₂ (0.1)	Xantphos (0.12)	Cs ₂ CO ₃ (2)	Dioxane	90	60	-
7 ^a	2	Pd(OAc) ₂ (0.1)	Xantphos (0.12)	NaO ^t Bu (2)	DMSO	90	60	-
8 ^c	1.5	CuI (0.1)	DMEDA (0.5)	K ₂ CO ₃ (2)	Toluene	120	48	-
9 ^c	1.2	CuI (0.1)	DMEDA (0.1)	K ₂ CO ₃ (2)	Toluene	100	18	-
10 ^d	1.2	CuI (0.1)	-	K ₂ CO ₃ (2)	-	100	18	-
11 ^d	1.2	CuI (0.1)	-	KOH (2)	H ₂ O	100 and RT	18	-
12	3	CuI (2)	L-proline (0.4)	-	DMSO	RT then -	42	29
13	3	CuI (2)	L-proline (0.4)	-	DMSO	60	168	62

Note reactions were always degassed via freeze-pump-thaw in triplicate and the reactions conducted under argon. ^a Procedure identified by Kanazawa *et al.*;^[8] ^b procedure identified by Ma *et al.*;^[13] ^c procedure identified by Huang *et al.*^[14] and ^d procedure identified by Ding *et al.*^[15]

Finally, deprotection of the acetyl group was achieved in the same way as the 3-phenoxazine series, i.e. conc. HCl in EtOH, returning a 60% yield. Although base methods are more usual for acetyls, we avoided this for two reasons: 1) the problem encountered with base in the previous reaction, and 2) it was hoped that the HCl salt of the product would be stable; it was not. Rather it was found that the material fairly

rapidly changed colour to a deep orange. After some investigation, it was found that the purity of the compound was sufficient for α -hematin testing, provided it was freshly prepared and used within 24 hours. LC-HRMS provided the initial clue as to what the compound was 'degrading' into, as a peak twice that of the molecular ion (less 2 hydrogen atoms) was detected suggesting the formation of a covalent dimer.

The coupling reactions for the aniline and cyclohexylamine sidechains proceeded under the conditions described for the chloroquine sidechain, again requiring long reaction times. Even so, the aniline sidechain only produced a meagre 17% yield after the coupling reaction. Deprotection was also successful under the ethanolic HCl procedure. For the cyclohexyl derivative (**P2b**) a crystal structure was obtained, as well as a crystal structure of the purported dimer, confirming the hypothesis formed on observing the large molecular mass via HRMS. The details for both structures can be found in Table S12 and Figure S5 in Section 2 above.

Experimental details

General

All chemicals were bought from Sigma-Aldrich or Merck and used as is, unless otherwise stated. Tetrahydrofuran and toluene were distilled under nitrogen from sodium wire using benzophenone as an indicator. Dichloromethane and acetonitrile were distilled under nitrogen from calcium hydride. N-Bromo succinimide was recrystallized from H₂O. Aniline was dried with KOH and distilled under vacuum. Cyclohexylamine was dried on CaCl₂ and distilled from KOH under vacuum. ¹H NMR and ¹³C NMR spectra were obtained using Varian 300 MHz VNMRs, Varian 400 MHz Unity INOVA and Varian 600 MHz Unity INOVA NMR instruments. Chemical shifts (δ) were recorded using the residual chloroform-d peaks (δ 7.26 ppm for ¹H NMR and δ 77.16 ppm for ¹³C NMR), DMSO-d peaks (δ 2.50 ppm for ¹H NMR and δ 39.52 ppm for ¹³C NMR) and D₂O peaks (δ 4.79 ppm for ¹H NMR and no signal for ¹³C NMR). All chemical shifts are reported in ppm and all spectra were obtained at 25 °C unless otherwise stated. Mass spectra were collected using positive ESI on a Waters SYNAPT G2 QTOF mass spectrometer by the Central Analytical Facility at Stellenbosch University. Column chromatography was performed using 230 – 400 nm silica gel or neutral alumina, and thin layer chromatography was performed using

Macherey-Nagel DC-Fertigfolien ALUGRAM Xtra SIL G/UV254 or Alox N/UV254 TLC plates. Petroleum ether, ethyl acetate, dichloromethane and/or methanol were used individually or in combination as solvents for all chromatography. Compounds were visualized on TLC using UV light (254 nm).

Towards the 2-substituted phenoxazines

4-bromo-1-(2-iodophenoxy)-2-nitrobenzene 2-Iodophenol (1.08 g, 4.91 mmol, 1.00 eq.), 2,5-dibromonitrophenol (1.38 g, 4.91 mmol, 1.00 eq.) and K_2CO_3 (1.36 g, 9.82 mmol, 2.00 eq.) were added to DMSO (7.5 mL) in a round-bottom flask. The mixture was stirred at 100 °C for 5 h. Thereafter it was cooled, diluted with H_2O (20 mL), washed with EtOAc (3 × 30 mL) in triplicate and washed with 2M NaOH (3 × 30 mL) in triplicate. The organic layer was then dried with $MgSO_4$, concentrated on the rotary evaporator and purified via column chromatography (EtOAc:Hexane 1:5), providing the product, a yellow solid, with a mass of 1.71 g and in a yield of 83%.

The characterization data collected for this compound compared well to literature data.^[10]

1H NMR (400 MHz, $CDCl_3$) δ 8.11 (d, $^4J = 2.4$ Hz, 1H, ArH), 7.88 (dd, $^3J_{HH} = 7.8$ Hz, $^4J = 1.4$ Hz, 1H, ArH), 7.57 (dd, $^3J_{HH} = 8.9$ Hz, $^4J_{HH} = 2.4$ Hz, 1H, ArH), 7.37 (ddd, $^3J_{HH} = 8.2$ Hz, $^3J_{HH} = 7.8$, $^4J_{HH} = 1.4$ Hz, 1H, ArH), 7.03 – 6.95 (m, 2H, ArH), 6.72 (d, $^3J_{HH} = 8.9$ Hz, 1H, ArH). **^{13}C NMR (400 MHz, $CDCl_3$)*** δ 154.56, 149.53, 140.95, 140.50, 137.16, 130.26, 128.73, 127.27, 120.66, 120.59, 115.09, 89.11.

5-bromo-2-(2-iodophenoxy)aniline. 1-Bromo-3-(2-iodophenoxy)-2-nitrobenzene (3.86 g, 9.19 mmol, 1.00 eq), glacial acetic acid (18.4 mL, 321 mmol, 35.0 eq), iron filings (2.57 g, 44.0 mmol, 5.00 eq) and EtOH (18.4 mL) were added to distilled water (9.2 mL), and the reaction was sonicated for 2 hours at 30 °C. The mixture was allowed to cool, neutralized with 1M NaOH and then extracted with ethyl acetate (3 × 12 mL) in triplicate. The organic layer was washed with water and dried $MgSO_4$ and vacuum filtered. The excess solvent was removed, yielding a dark yellow oil. The product, a pale yellow solid, was purified by column chromatography (Hexane:EtOAc 100:1), to provide the product in a mass of 3.19 g and with a yield of 89%.

The characterization data collected for this compound compared well to literature data.^[10]

¹H NMR (400 MHz, CDCl₃) δ 7.84 (dd, ³J_{HH} = 8.0 Hz, ⁴J_{HH} = 1.6 Hz, 1H, ArH), 7.26 (ddd, ³J_{HH} = 8.0 Hz, ³J_{HH} = 7.6 Hz, ⁴J_{HH} = 1.6 Hz, 1H, ArH), 6.96 (d, ⁴J_{HH} = 2.3 Hz, 1H, ArH), 6.85 (td, ³J_{HH} = 7.6 Hz, ⁴J_{HH} = 1.4 Hz, 1H, ArH), 6.81 (dd, ³J_{HH} = 8.0 Hz, ⁴J_{HH} = 1.4 Hz, 1H, ArH), 6.79 (dd, ³J_{HH} = 8.5 Hz, ⁴J_{HH} = 2.3 Hz, 1H, ArH), 6.63 (d, ³J_{HH} = 8.5 Hz, 1H, ArH), 3.92 (s, 2H, NH).

***N*-[2-(4-bromo-2-iodophenoxy)phenyl]acetamide.**

5-Bromo-2-(2-

iodophenoxy)aniline (0.402 g, 1.03 mmol, 1.00 eq.) and acetic anhydride (0.298 mL, 3.15 mmol, 3.06 eq.) were stirred together in a round-bottom flask at room temperature for 18 h. The reaction mixture was then quenched with saturated aqueous Na₂CO₃ (50 mL), followed by extraction into EtOAc (3 × 20 mL) in triplicate. The organic layer was then dried with MgSO₄, filtered and concentrated on the rotary evaporator. The product was purified via column chromatography (EtOAc:Hexane 1:5), giving a white solid with a mass of 374 mg and in a yield of 84%.

The characterization data collected for this compound compared well to literature data.^[10]

¹H NMR (400 MHz, CDCl₃) δ 8.65 (d, ⁴J_{HH} = 2.2 Hz, 1H, ArH), 7.87 (dd, ³J_{HH} = 8.3 Hz, ⁴J_{HH} = 1.5 Hz, 1H, ArH), 7.35 – 7.30 (m, 1H, ArH), 7.08 (dd, ³J_{HH} = 8.7 Hz, ⁴J_{HH} = 2.2 Hz, 1H, ArH), 6.95 (m, 2H, ArH), 6.57 (d, ³J_{HH} = 8.7 Hz, 1H, ArH), 2.20 (s, 3H, C(O)CH₃).

1-(2-bromo-10*H*-phenoxazin-10-yl)ethan-1-one.

N-(5-Bromo-2-(2-iodophenoxy)phenyl)-acetamide (1.00 g, 2.29 mmol, 1.00 eq.) and K₂CO₃ (0.633 g, 4.58 mmol, 2.00 eq.) were added to a Schlenk flask and an argon atmosphere was established. DMEDA (24.7 μL, 0.229 mmol, 0.100 eq.) and distilled toluene (10 mL) were then added and the reaction mixture was heated to 135 °C for 24 h. The reaction mixture was cooled, diluted with DCM (20 mL) and filtered through Celite. The reaction mixture was concentrated using the rotary evaporator and purified via column chromatography (EtOAc: Hexane 1:5), producing the product, a white solid, with a mass of 0.827 g in a yield of 84%.

The characterization data collected for this compound compared well to literature data.^[10]

¹H NMR (400 MHz, CDCl₃) δ 7.69 (d, ⁴J_{HH} = 2.3 Hz, 1H, ArH), 7.39 (dd, ⁴J_{HH} = 7.9 Hz, ⁴J_{HH} = 1.6 Hz, 1H, ArH), 7.29 (dd, ³J_{HH} = 8.7 Hz, ⁴J_{HH} = 2.3 Hz, 1H, ArH), 7.20 (dd, ³J_{HH} = 7.9 Hz, ⁴J_{HH} = 1.6 Hz, 1H, ArH), 7.13 (m, 2H, ArH), 6.98 (d, J = 8.7 Hz, 1H, ArH), 2.33 (s, 3H, C(O)CH₃).

3-bromo-10H-phenoxazine. 10H-Phenoxazine (500 mg, 2.56 mmol, 1.00 eq.) was added to an oven-dried three-neck round-bottom flask. An argon atmosphere was established, and the flask was covered in tinfoil to eliminate all light. THF (10 mL) was added and the reaction flask and cooled to 0 °C while stirring for 10 min. The NBS (456 mg, 2.56 mmol, 1.00 eq.) was dissolved in THF (7.5 mL) and cooled to 0 °C. The NBS solution was then added dropwise to the three-neck round-bottom flask over a 30-minute period, the reaction was then allowed to stir on ice for a further 30 minutes. The reaction was then quenched with H₂O (10 mL) and diluted with EtOAc (30 mL) and separated. The organic layer was washed in triplicate with H₂O (3 × 30 mL) and subsequently dried with MgSO₄, filtered and reduced on a rotary evaporator. The product was purified via column chromatography (Hexane:EtOAc 5:1), producing a white solid with yield of 46% (307 mg).

IR (ATR, cm⁻¹): 3377 (N-H), 1487 (C=C), 745 (C-H). **¹H NMR (400 MHz, CDCl₃)** δ 6.83 (dd, ³J_{HH} = 8.2 Hz, ⁴J_{HH} = 2.0 Hz, 1H, ArH), 6.79 (d, ⁴J_{HH} = 2.0 Hz, 1H, ArH), 6.78 – 6.72 (m, 1H, ArH), 6.71 – 6.62 (m, 2H, ArH), 6.37 (d, ³J_{HH} = 7.4 Hz, 1H, ArH), 6.23 (d, ³J_{HH} = 8.2 Hz, 1H, ArH), 5.11 (s, 1H, NH). **¹³C NMR (400 MHz, CDCl₃)** δ 144.20, 143.02, 130.85, 130.79, 126.20, 123.97, 121.73, 118.90, 115.87, 114.21, 113.49, 112.39. **HRMS–Positive:** *m/z*[M+H]⁺ calculated for C₁₂H₉BrNO: 261.9868; found: 261.9881. The [M]⁺ ion was also found: 260.9791, calculated for C₁₂H₈BrNO, 260.9789

Towards the 3-substituted phenoxazines

Whilst the purity of these could not be unambiguously determined, the experimental details are recorded here as a full record of what was done.

N¹,N¹-diethyl-N⁴-(10H-phenoxazin-3-yl)pentane-1,4-diamine P3a. **N-Boc-P3a** (50.0 mg, 0.114 mmol, 1.00 eq.) was added to distilled H₂O (1.8 mL) and sonicated until dissolved. The reaction mixture was heated to 90 °C. There after 37% HCl (3

drops) was added, and the reaction was stirred at 90 °C until reaction was complete (10 - 20 min). The reaction was allowed to cool and neutralized with 2 M NaOH, monitored by pH paper. The neutralized solution was then diluted with DCM (5 mL). The mixture was separated, and the aqueous phase was extracted with DCM (50 mL) six times, or until the water layer was clear. The organic phase was dried with MgSO₄ and concentrated on the rotary evaporator. The product was purified via column chromatography (methanol: DCM 3:20). A yield of 59% was attained for the final product, a bright yellow oil with a mass of 22.8 mg. **HRMS(ESI⁺)** found [M+H]⁺ 340.2393, C₂₁H₃₀N₃O required 340.2389; found oxidised form [M-H]⁺ 338.2238 C₂₁H₂₈N₃O required 338.2232

(E)-4-[(3H-phenoxazin-3-ylidene)amino]-N,N-diethylpentan-1-amine HCl salt P3a'. **P3a** (28.3 mg, 0.083 mmol, 1.00 eq) added to THF (5 mL). Three drops of 4 M HCl dioxane was added, the precipitate was allowed to settle and the THF decanted. Acetone (3mL) was then added and the solid was filtered and dried under high vacuum, producing a red solid with a mass of 10.3 mg, in a yield of 33%. LC-MS analysis showed a purity of 82%.

N-cyclohexyl-10H-phenoxazin-3-amine P3b. The same hydrolysis protocol for **P2a** was followed. **N-Boc-P3b** (99 mg) was added to a degassed 0.24 M HCl ethanol solution (5.0 eq. of HCl), the reaction was heated under reflux. Thereafter the reaction mixture was concentrated on the rotary evaporator until approximately a quarter of the solution remained after which it was topped with a layer of EtOAc. The product precipitated out of solution overnight (65% yield) and the solid was filtered and washed with cold EtOAc, dried under high vacuum for 24 hours and stored under argon. LC-MS analysis gave a purity of 90%; **HRMS(ESI⁺)** calculated for C₁₈H₂₁N₂O: 281.1654, found [M+H]⁺ 281.1664.

Spectra for new compounds reported in the manuscript

1-(2-((5-(diethylamino)pentan-2-yl)amino)-10H-phenoxazin-10-yl)ethan-1-one

(*N*-Ac-P2a)

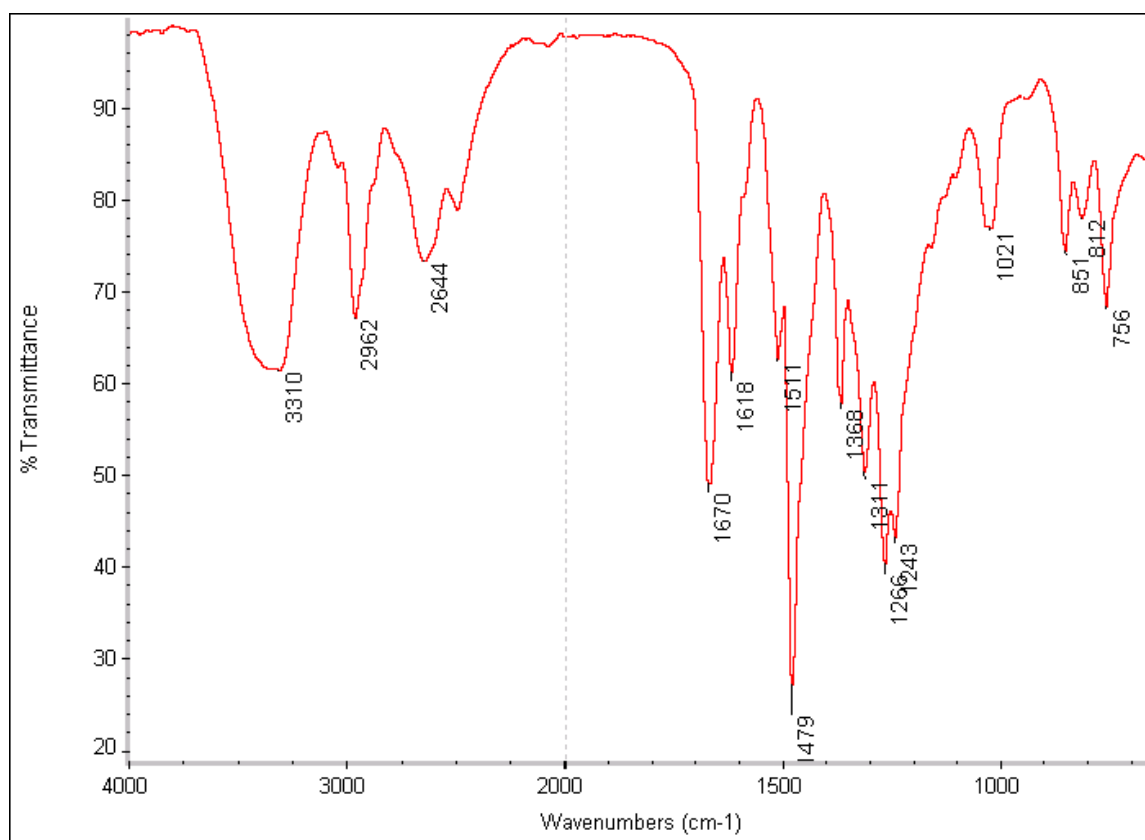


Figure S3.1 Infra-red spectrum (ATR) of *N*-Ac-P2a

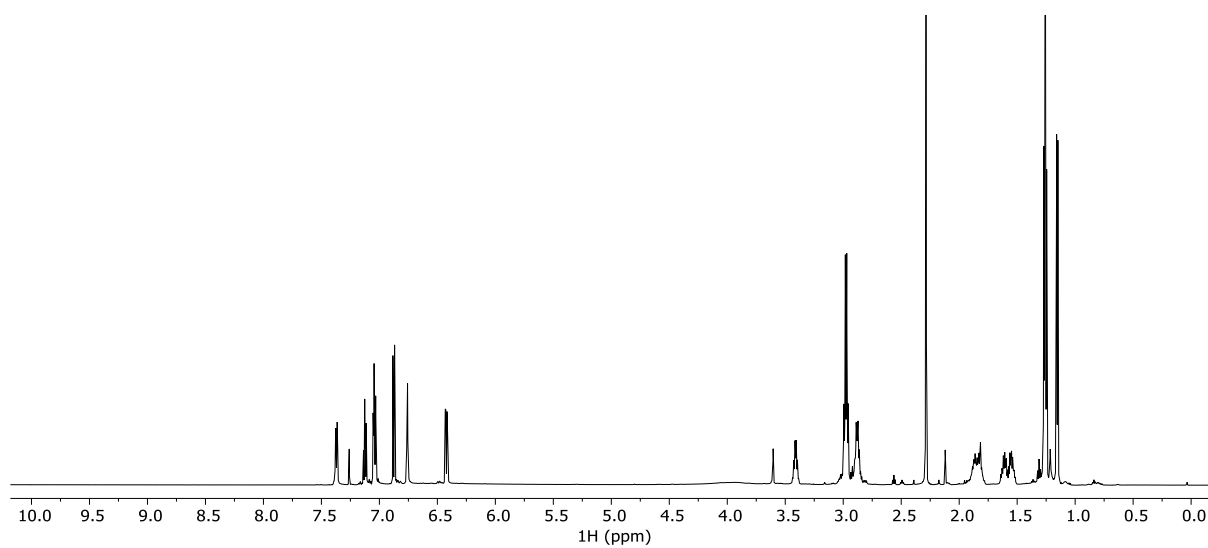


Figure S3.1 ¹H NMR spectrum (600 MHz, CDCl₃) of *N*-Ac-P2a

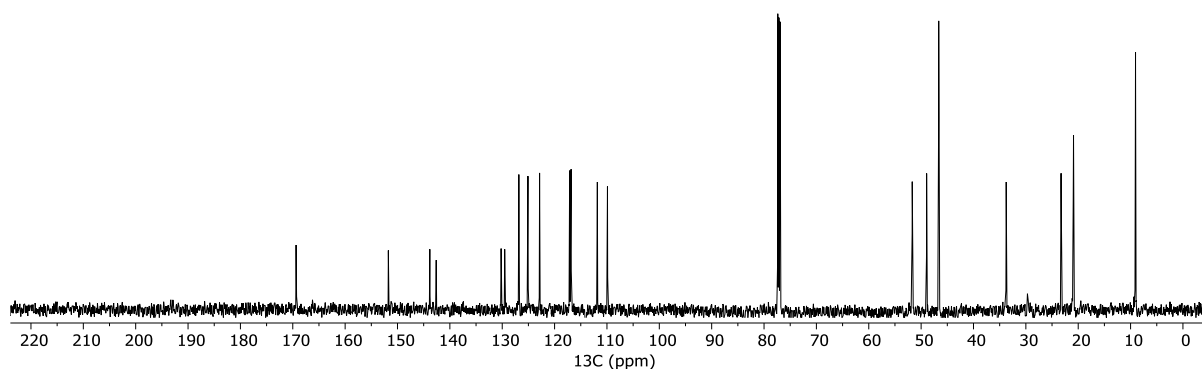


Figure S3.2 ¹³C NMR spectrum (151 MHz, CDCl₃) of *N*-Ac-P2a

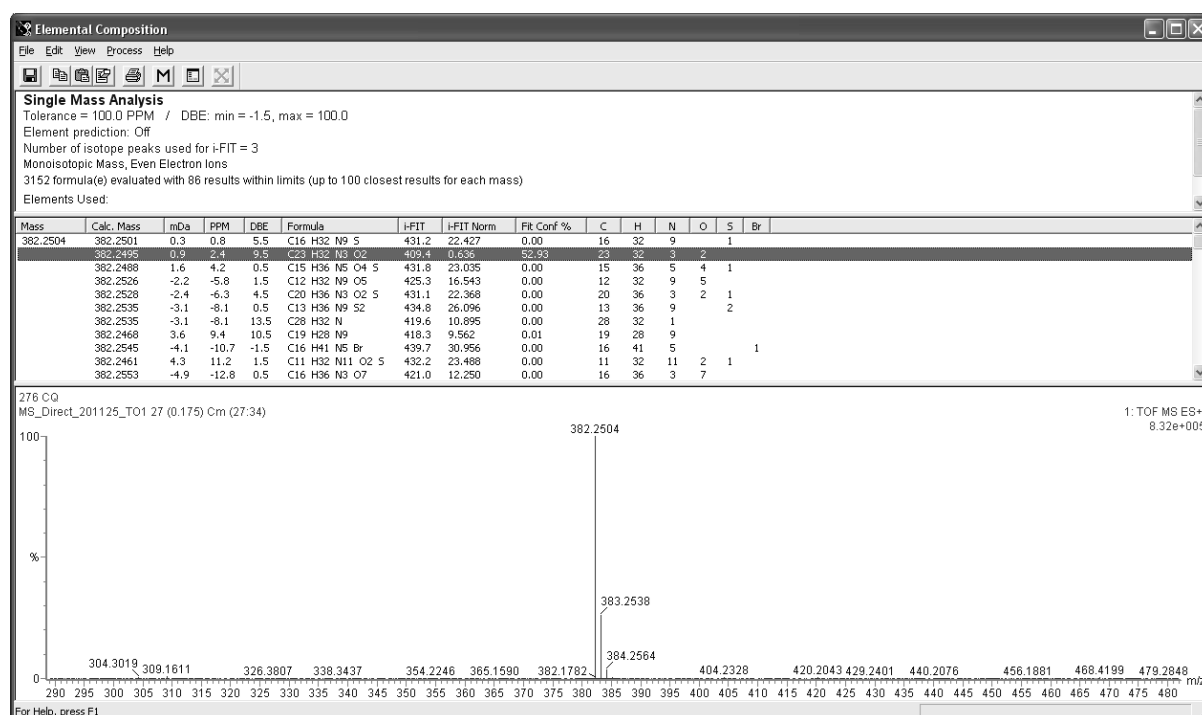


Figure S3.3 HRMS spectrum of *N*-Ac-P2a

*N*¹,*N*¹-diethyl-*N*⁴-(10*H*-phenoxazin-2-yl)pentane-1,4-diamine (**P2a**)

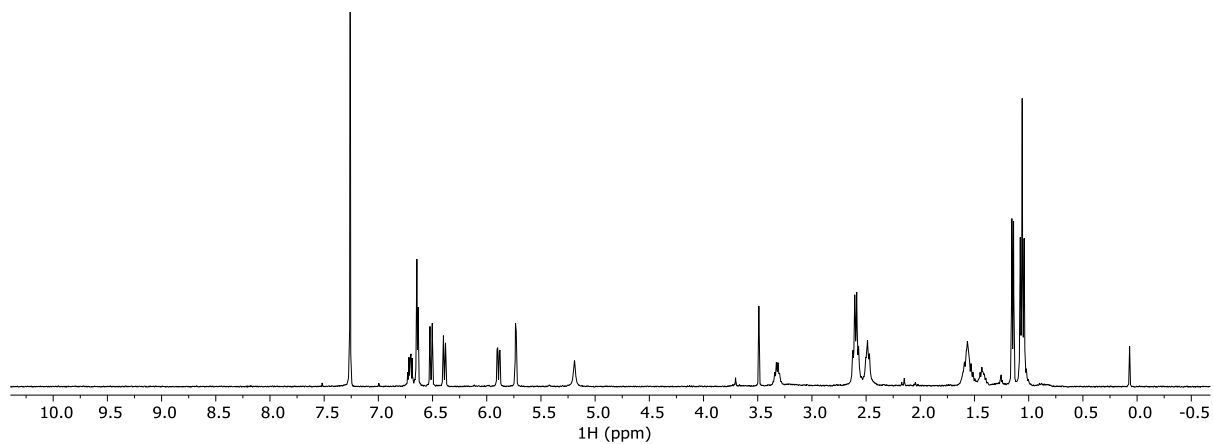


Figure S3.4 ¹H NMR spectrum (400 MHz, CDCl₃) of **P2a**

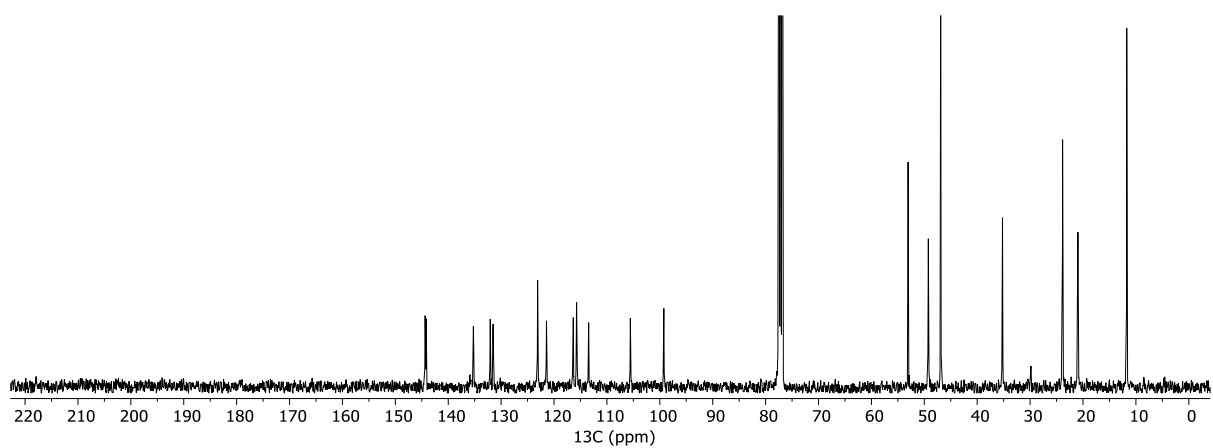


Figure S3.5 ¹³C NMR spectrum (101 MHz, CDCl₃) of **P2a**

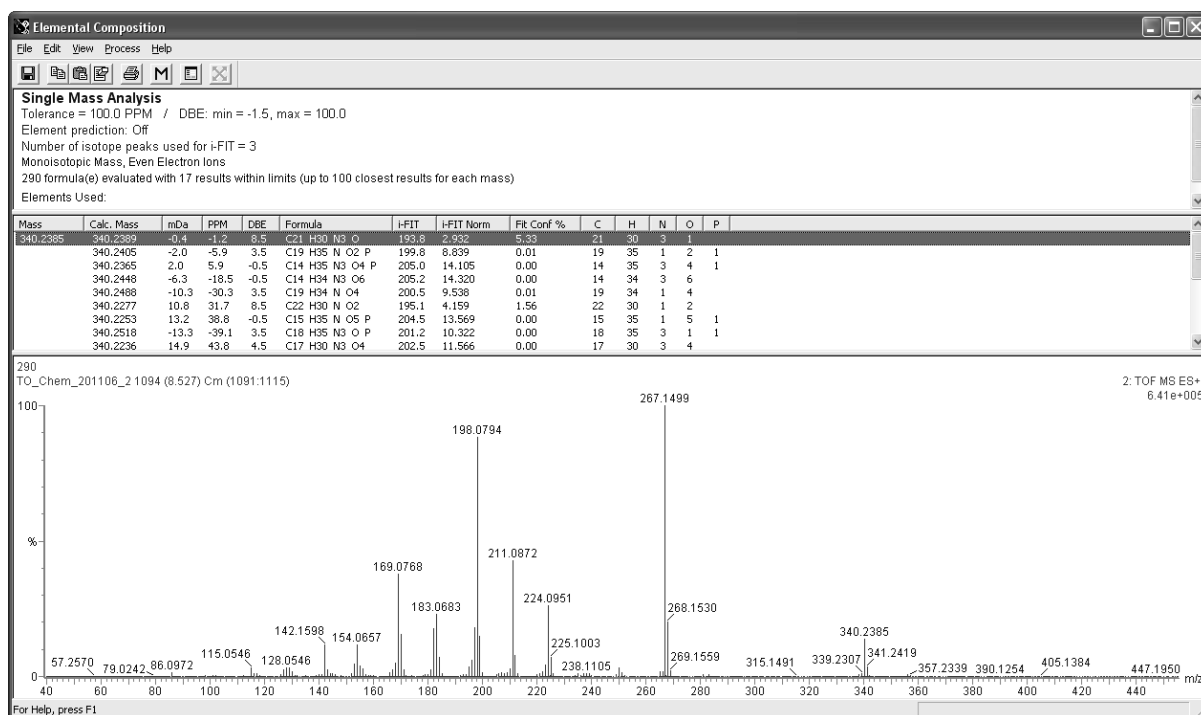


Figure S3.6 HRMS spectrum of **P2a**

1-(2-(cyclohexylamino)-10*H*-phenoxazin-10-yl)ethan-1-one (**N-Ac-P2b**)

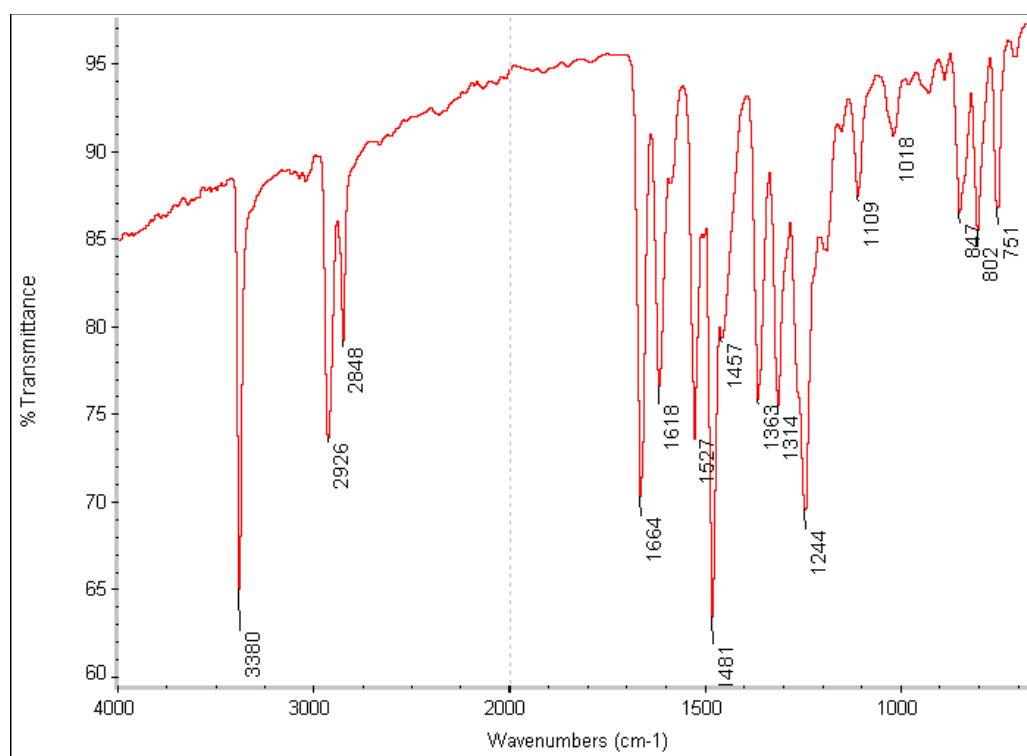


Figure S3.7 Infra-red spectrum (ATR) of **N-Ac-P2b**

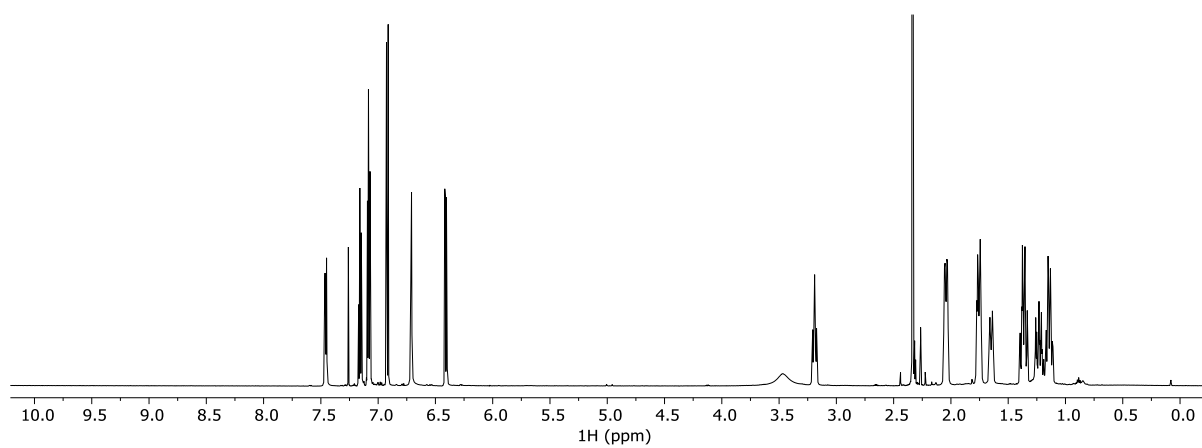


Figure S3.8 ¹H NMR spectrum (600 MHz, CDCl₃) of *N*-Ac-P2b

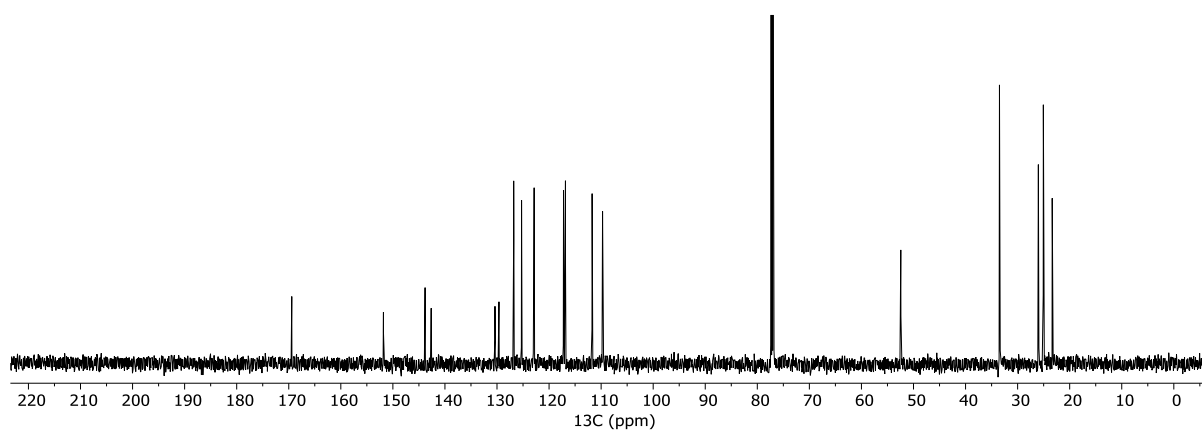


Figure S3.9 ¹³C NMR spectrum (151 MHz, CDCl₃) of *N*-Ac-P2b

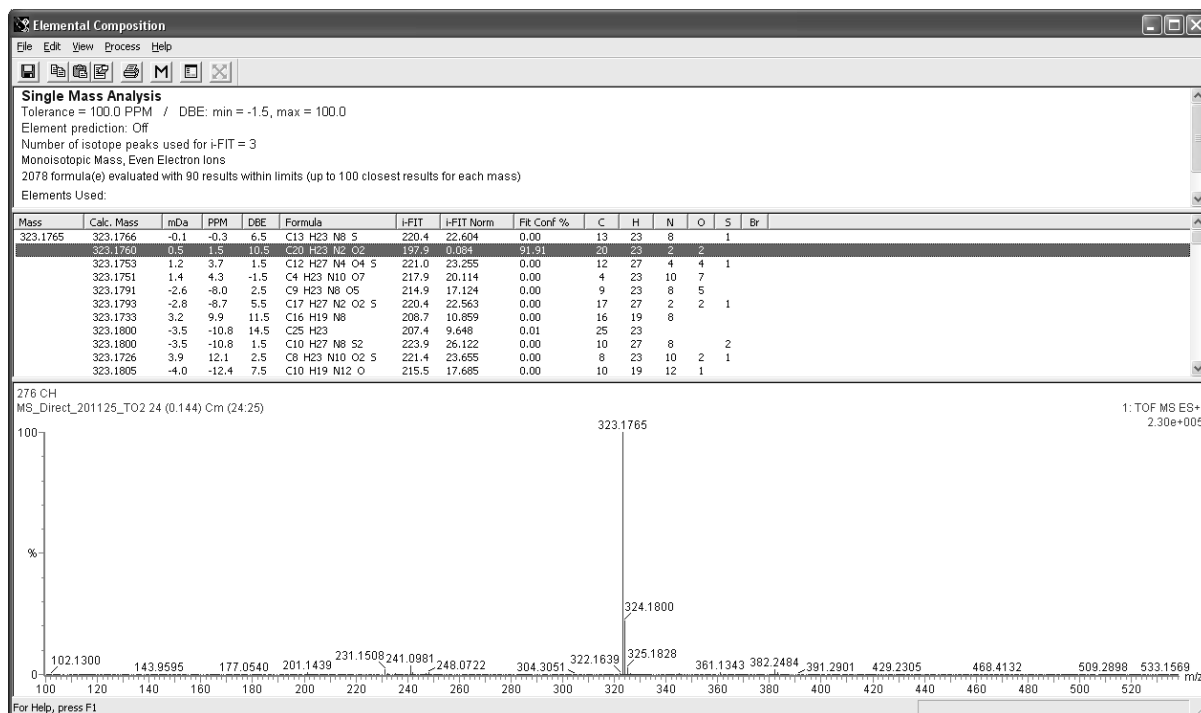


Figure S3.10 HRMS spectrum of **N-Ac-P2b**

N-cyclohexyl-10*H*-phenoxazin-2-amine (**P2b**)

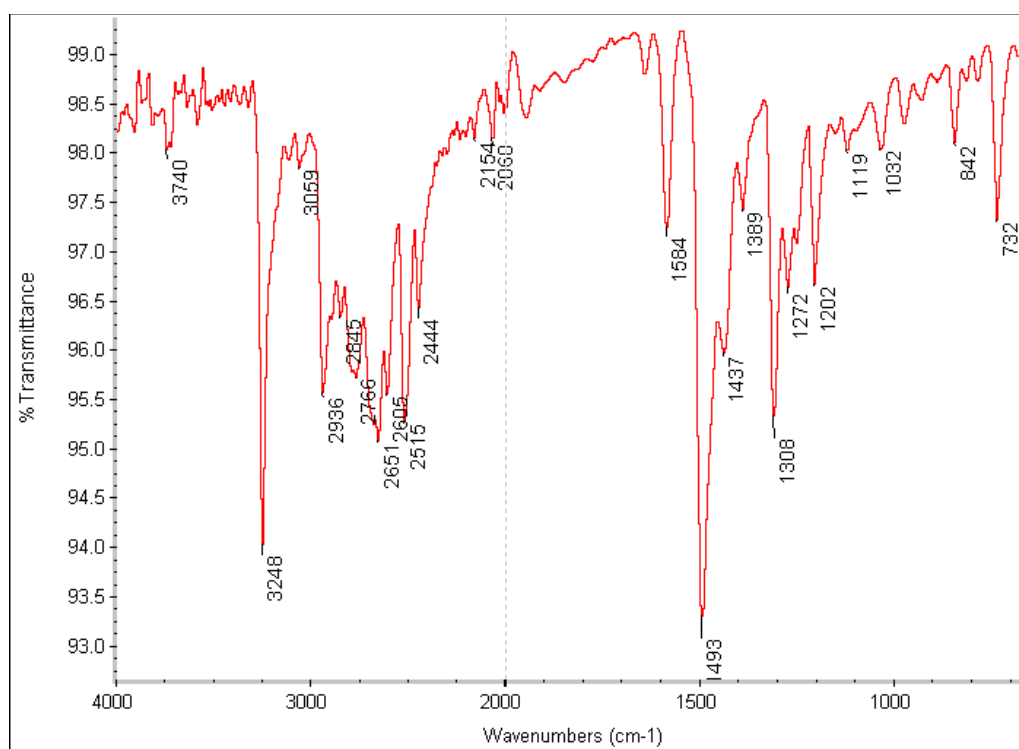


Figure S3.11 Infra-red spectrum (ATR) for **P2b**

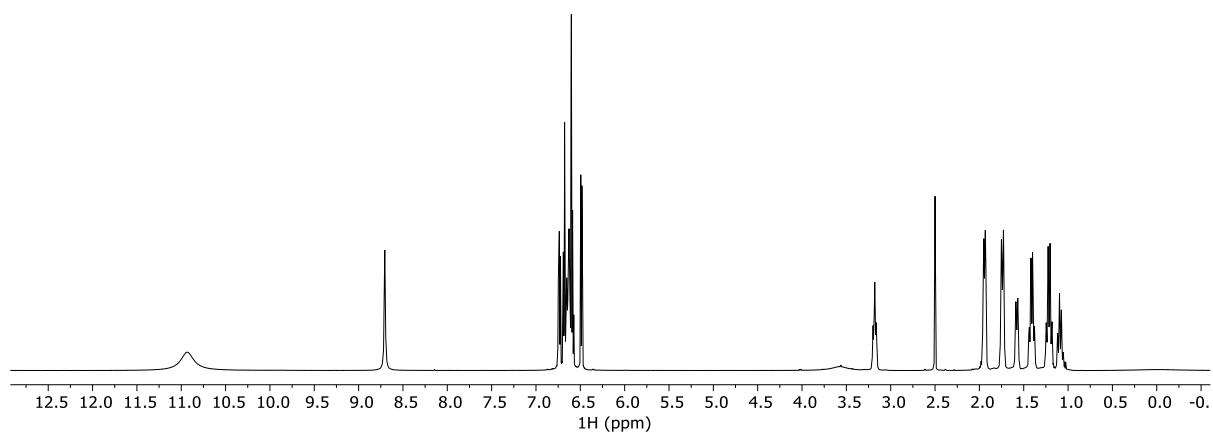


Figure S3.12 ^1H NMR spectrum (600 MHz, CDCl_3) of **P2b**

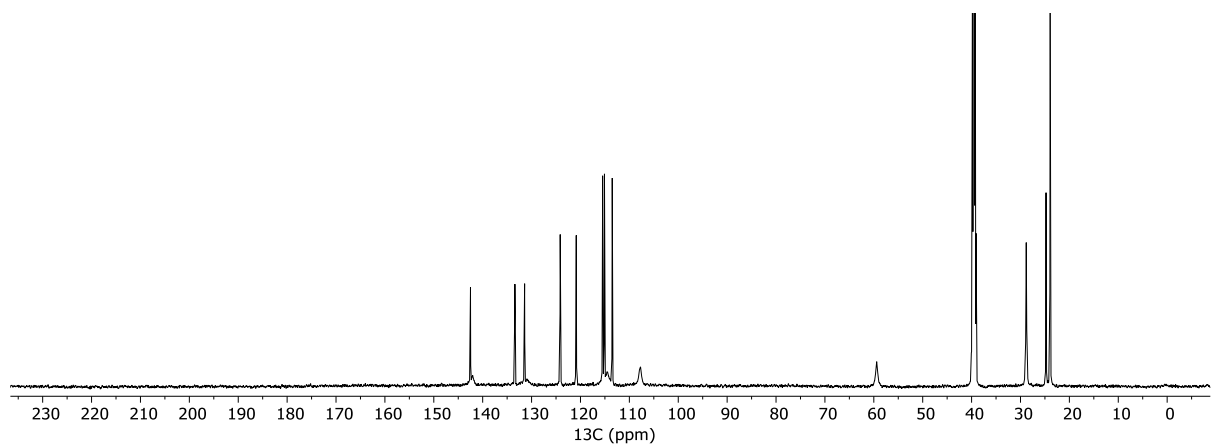


Figure S3.13 ^{13}C NMR spectrum (151 MHz, CDCl_3) of **P2b**

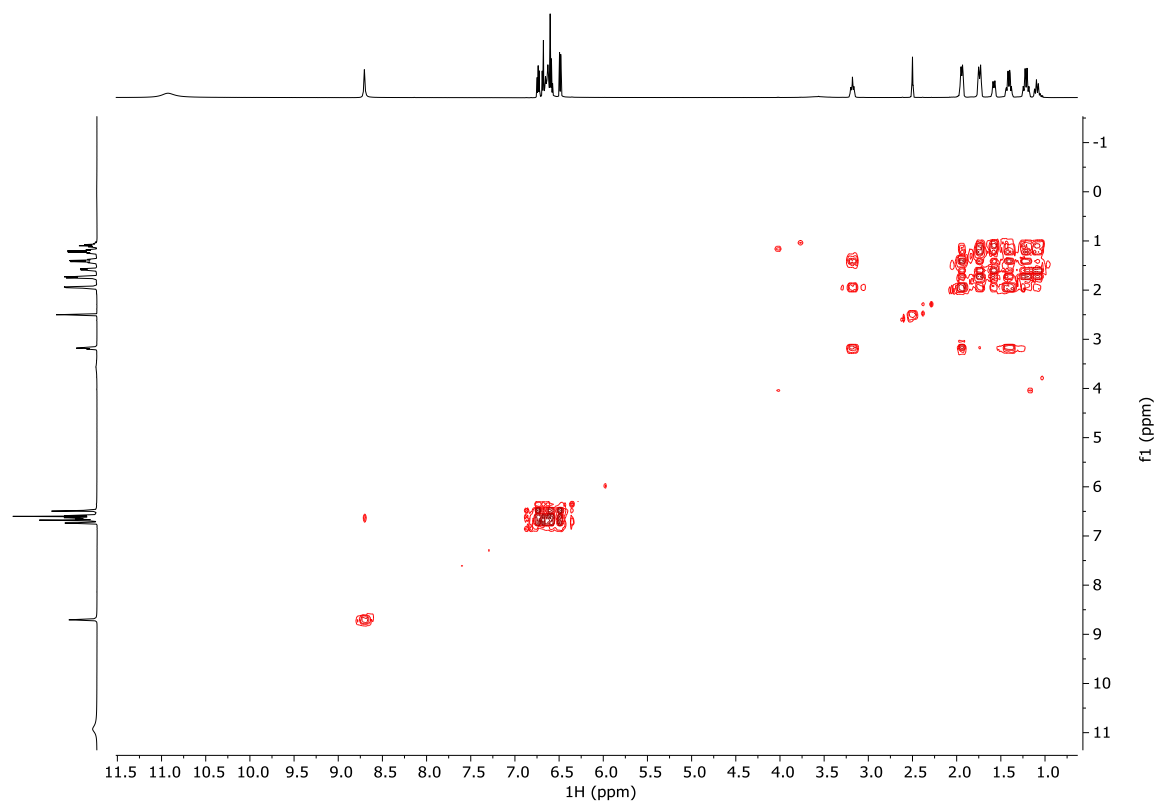


Figure S3.14 gCOSY spectrum (600 MHz, DMSO- d_6) of **P2b**

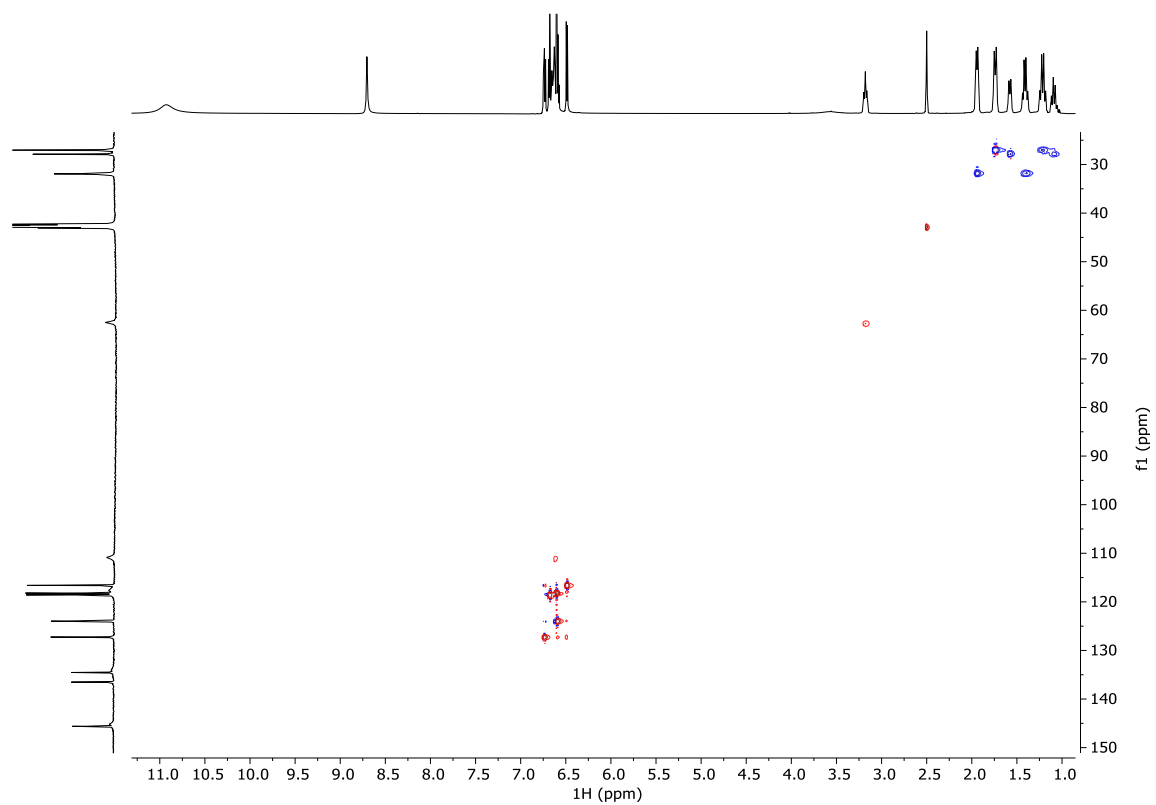


Figure S3.15 gHSQCAD spectrum (600/151 MHz, DMSO- d_6) of **P2b**

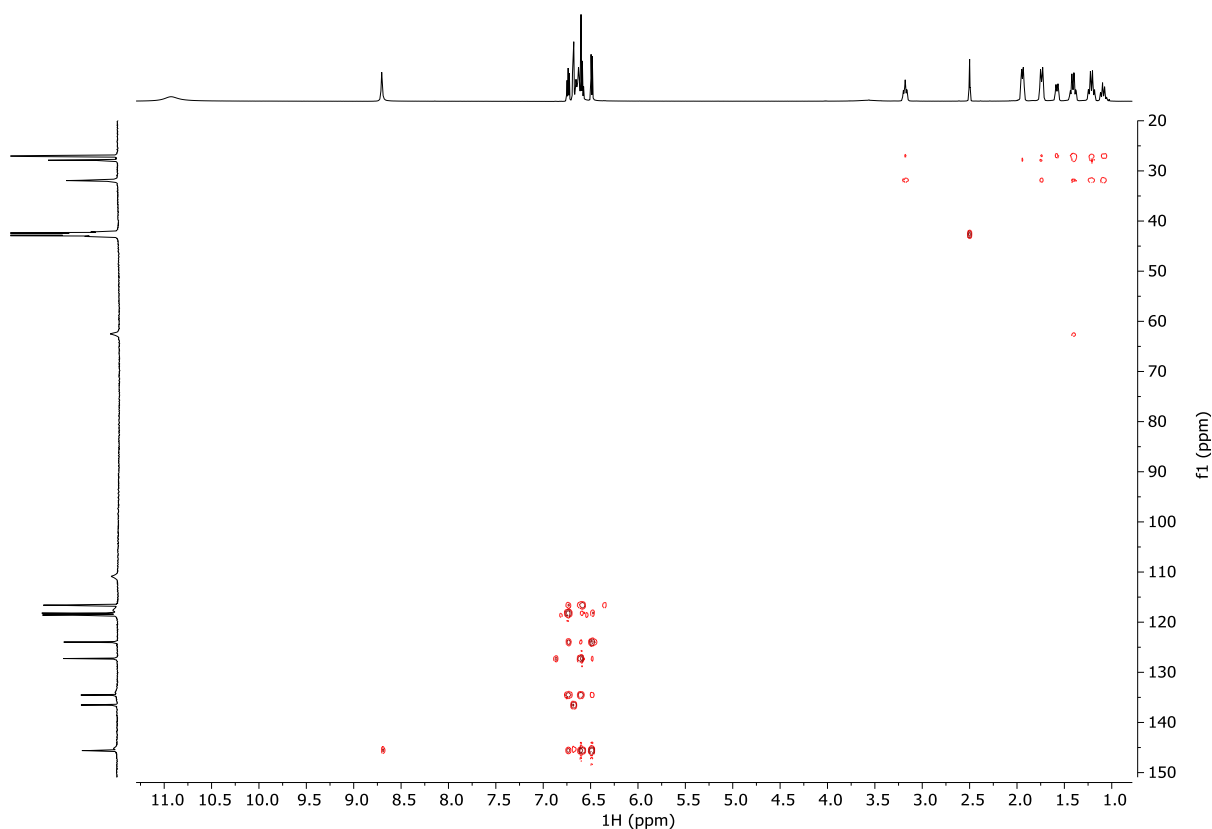


Figure S3.16 gHMBCAD spectrum (600/151 MHz, DMSO- d_6) of P2b

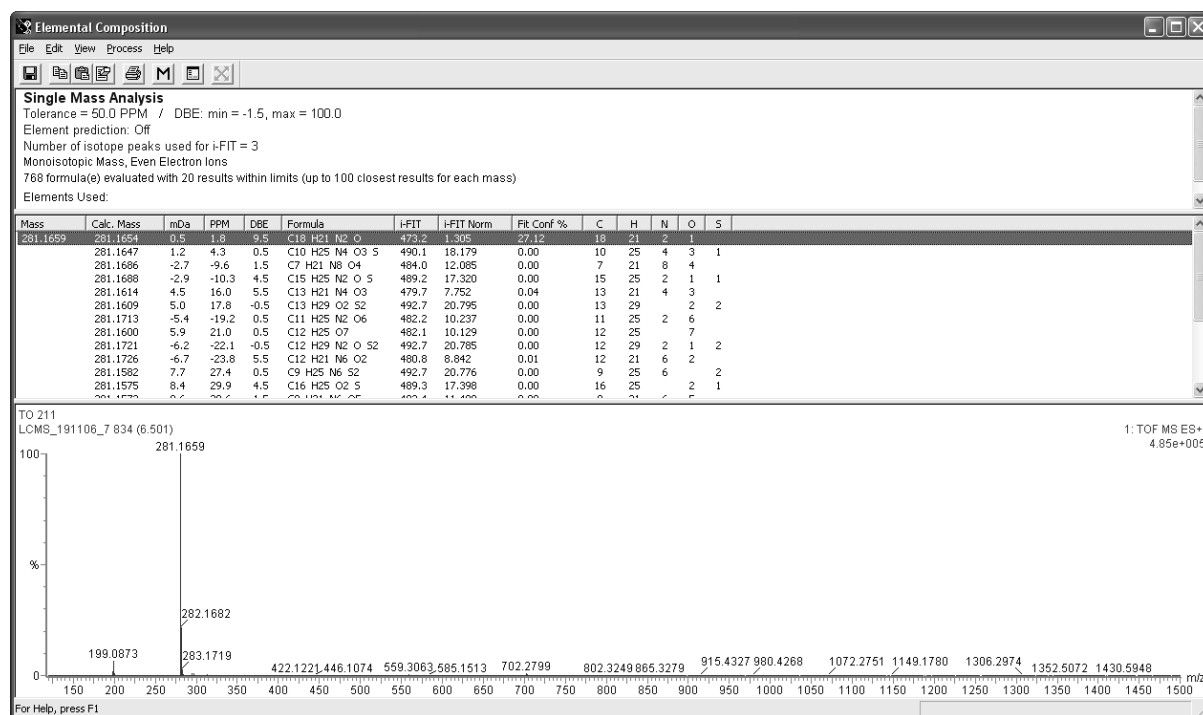


Figure S3.17 HRMS spectrum of P2b

1-(2-(phenylamino)-10H-phenoxazin-10-yl)ethan-1-one (**N-Ac-P2c**)

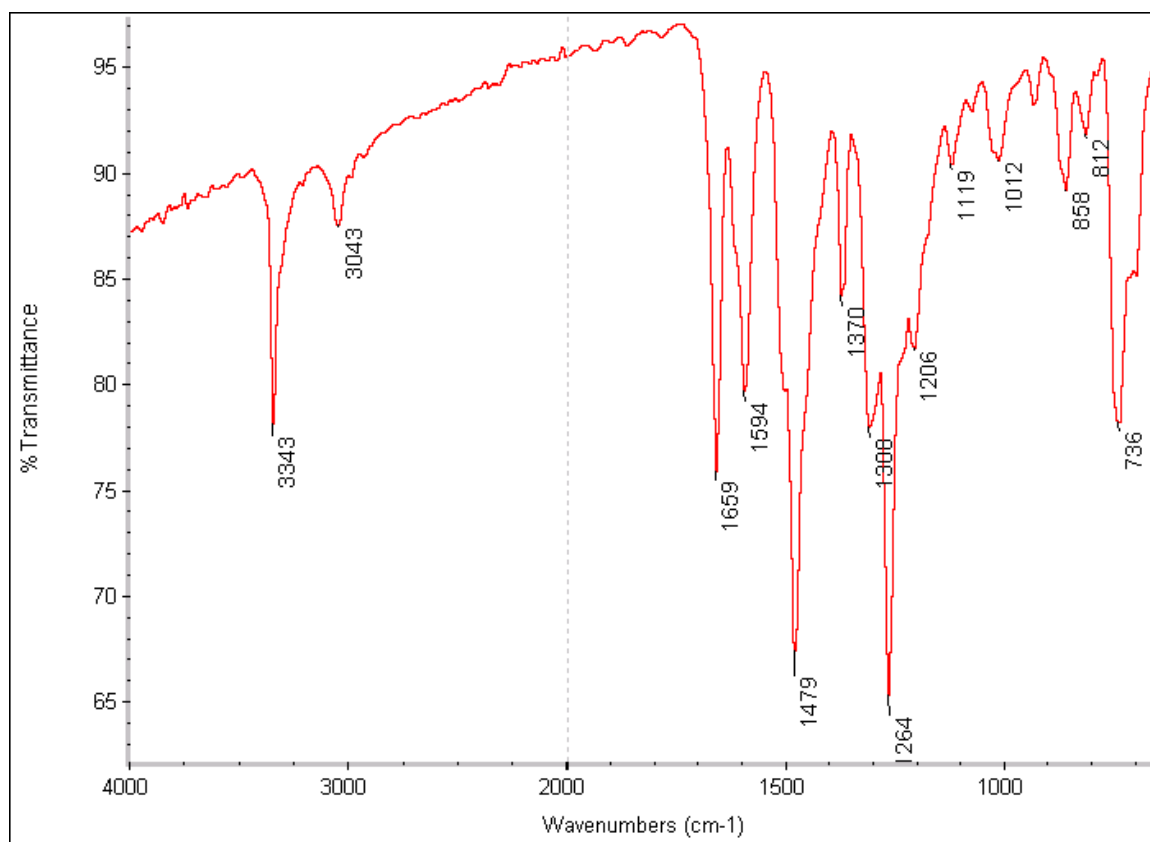


Figure S3.18 Infra-red spectrum (ATR) for **N-Ac-P2c**

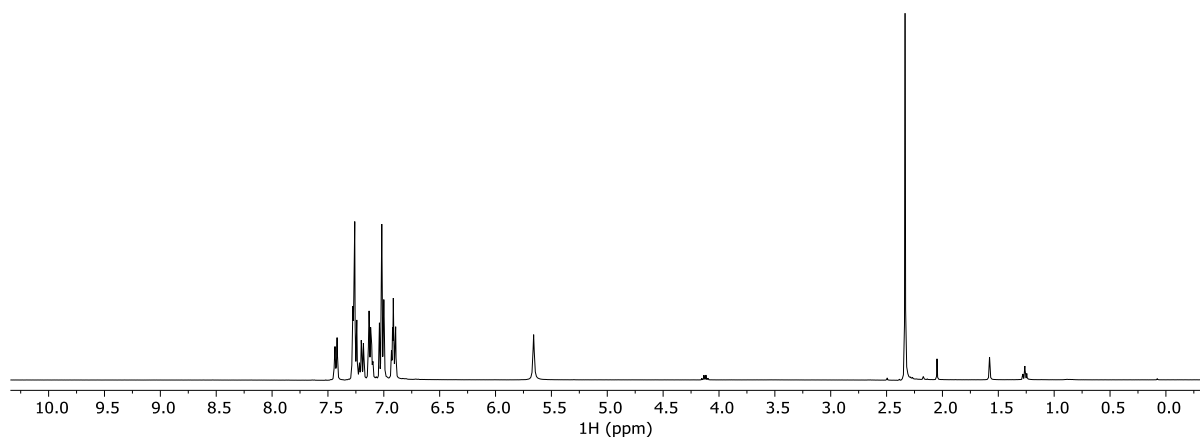


Figure S3.19 ¹H NMR spectrum (400 MHz, CDCl₃) for **N-Ac-P2c**

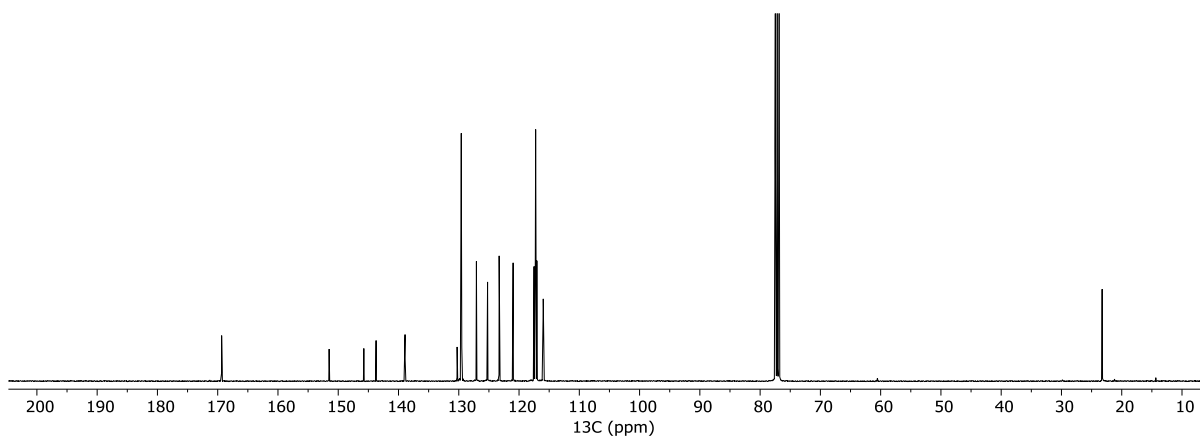


Figure S3.20 ^{13}C NMR spectrum (101 MHz, CDCl_3) for *N*-Ac-P2c

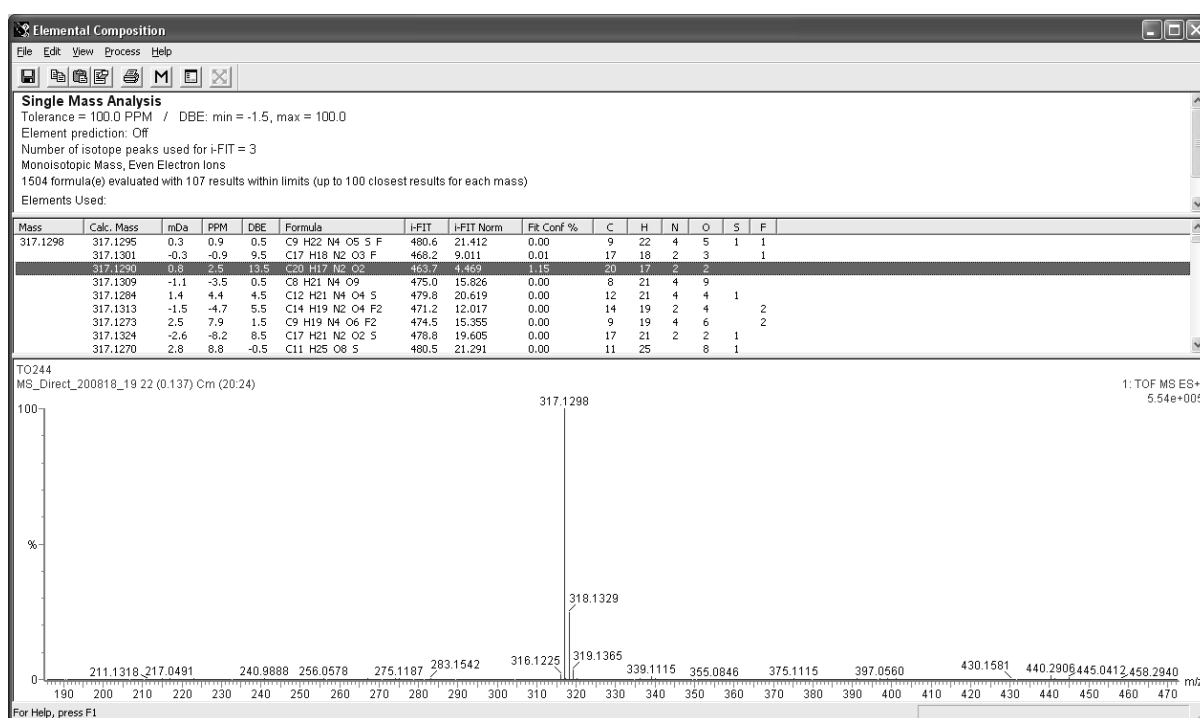


Figure S3.21 HRMS spectrum (ES+) for *N*-Ac-P2c

N-phenyl-10*H*-phenoxazin-2-amine (**P2c**)

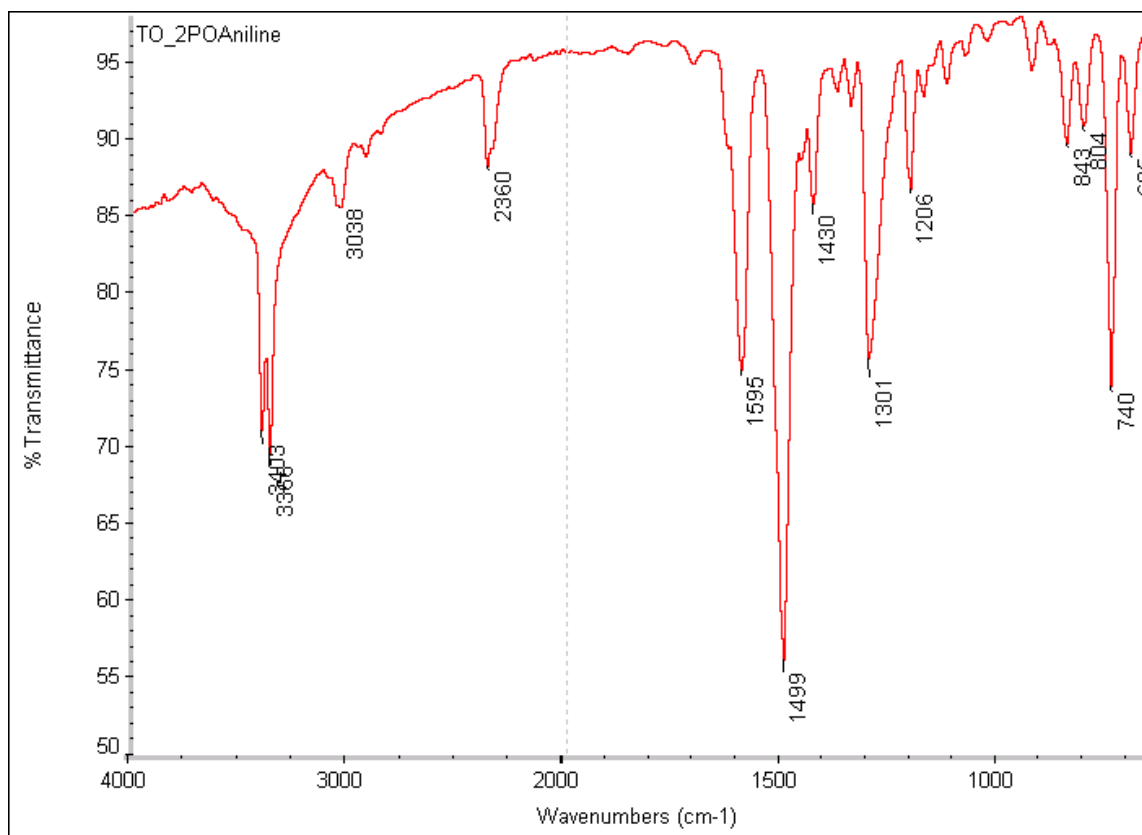


Figure S3.22 Infra-red spectrum (ATR) for **P2c**

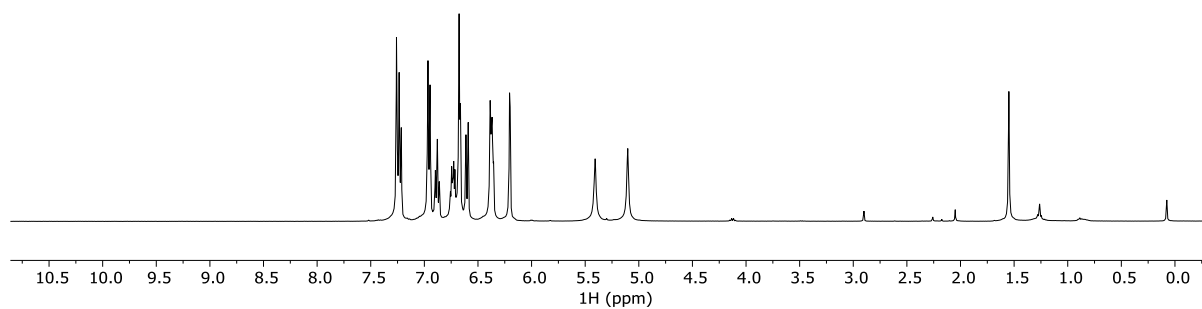


Figure S3.23 ¹H NMR spectrum (400 MHz, CDCl₃) for **P2c**

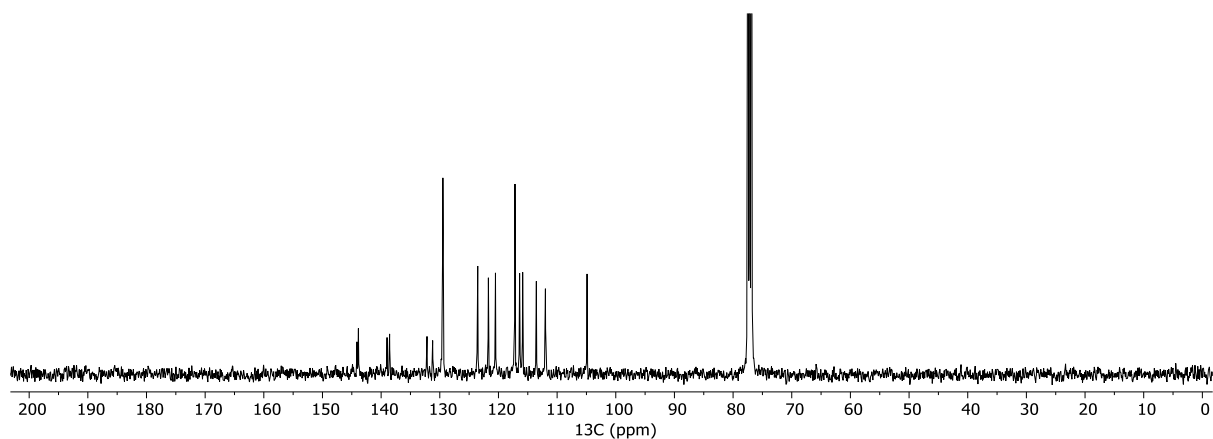


Figure S3.24 ^{13}C NMR spectrum (101 MHz, CDCl_3) for **P2c**

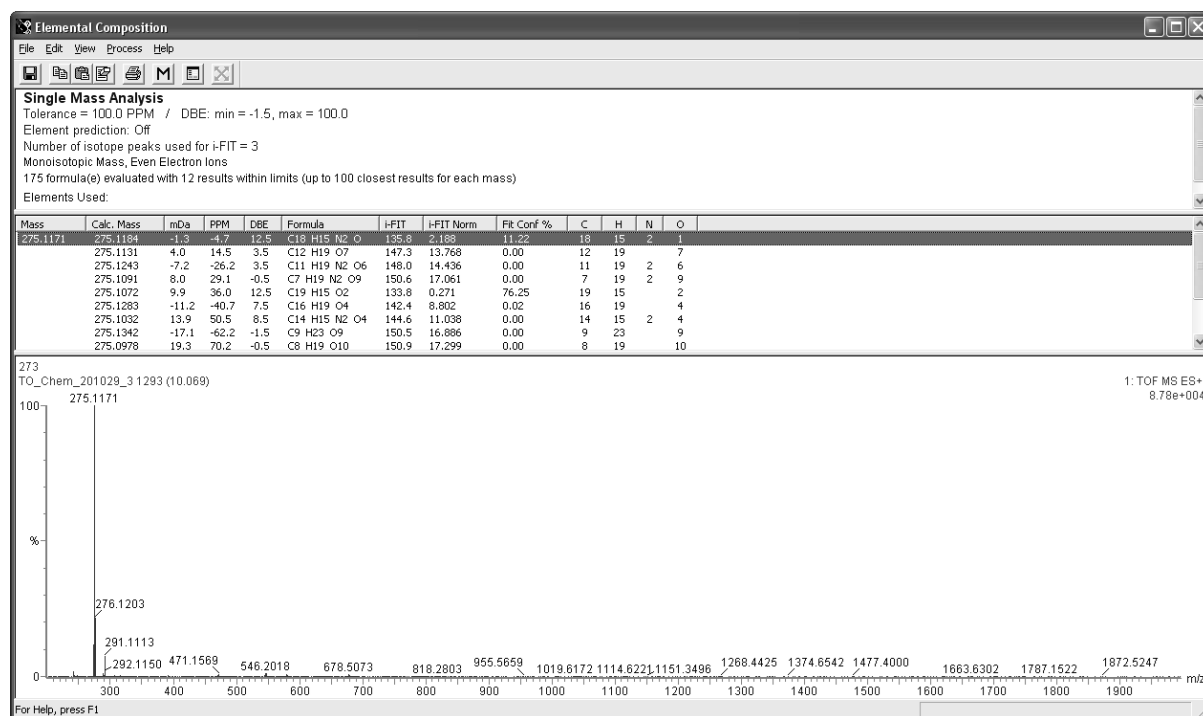


Figure S3.25 HRMS spectrum (ES+) for **P2c**

tert-butyl 3-bromo-10*H*-phenoxazine-10-carboxylate (Boc-protected **2**)

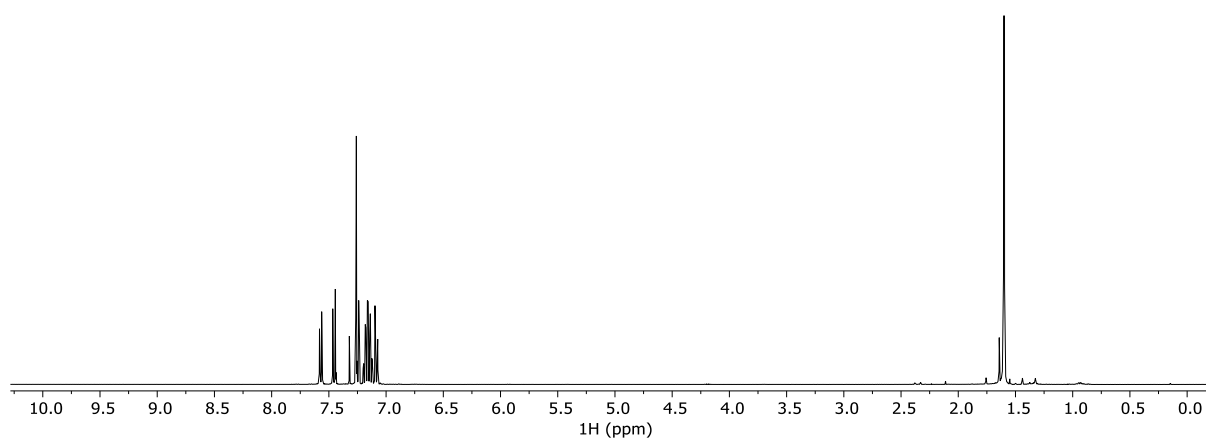


Figure S3.26 ¹H NMR spectrum (400 MHz, CDCl₃) for Boc-protected **2**

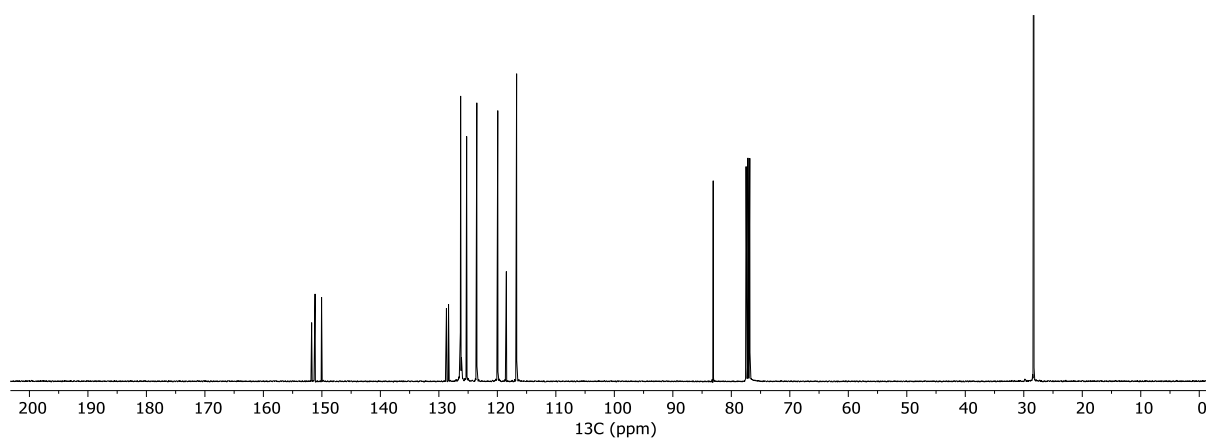


Figure S3.27 ¹³C NMR spectrum (101 MHz, CDCl₃) for Boc-protected **2**

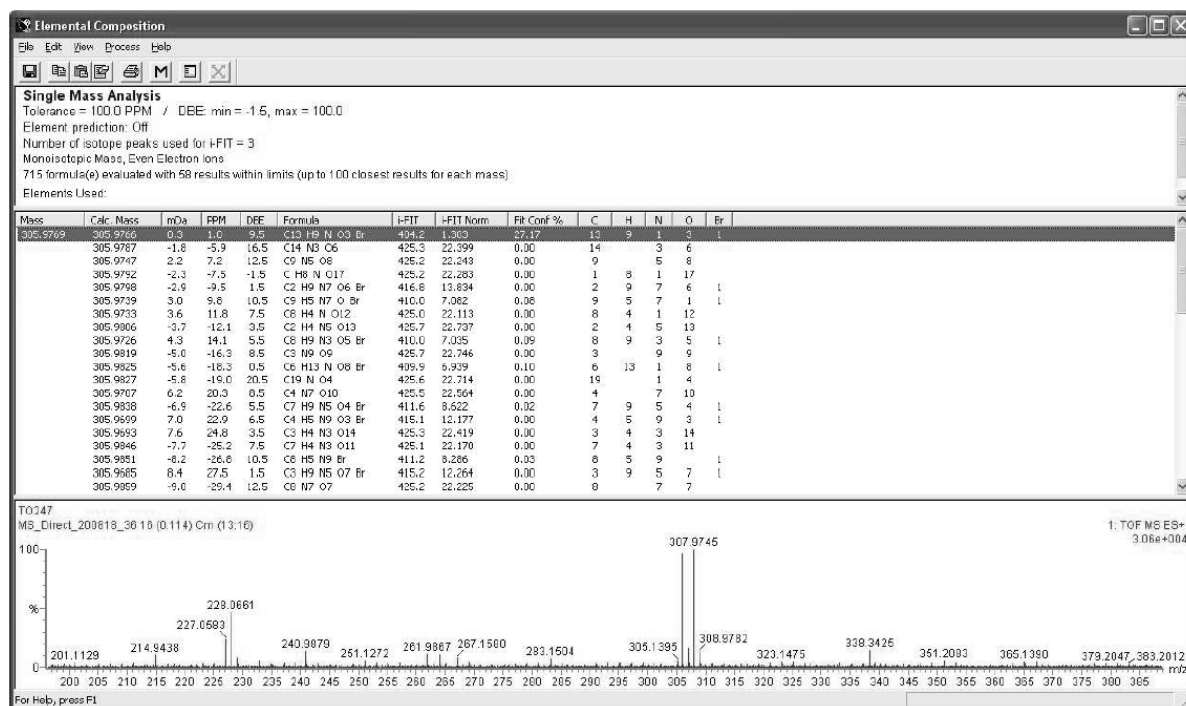


Figure S3.28 HRMS spectrum (ES+) for Boc-protected 2

tert-butyl 3-([5-(diethylamino)pentan-2-yl]amino)-10*H*-phenoxazine-10-carboxylate
(*N*-Boc-P3a)

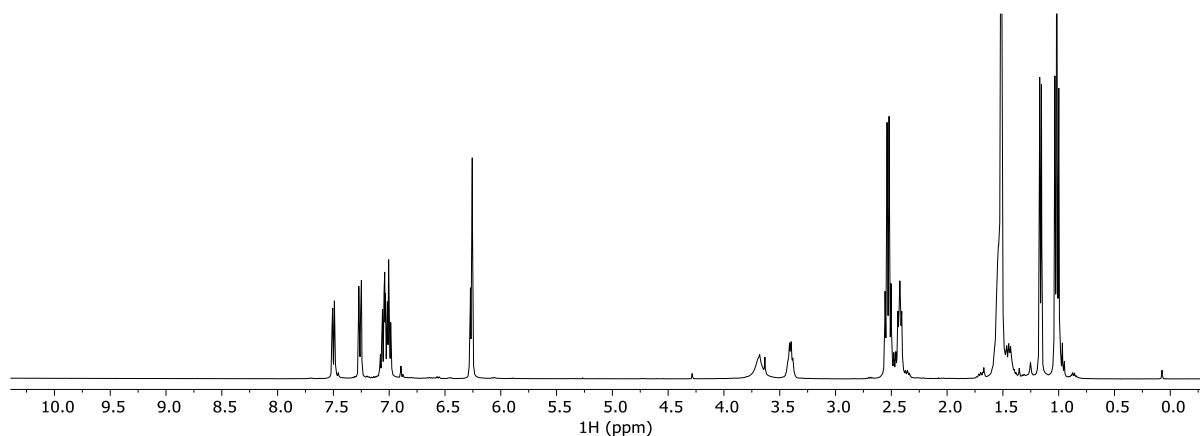


Figure S3.29 ¹H NMR spectrum (400 MHz, CDCl₃) for *N*-Boc-P3a

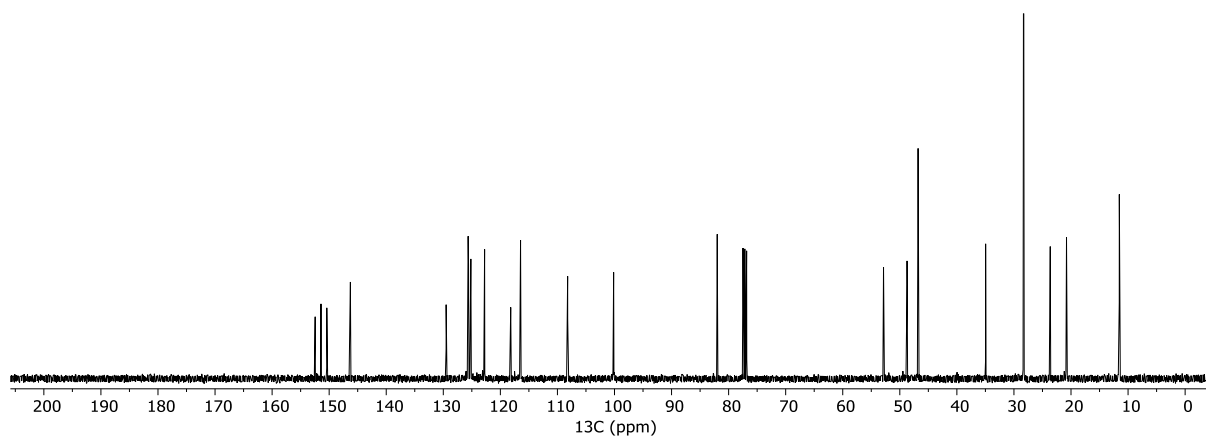


Figure S3.30 ^{13}C NMR spectrum (101 MHz, CDCl_3) for *N*-Boc-P3a

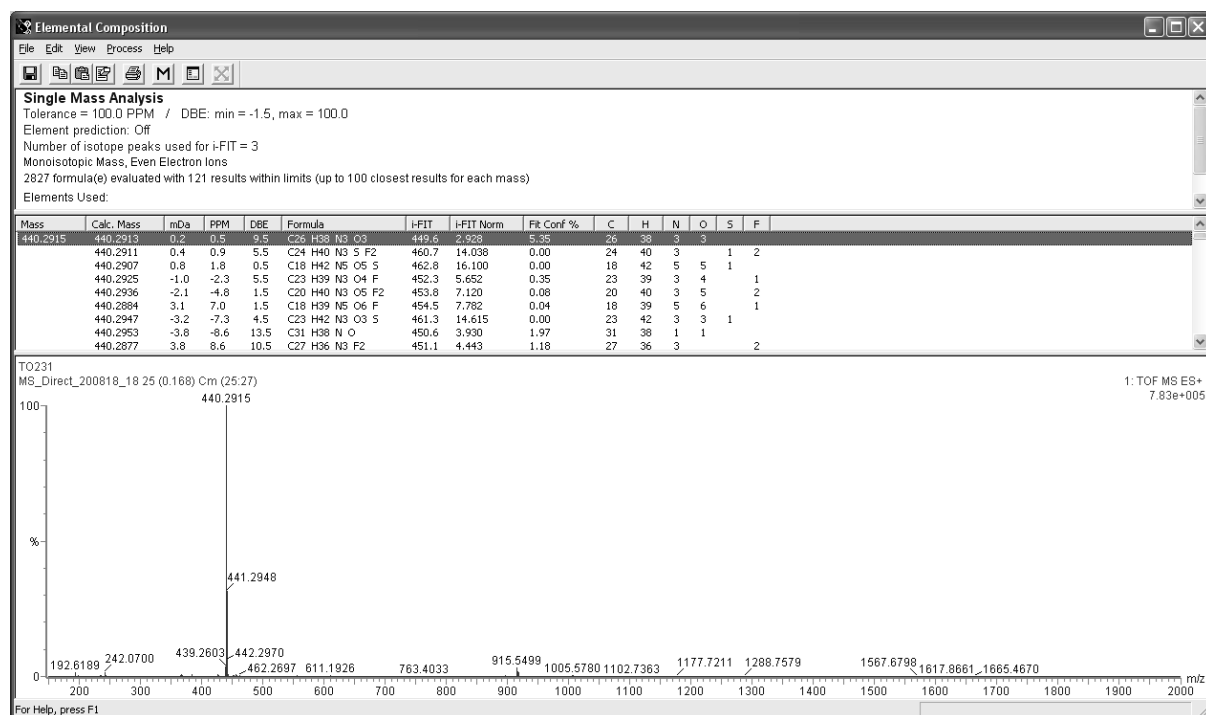


Figure S3.31 HRMS spectrum (ES+) for *N*-Boc-P3a

tert-butyl 3-(cyclohexylamino)-10*H*-phenoxazine-10-carboxylate (**N-Boc-P3b**)

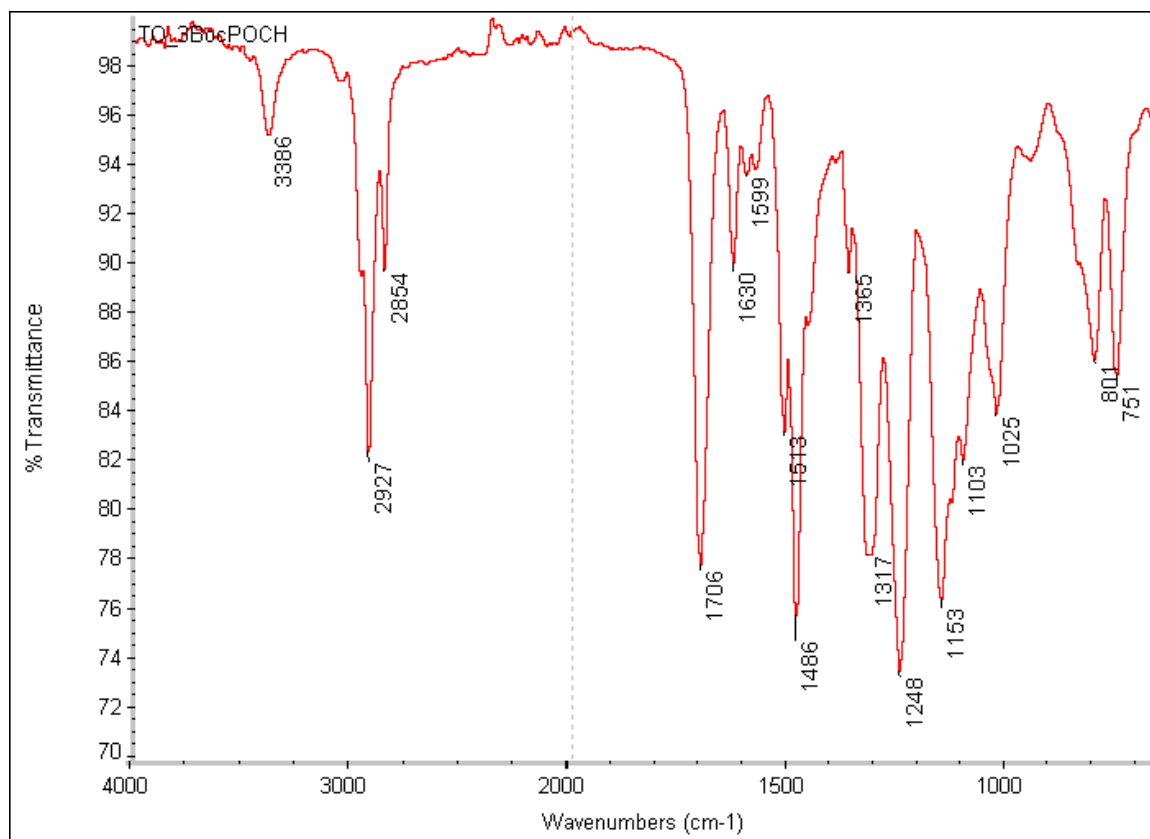


Figure S3.32 Infra-red spectrum (ATR) for **N-Boc-P3b**

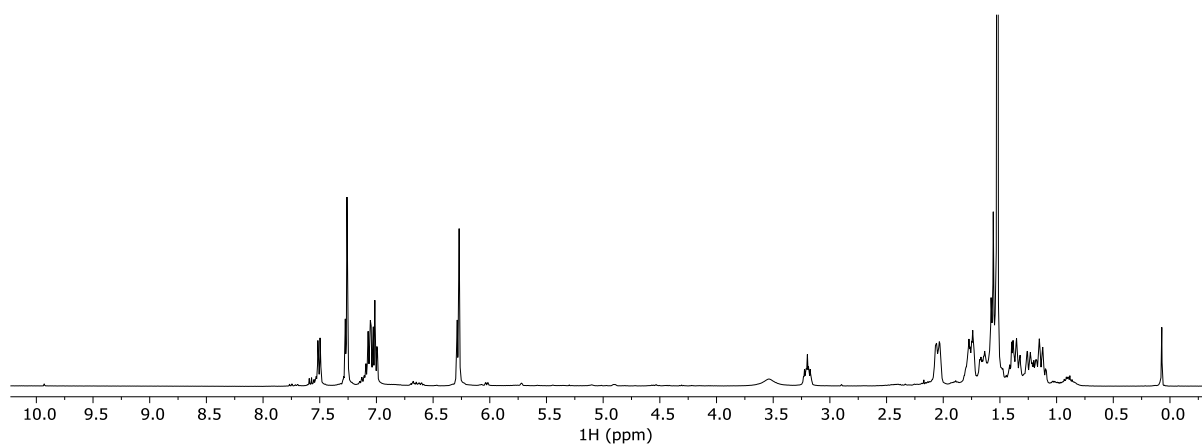


Figure S3.33 ¹H NMR spectrum (400 MHz, CDCl₃) for **N-Boc-P3b**

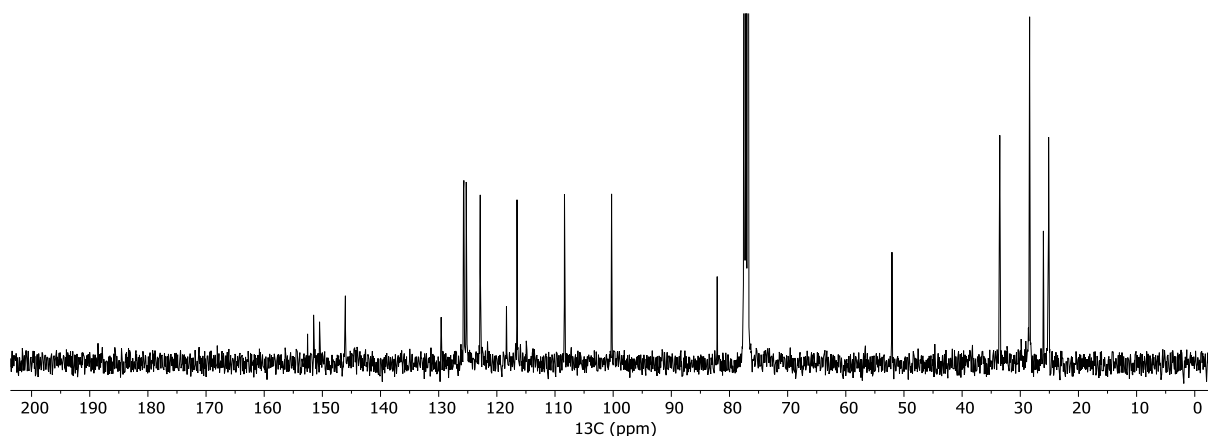


Figure S3.34 ^{13}C NMR spectrum (101 MHz, CDCl_3) for *N*-Boc-P3b

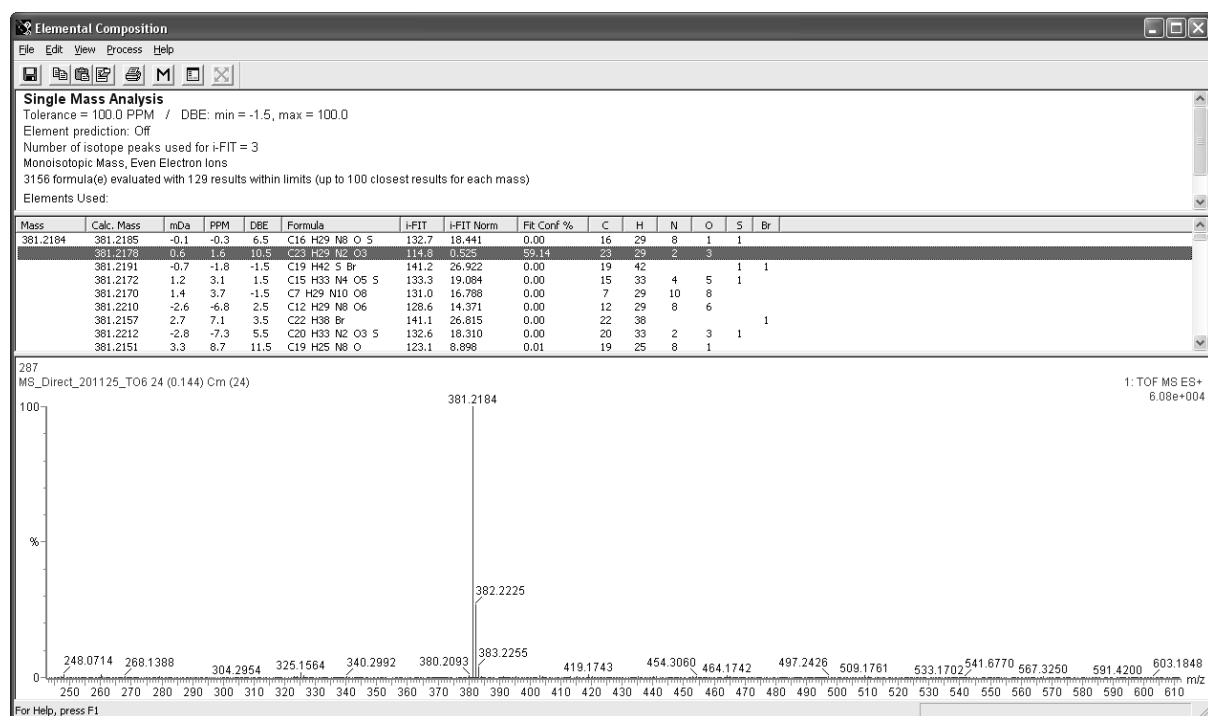


Figure S3.35 HRMS spectrum (ES+) for *N*-Boc-P3b

N,N-diethyl-*N*-(10*H*-phenoxazin-3-yl)pentane-1,4-diamine (**P3a**)

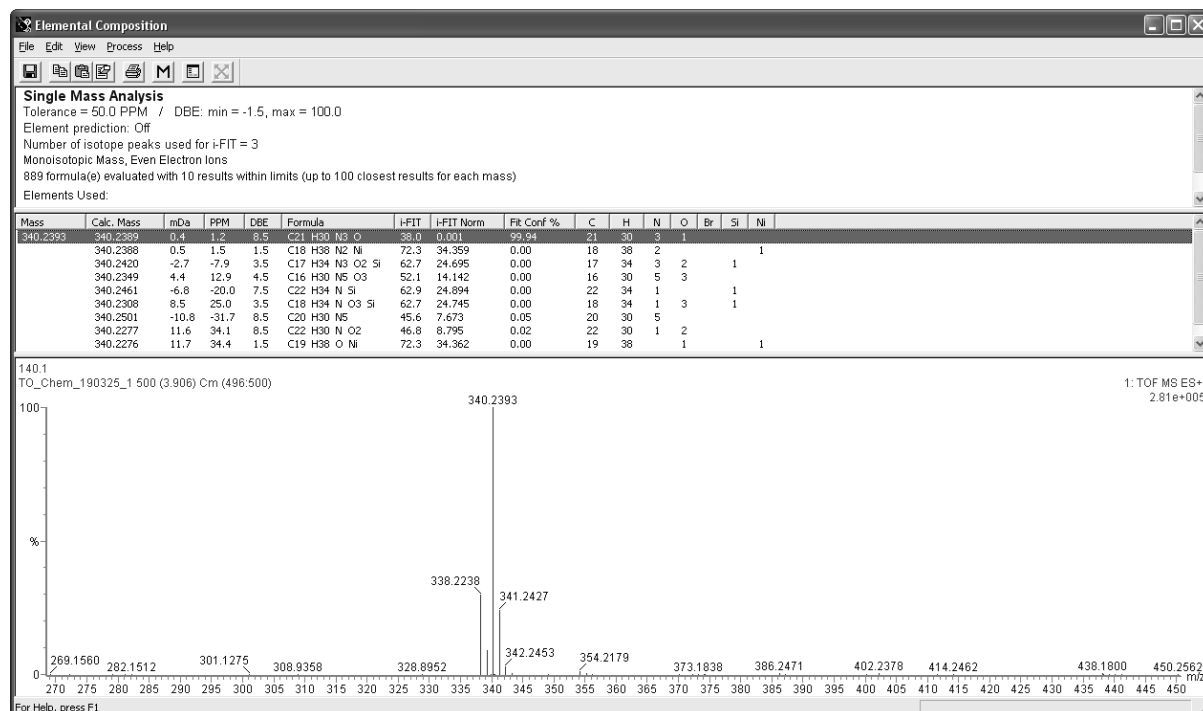


Figure S3.36 HRMS spectrum of **P3a** showing contamination by **P3a'**

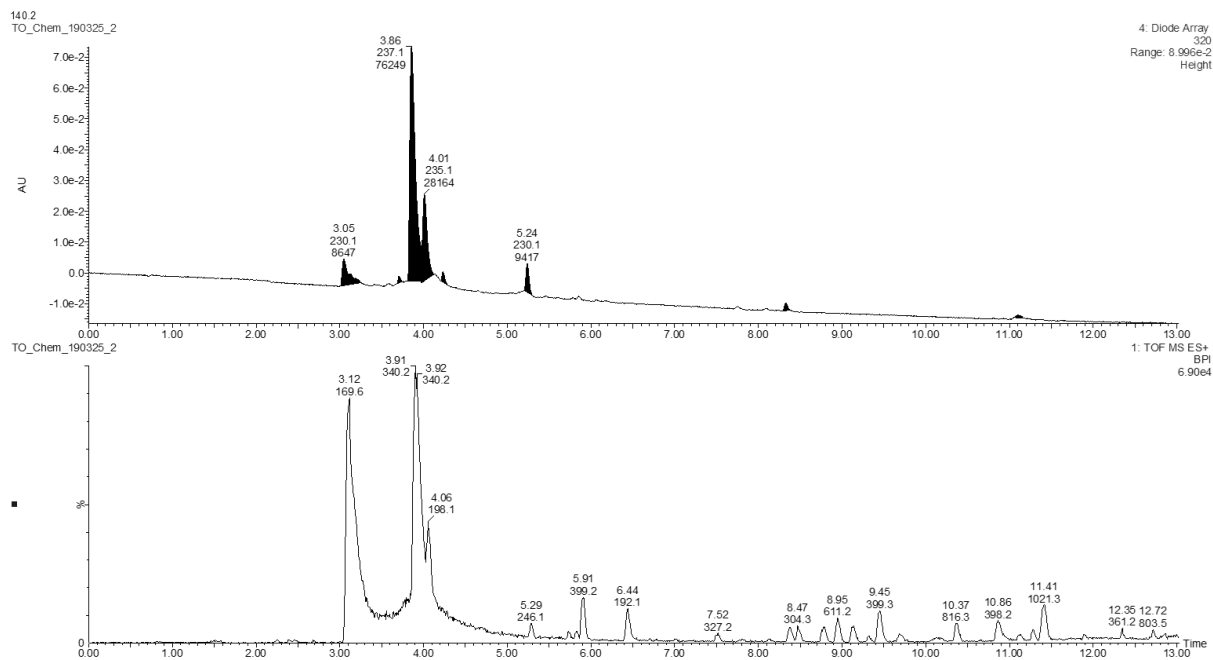


Figure S3.37 LCMS trace of **P3a** showing poor purity

(E)-4-[(3H-phenoxazin-3-ylidene)amino]-N,N-diethylpentan-1-amine HCl salt (**P3a'**)

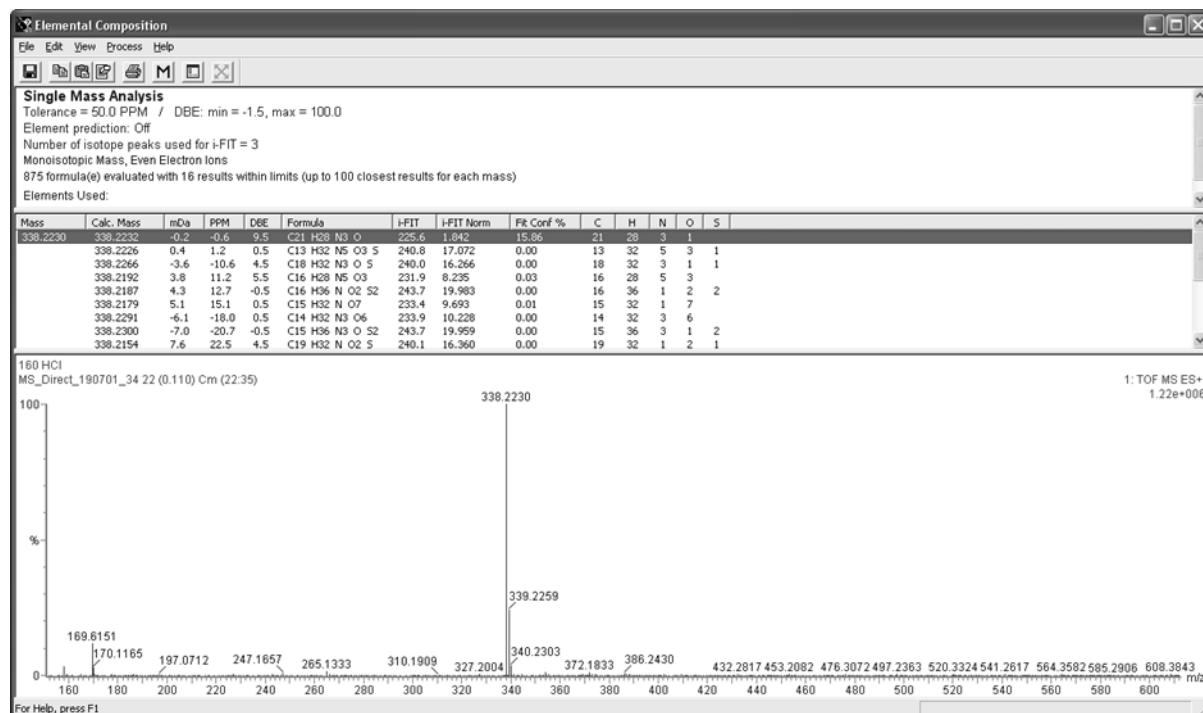


Figure S3.38 HRMS of **P3a'**·HCl

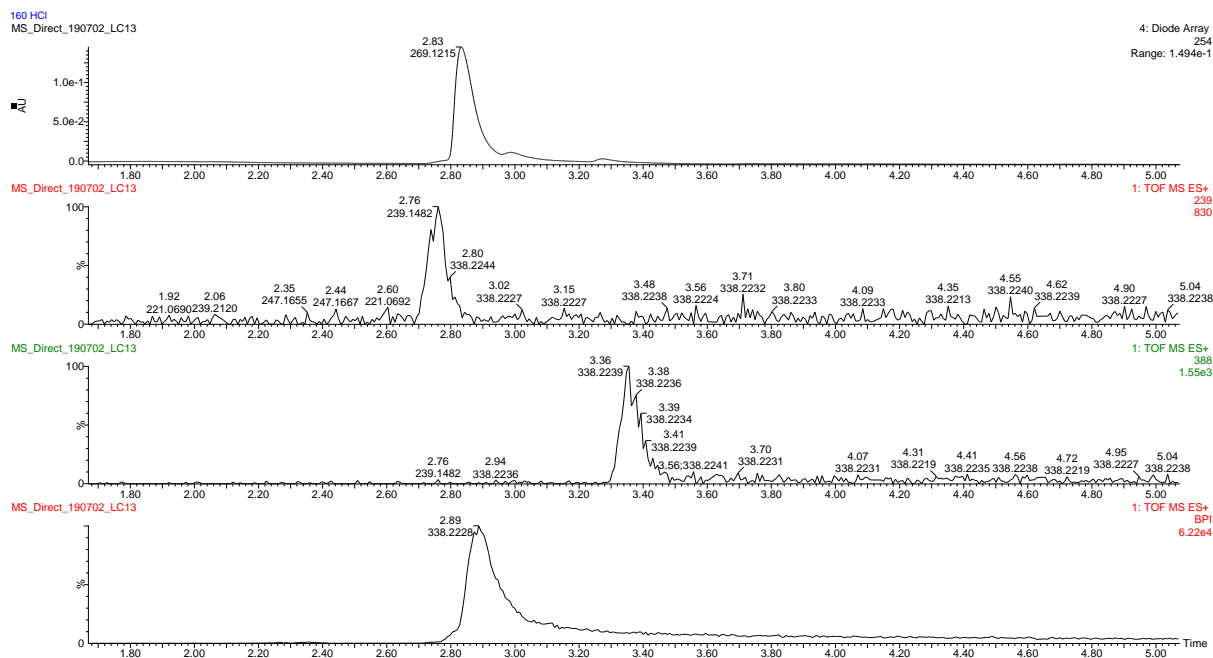


Figure S3.39 LCMS purity measurements, calculated to be 88% for **P3a'**·HCl

N-cyclohexyl-10H-phenoxazin-3-amine (P3b)

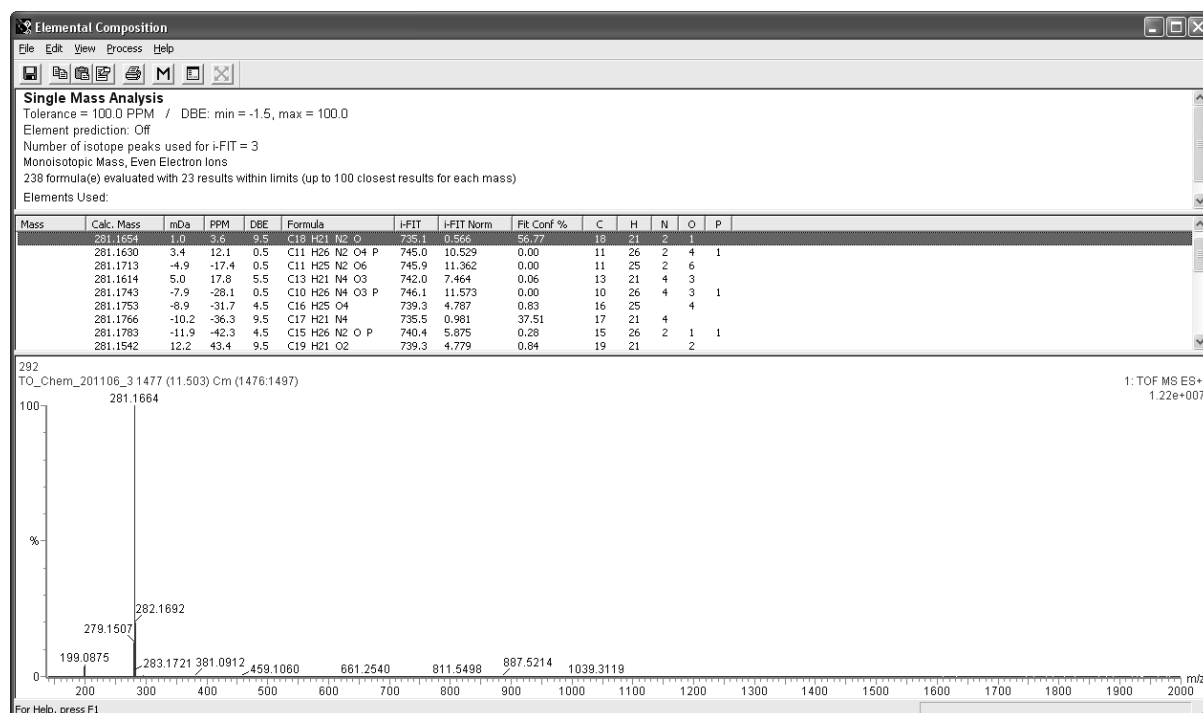


Figure S3.40 HRMS of P3b, revealing some contamination of P3b' (279.1507)

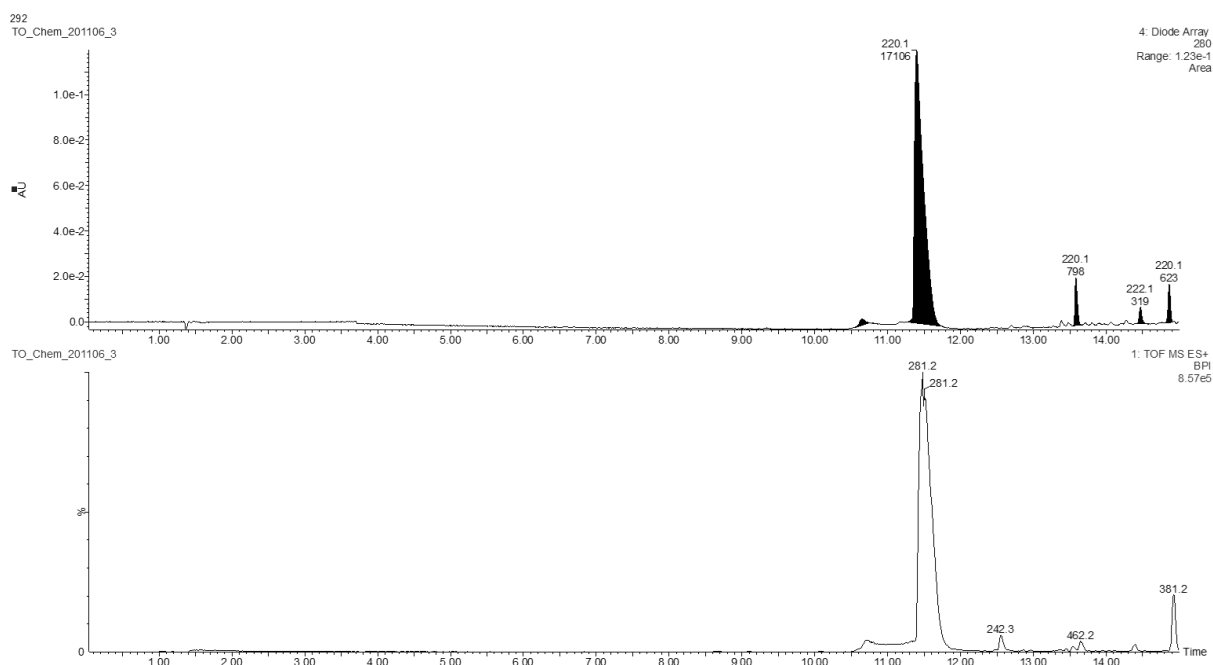


Figure S3.41 LC-MS purity measurement for P3b giving a purity of 90.8%

4. References

- [1] R. Buller, M. L. Peterson, Ö. Almarsson, L. Leiserowitz, *Cryst. Growth Des.* **2002**, *2*, 553-562.
- [2] BIOVIA, 6.0 ed., Dassault Systèmes BIOVIA, San Diego.
- [3] MarvinSketch, ChemAxon Ltd., Budapest, **2011**.
- [4] a) M. D. Carter, V. V. Phelan, R. D. Sandlin, B. O. Bachmann, D. W. Wright, *Comb. Chem. High Throughput Screen.* **2010**, *13*, 285-292; b) R. D. Sandlin, M. D. Carter, P. J. Lee, J. M. Auschwitz, S. E. Leed, J. D. Johnson, D. W. Wright, *Antimicrob. Agents Chemother.* **2011**, *55*, 3363-3369.
- [5] S. R. Hawley, P. G. Bray, M. Mungthin, J. D. Atkinson, P. M. O'Neill, S. A. Ward, *Antimicrob. Agents Chemother.* **1998**, *42*, 682-686.
- [6] J. W. M. Nissink, *J. Chem. Inf. Model.* **2009**, *49*, 1617-1622.
- [7] M. Jahanfar, K. Suwa, K. Tsuchiya, K. O. Ogino, *Open J. Org. Polym. Mater.* **2013**, *03*, 46-52.
- [8] Y. Kanazawa, T. Yokota, H. Ogasa, H. Watanabe, T. Hanakawa, S. Soga, M. Kawatsura, *Tetrahedron* **2015**, *71*, 1395-1402.
- [9] C. Zinelaaibidine, O. Souad, J. Zoubir, B. Malika, A. Nour-Eddine, *Int. J. Chem.* **2012**, *4*, 73-79.
- [10] I. Thomé, C. Bolm, *Org. Lett.* **2012**, *14*, 1892-1895.
- [11] A. B. Gamble, J. Garner, C. P. Gordon, S. M. J. O'Conner, P. A. Keller, *Synth. Commun.* **2007**, *37*, 2777-2786.
- [12] C. Deldaele, G. Evano, *ChemCatChem* **2016**, *8*, 1319-1328.
- [13] D. Ma, Q. Cai, H. Zhang, *Org. Lett.* **2003**, *5*, 2453-2455.
- [14] Y.-B. Huang, C.-T. Yang, J. Yi, X.-J. Deng, Y. Fu, L. Liu, *J. Org. Chem.* **2010**, *76*, 800-810.
- [15] X. Ding, M. Huang, Z. Yi, D. Du, X. Zhu, Y. Wan, *J. Org. Chem* **2017**, *82*, 5416-5423.